Elucidating the Role of EPAC-Rap1 Signaling Pathway in the Blood-Retinal Barrier

By

Carla Jhoana Ramos

A dissertation submitted in partial fulfillment
of the requirements for the degree of
Doctor of Philosophy
(Cellular and Molecular Biology)
in The University of Michigan
2017

Doctoral Committee:

Professor David A. Antonetti, Chair
Professor Christin Carter-Su
Associate Professor Philip J. Gage
Professor Ben Margolis
Assistant Professor Ann L. Miller

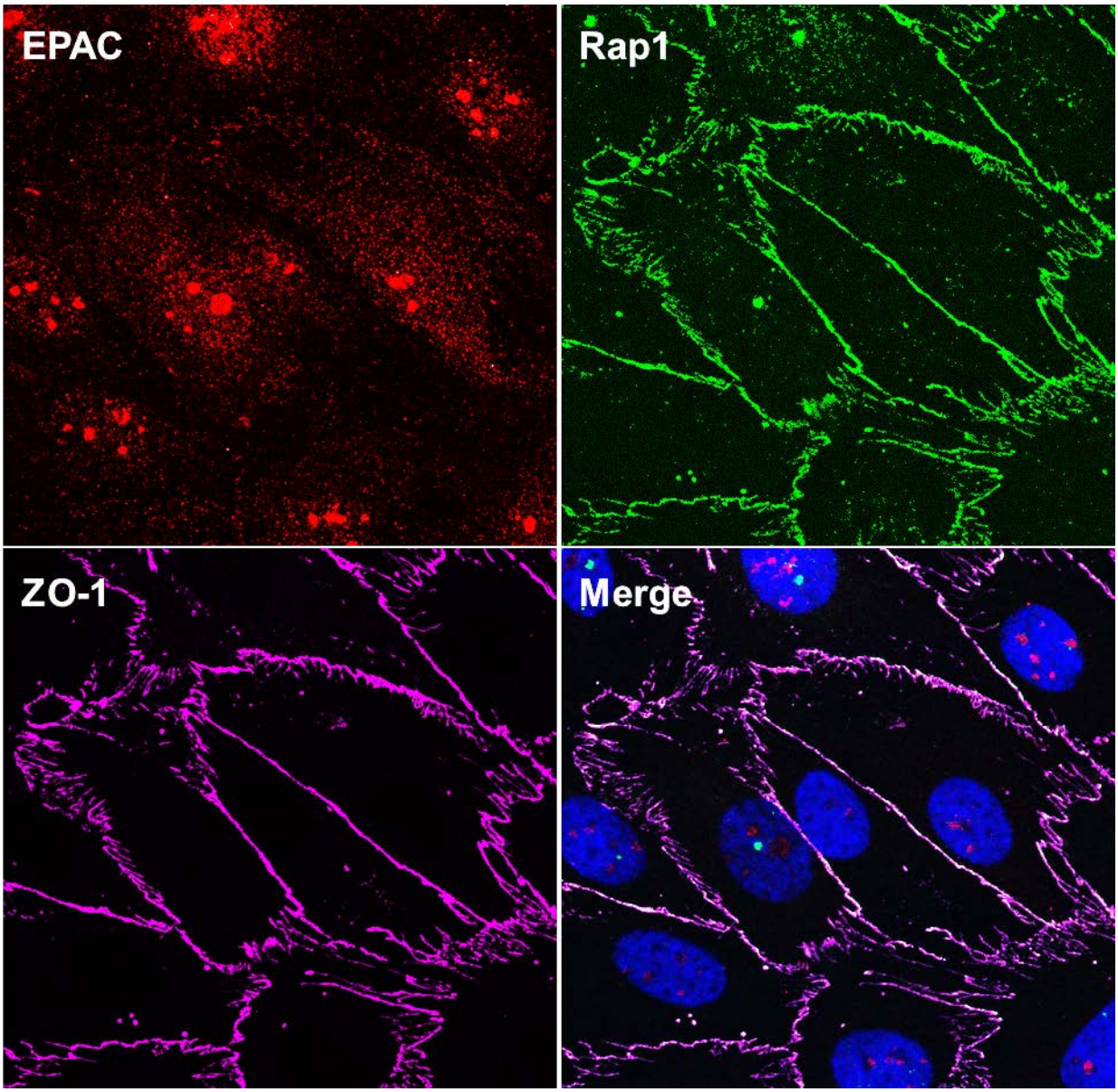

Image of exchange factor directly activated by cAMP (EPAC), Ras-related protein (Rap1) and Zonula occludens-1 (ZO-1) immunofluorescent staining in bovine retinal endothelial cells, obtained by confocal microscopy.

Carla Jhoana Ramos

cjram@umich.edu

ORCID iD: 0000-0001-5041-6758

DEDICATION

This dissertation is dedicated to my mother Victoria de Jesus Larios de Ramos, my father Jose Carlos Ramos, and my younger brother Hilmar Ramos. My parents migrated from El Salvador to the USA in search of better opportunities and dedicated their lives to providing us with a good education. They have instilled in me determination, perseverance and strength. Finally, my experience observing my mother cope with more than 26 years of diabetes and 10 years of mild diabetic retinopathy led me into diabetes research at the University of Michigan.

ACKNOWLEDGEMENTS

The completion of this dissertation has been made possible by the support from my community of mentors, friends and family. I would like to first thank my mentor David Antonetti, who gave me the opportunity to train in his laboratory under his guidance during these last 6 years. Additionally, I would like to thank my thesis committee: Ben Margolis, Christin Carter-Su, Philip Gage, and Ann Miller whose suggestions, questions, and scientific discussions helped improve the quality of this thesis and for their constant support and encouragement.

I dedicate a special thank you to laboratory members that have helped me in my dissertation research. Xuwen Liu, has been a mentor, friend, and role model. Cheng-mao Lin trained me in all the animal protocols and I thank him for his kindness and patience. Ari Muthusamy was the first person who trained me and provided his ongoing support. Moreover, I thank Monica Diaz Coranguez and Andreia Gonçalves for their contribution to my scientific training and thinking and for their guidance and friendship.

I would also like to thank my friends inside and outside the laboratory, my Sacnista family, and the CMB department for their continuous support and inspiration.

I am extremely grateful to my parents, Vicky and Jose Ramos, and my younger brother Hilmar Ramos for their unconditional love, support, and sacrifice. They have been my strength during difficult times. I also want to express my gratitude to my new family: David and Sherry Ketchesin, Nana Peggy, Nana Ketchesin and the Spurlocks for providing a loving home away from home and for their support. Finally, I dedicate a special thank you to my boyfriend Kyle

Ketchesin who has been my support, strength, friend, partner, and editor during these last 4.5 years.

TABLE OF CONTENTS

LIST OF FIGURES

LIST OF TABLES

ABSTRACT

Abnormalities in retinal vascular permeability can result in macular edema, the buildup of fluid in the retina, which causes the retina to swell and thicken, and leads to neuronal cell death and vision loss. Increased retinal vascular permeability is found in many eye pathologies, including diabetic retinopathy (DR), age-related macular degeneration (AMD), and retinal vein occlusion (RVO). The pathological changes in vascular permeability are driven by elevated levels of growth factors such as vascular endothelial growth factor (VEGF) and pro-inflammatory cytokines such as tumor necrosis factor (TNF-α). The use of VEGF-neutralizing antibodies as a form of treatment improves vision in about half of patients treated. However, these treatments are invasive, secondary complications are observed, and half of the patients treated do not improve. Therefore, understanding mechanisms that block vascular permeability and restore the blood-retinal barrier (BRB) are important for developing novel therapies promoting barrier restoration.

The small guanosine triphosphatase (GTPase) Rap1 and its guanine-nucleotide-exchange factor (GEF), EPAC, have been identified as key regulators of barrier formation, promoting cell-cell adhesion, cell-extracellular matrix (ECM) adhesion, and the assembly of junctional complexes in human umbilical vein endothelial cells (HUVEC) and epithelial cells. However, it is unknown whether the EPAC-Rap1 signaling pathway regulates the tight junctions (TJs) of retinal endothelial cells and the relationship between EPAC-Rap1 and VEGF signaling in retinal permeability is poorly understood. The goals of this thesis are to: 1) determine whether EPAC-

Rap1 signaling regulates the barrier properties of the BRB, and 2) gain insight into the mechanisms of endothelial cell permeability to identify novel therapeutic targets.

To investigate the role of EPAC-Rap1 signaling in the BRB, EPAC was activated using the membrane permeable cAMP analog, 8-pCPT-2´-O-Me-cAMP-AM (8CPT-AM). 8CPT-AM treatment blocked and, importantly, reversed permeability induced by VEGF and TNF-α both *in vivo* and *in vitro* and promoted TJ organization in bovine retinal endothelial cells (BREC). Additionally, inhibition of EPAC2 or knockdown of Rap1B led to an increase in basal permeability. Rap1B knockdown alone recapitulated the TJ disorganization observed with VEGF. Furthermore, pretreatment of cells with 8CPT-AM prior to VEGF, decreased VEGF-induced phosphorylation of VEGFR2 and Erk1/2. Together, these data show that activation of EPAC-Rap1 signaling can promote and restore barrier properties by blocking permeability inducing agents, attenuate VEGF-Erk1/2 signaling, and promote organization of the TJ complex.

To further explore and gain insight into the mechanisms of VEGF signaling in retinal endothelial permeability, mass-spectrometry based phosphoproteomics was performed on BREC. 1,724 proteins were identified. From these proteins, 107 phosphoproteins that had a 25% phosphorylation change in the presence of VEGF and were present in more than one mass spectrometry analysis were identified and used to develop protein interaction networks using Cytoscape. One of the protein interaction networks obtained consists of the proteins EPAC, rasip1, and afadin (AF-6), all of which show significant changes in phosphorylation in the presence of VEGF.

The results presented here provide new evidence that EPAC-Rap1 signaling contributes to the barrier properties of the BRB via regulation of the TJ complex. Additionally, the phosphoproteome analysis suggests how VEGF may increase permeability through

phosphorylation and regulation of the EPAC/Rap/rasip1 pathway. Overall, the results from this thesis expand our knowledge on the role of EPAC2 and Rap1B in regulating retinal endothelial barrier properties and permeability. Further, these data identify specific targets for novel therapies addressing abnormalities in retinal vascular permeability.

CHAPTER 1

Introduction*

1. 1 Barriers of the Central Nervous System

In 1885, Paul Ehrlich published the first observation of a Central Nervous System (CNS) barrier. Ehrlich observed that water-soluble dyes, injected subcutaneously, stained all organs except the brain and spinal cord [1]. It was not until 1900 that the concept of a CNS barrier was introduced by Lewandosky who termed it "capillary wall." Later, in 1918, the term "barrier" was proposed by Lina Stern [2]. The pioneering work performed by Ehrlich, Lewandosky, Stern and other scientists led to the recognition of the blood-brain barrier (BBB).

The earliest observations of the blood-retinal barrier (BRB) were reported by Schnaudigel in 1913 and Palm in 1947. Intravenous injection of trypan blue into rabbits stained all organs, but not the CNS or the retina [3]. These initial observations were later supported at the ultrastructural level by Cunha-Vaz [4, 5]. Thus, the BBB and the BRB were discovered to form part of the barriers of the CNS. We now understand that the BBB and BRB provide tight control of the neuronal environment by regulating the flux of blood borne material into the neural parenchyma. These barriers maintain proper neural homeostasis and protect the neural tissue from potential blood-borne toxicity.

**Note: Portions of this introduction were published previously in two articles entitled, "The inner blood-retinal barrier: Cellular basis and development" (Díaz-Coránguez et al., 2017) and "The role of small GTPases and EPAC-Rap1 signaling in the regulation of the blood-brain and blood-retinal barriers" (Ramos and Antonetti, 2017).*

Understanding how barriers of the CNS develop in order to supply the required metabolic support for neural tissue and sustain the proper environment for synaptic signaling remains an area of active investigation. The vasculatures in both the brain and retina have well-developed tight junction (TJ) complexes, which restrict paracellular flux by maintaining precise control of proteins, metabolites and cells that can enter the neural tissue. Additionally, these vascular endothelial cells exhibit limited fenestrae and low endocytic vesicle formation in order to maintain a tight barrier [6, 7].

Loss of these barriers is observed in a variety of pathologies associated with high morbidity and mortality. Brain tumors, dementia, Alzheimer's disease, Parkinson's disease, and a host of blinding eye diseases such as diabetic retinopathy, retinal vein occlusions, retinopathy of prematurity and age-related macular degeneration all have a "leaky" vascular barrier [6, 8, 9]. Vascular permeability involves both increased paracellular flux associated with changes in the cell junctional complexes that connect adjacent cells and increased transport through the transcellular pathway mediated by endocytic vesicles.

1.2 The Retinal Vasculature

The retina is a thin, highly organized, multi-layered and multi-cellular neural tissue responsible for vision. It is located on the posterior cavity of the eye between the choroid and the vitreous humor (Figure 1.1.A). The retina's function is to capture light stimuli and convert it into an electrical impulse that can be transmitted, via the optic nerve, to the brain's visual cortex and ultimately interpreted as visual input.

The retina, like the brain, is a high energy demanding system in the body because of neuronal activity [10]. However, the retina also requires low intra-retinal blood vessels in order to allow vision. Two vascular beds satisfy these competing requirements. The retina is divided

into two main parts, the inner and the outer retina (Figure 1.1.B). The inner retina consists of three layers: the ganglion cell layer (GCL), the inner plexiform layer (IPL) and the inner nuclear layer (INL) (Figure 1.1.B). The outer retina extends from the outer plexiform layer (OPL), through the outer nuclear layer (ONL) to the retinal pigment epithelium (RPE) (Figure 1.1.B). The outer retina is avascular and contains photoreceptors which are highly oxygen demanding and consumes 8% of the basal metabolic rate [11, 12]. In order to support the demands from the different retinal regions, the retina has a dual blood supply system, which arises from the central retinal artery circulation [13]. The inner retina is nourished by the retinal vasculature, which provides nutritional support and waste product removal (Figure 1.2). The oxygen levels of the inner retina are regulated and maintained at a relative hypoxic state, PO_2 of 20mmHg [14]. The retinal vasculature is further divided into the inner superficial vasculature and the deep vasculature. The inner superficial vasculature is located at the GCL and the deep vasculature is located at the inner and outer edges of the inner nuclear layer (INL) (Figure 1.2) [13]. The outer retina is nourished by the choroidal vasculature separated from the retina by the RPE which controls metabolic nourishment and waste removal (Figure 1.1.B) [13].

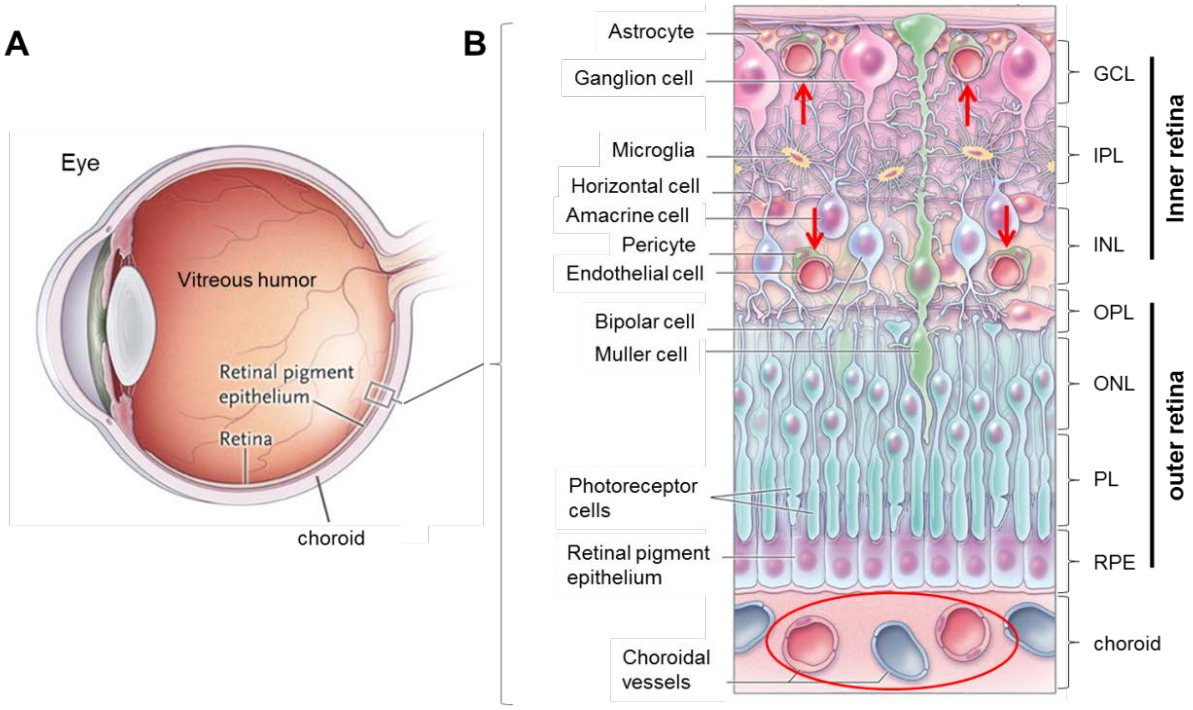

Figure 1.1 Anatomy of the Retina. **A.** Schematic of the human eye and localization of the retina. **B.** Schematic of retina cross section enlargement showing cell types and layers. The red arrows show the retinal vasculature of the inner retina and the red circle in the choroid layer shows the choroidal vasculature of the outer retina (adapted from Antonetti et al., 2012).

1.2.1 Development of the Retina Vasculature

In early human retinal development, a hyaloid network of vasculature emerges from the central hyaloid artery in the optic nerve, providing vascular support for the whole eye. In humans, hyaloid vessels regress and the retinal vasculature begins developing around week 14 of gestation (WG) and continues until the day of birth [15]. The retinal vasculature development is conducted by two different mechanisms: vasculogenesis, which refers to the maturation of progenitor cells to the primary vascular bed; and angiogenesis, which is the sprouting of vessels from the pre-existing vasculature.

In humans, retinal vasculogenesis occurs from WG 14 to WG 18. Vasculogenesis is followed by angiogenesis at WG 18 [15]. The primary sprouts come from the optic nerve head and expand radially along the vitreal surface in the retina, attracted by the VEGF secreted from astrocytes. In the primary plexus, the differentiation of major arteries and veins takes place, followed by sprouting into the deep retinal tissue. At WG 21, the first capillary bed in the outer layer is apparent, and the sprouting continues to the inner plexus in a process that coincides with the eye opening. In humans, this process culminates by WG 32, when hyaloid vasculature regression has been completed.

However, much of our understanding of retinal vascular development comes from mice, whose hyaloid regression and retinal vascular development begins after birth. In mice, retinal angiogenesis starts at the day of birth, as does the formation of the superficial plexus that covers the retinal surface by post-natal day 8 (P8). This is followed by vascular sprouting into the deep and intermediate plexus layers, formed at P7–P12 and P14–P21, respectively.

Retinal angiogenesis is mainly governed by the expression of the VEGF receptor (VEGFR2), which regulates endothelial migration and proliferation in response to VEGFA

secreted by glia and neurons [16, 17]. During the angiogenic process, two endothelial cell types can be distinguished: endothelial tip cells, which establish the direction of the sprouting by extending their filopodia toward the VEGF source; and stalk cells, an intermediate population of cells in the vascular plexus that proliferate and extend the length of the vessels. Tip cells express delta like 4 (Dll4), Platelet Derived Growth Factor Subunit B (PDGFB) and apelin ligands [18-20], while the netrin receptor Unc5b and VEGFR are upregulated in stalk cells [21, 22].

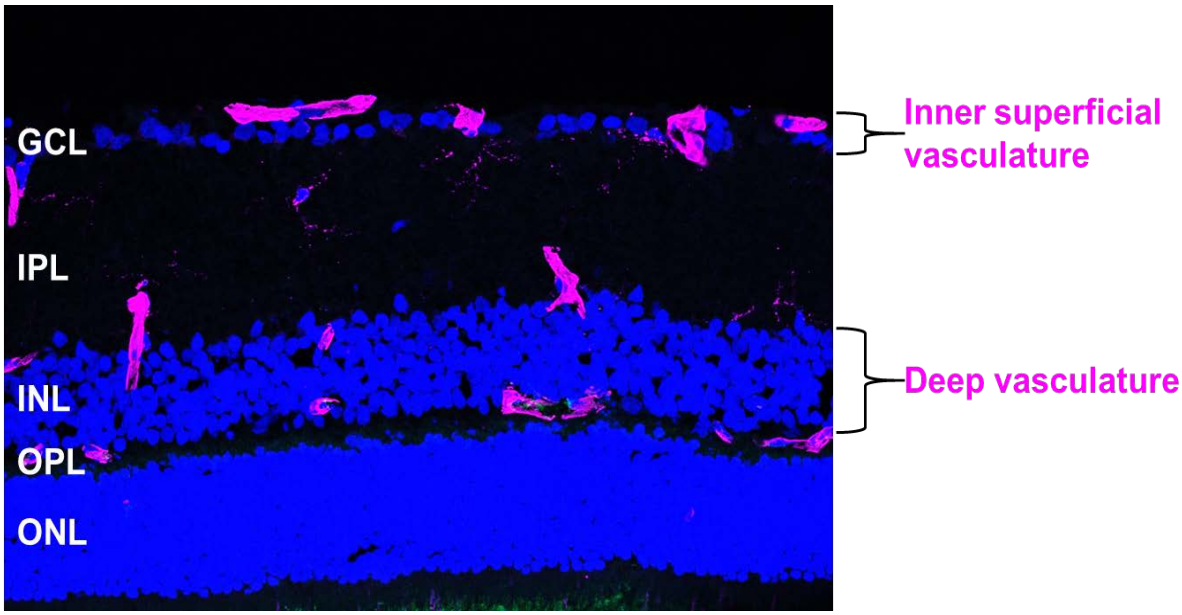

Figure 1.2 The Retinal Vasculature. Immunofluorescence staining using IB4 (pink) was used to detect the retinal vasculature in a rat retina cross section. The inner superficial vasculature is observed in the ganglion cell layer (GCL). The deep vasculature is at the inner and outer edges of the inner nuclear layer (INL).

1.3 Blood-Retinal Barrier

The retina, similar to the brain possesses a blood-retinal barrier. Structurally, the BRB consists of two distinct barriers, the outer BRB (oBRB) and the inner BRB (iBRB). The oBRB consists of the retinal pigment epithelium (RPE) that regulates movement from the choroidal vasculature to the inner retina. The iBRB is comprised of the retinal endothelial cells, astrocytes, and pericytes all which form the neurovascular unit. The iBRB provides oxygen and glucose for neuronal function and regulates transport of ions, nutrients, and toxins across the retinal capillaries [23, 24]. Loss of the iBRB contributes to the pathophysiology of a number of retinal diseases, including diabetic retinopathy [23, 25].

1.3.1 Flux and Permeability

The CNS barriers are highly selective, regulating the movement of ions, water, solutes and cells across capillaries [26]. Flux of a solute or water is defined as the net movement across a barrier over time, while permeability describes the property of the barrier, in this case, of the iBRB.

Fluid flux is the movement from the lumen of capillaries into the interstitial space. Starling's principle describes the net fluid flux (J_υ) across the capillary membrane as the difference between the hydrostatic pressure and oncotic pressure. This was later modified to include the permeability of the endothelium barrier, recognizing that different vascular beds possess differences in barrier properties [27]. Thus, the net movement of fluid flux across a semi-permeable membrane can be calculated by the equation below, where J_υ= net fluid flux (ml/min); K_f = the filtration coefficient (ml/min/mmHg); P_c = the capillary hydrostatic pressure (mmHg); P_i = the interstitial hydrostatic pressure (mmHg); σ = the reflection coefficient; π_c = the capillary oncotic pressure (mmHg); π_i = the interstitial oncotic pressure (mmHg):

$$J_v = K_f([P_c\text{-}P_i] - \sigma[\pi_c\text{-}\pi_i])$$

The filtration coefficient (K_f) is a constant that describes the barrier's permeability to water. The BRB, like the BBB, is less permeable than other vascular beds. The reflection coefficient (σ) is a correction factor for the membrane's permeability to the proteins involved in generating the oncotic pressure, i.e. albumin. The capillary hydrostatic pressure refers to the pressure of blood/plasma against the vessel walls. The capillary oncotic pressure is a form of osmotic pressure exerted by protein content in the blood plasma that absorbs water into the lumen of vessels. Studies testing Starling's principle have demonstrated that changes in the capillary oncotic pressure have a minimal effect on fluid filtration across the endothelium. Instead, the endothelial glycocalyx layer (EGL) plays a major regulatory role in capillary fluid filtration [28, 29]. The EGL is a mesh composed of membrane-bound glycoproteins and proteoglycans, located on the luminal side of endothelial cells. The EGL is semi-permeable to molecules like albumin and impermeable to dextran molecules $\geq$70kDa. In the CNS barriers, which are composed of non-fenestrated capillaries and continuous basement membrane, the EGL is also continuous.

On the other hand, permeability (P_o), across a barrier to a specified solute can be measured by calculating the rate of flux of the molecule. The P_o, is calculated by the equation below, where P_o = diffusive flux (cm/s); $[C]_A$ = basolateral concentration of the molecule of interest, often a labeled marker; $[C]_L$ = apical concentration; Δt = change in time; A = surface area of the filter (cm^2); V_A = volume of the basolateral chamber (cm^3):

$$P_o = ([C]_A V_A / \Delta t)/[C]_L A$$

Evan's blue dye, which tightly binds albumin, is often used to quantify the accumulation of albumin in the retina over a specified time, and differences in dye accumulation are interpreted as changes in permeability.

1.3.2 Routes of Permeability

Changes in permeability across the vascular bed may occur through changes in transport across the cells, broadly termed transcytosis, or through changes in the junctional complex organization, leading to flux around the cells or paracellular permeability. Both transcellular and paracellular routes are composed of multiple pathways that are not mutually exclusive, and may collectively contribute to altered flux.

1.3.2.1 Transcytosis

In 1960, Palade et al. described invaginations of the plasmalemma in the capillary endothelium that ‘‘pinch off” from the surface and form intracellular vesicles [30]. Electron microscopy revealed intracellular vesicles and invaginations, which suggested a regulated and directional transport [31]. Other groups observed a preference of localization for vesicles on one side of the membrane, suggesting a unidirectional flow [32]. However, this idea has been challenged by recent studies which reported invaginations on both sides [33].

In 1979, Nicolae Simionescu introduced the term transcytosis. In his electron microscopy studies, he identified the appearance of highly dense structures that he called specialized plasmalemma vesicles within endothelial cells [34]. We now know that transcellular transport across retinal endothelial cells is necessary for regulation of the retinal environment’s homeostasis.

There are a variety of routes that make up the transcellular transport [35]. Some small lipophilic molecules can passively diffuse along the retinal endothelial membrane and cross the BRB [36]. Other, larger, lipophilic molecules and hydrophilic molecules require ATP-dependent processes to cross the barrier, including: receptor-mediated vesicular transport, nonreceptor mediated pinocytosis, transporters and pumps (Figure 1.3). Brain and retinal endothelial cells

selectively regulate the transcellular movement of molecules from the blood to the neural tissue by controlling the expression of molecules at both the luminal and abluminal sides. Retinal endothelial cells express a low number of receptors, transporters and vesicle formation mediators, in combination with a high expression of efflux pumps [37], which collectively contribute to the BRB.

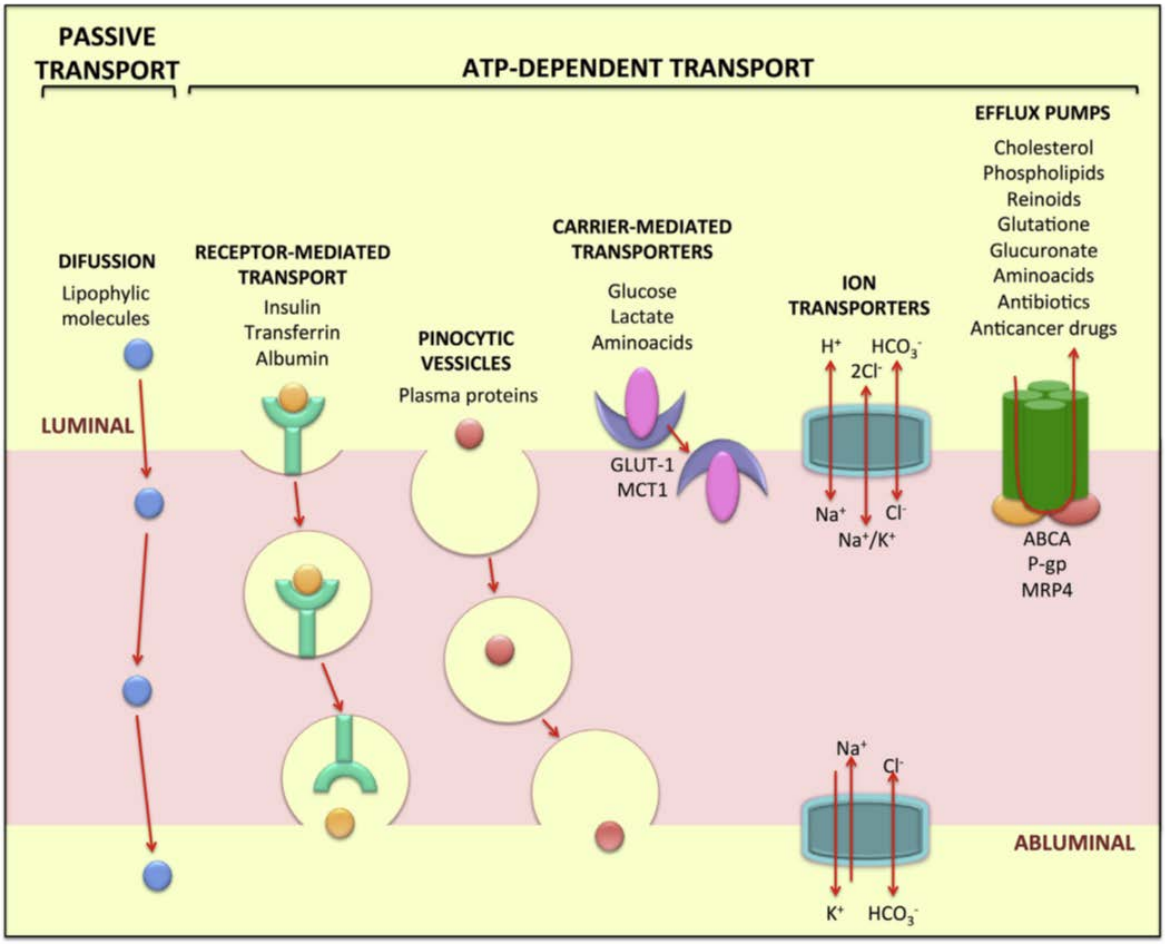

Figure 1.3 Mechanisms of Transcellular Transport Across Retinal Endothelial Cells. Some molecules can cross by diffusion due to their lipophilic properties. Other transport mechanisms are energy-dependent processes and include receptor-mediated transport, pinocytic vesicles, carrier-mediated transporters, ion transporters and efflux pumps. The endothelial cells that constitute the BRB, express a low number of these transporter mechanisms, some of the most important are indicated. (Figure from Díaz-Coránguez, M., et al.2017)

1.3.2.2 Paracellular Transport

In addition to transcellular transport, molecules can move via paracellular transport (Figure 1.4), which occurs through the intercellular space between adjacent cells. The intercellular space is highly regulated by the formation of junctional complexes, which include tight junctions (TJ), adherens junctions (AJ), gap junctions, and desmosomes, with TJs and AJs having a central role in barrier regulation.

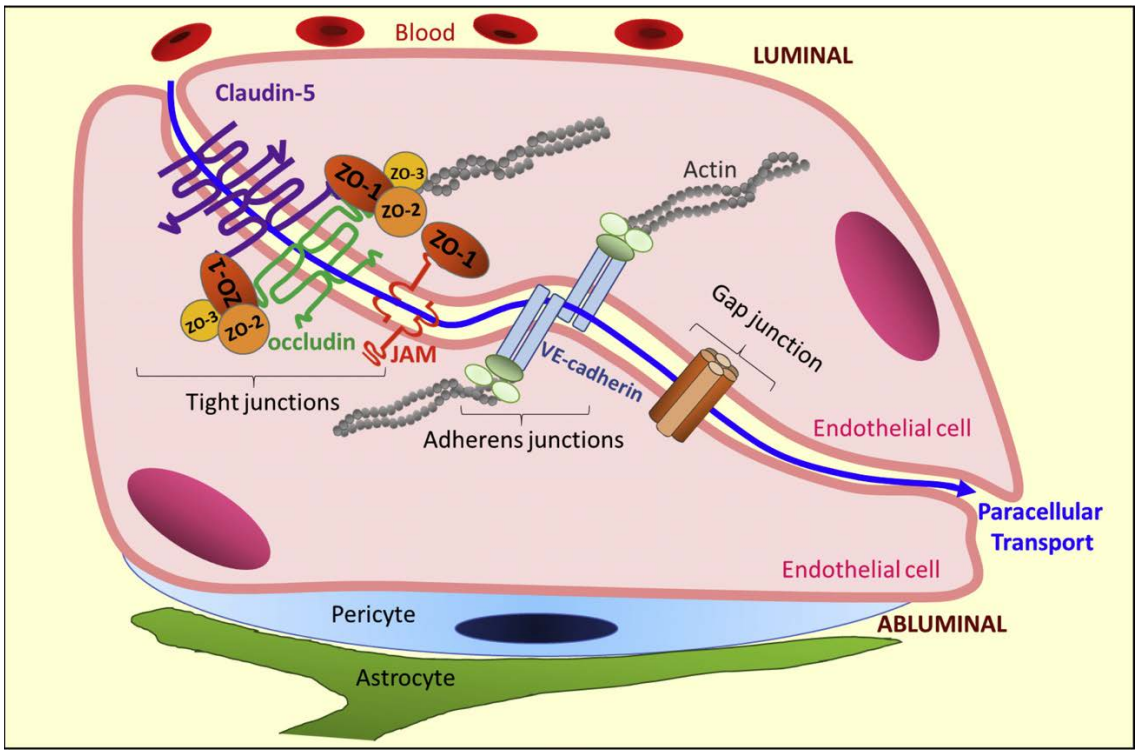

Figure 1.4 Paracellular Transport. In the BRB, molecules can move from the blood (luminal) into the retinal (abluminal) side via the paracellular space, which is located in between two adjacent cells (blue line). Some of the molecules central to control of paracellular transport of the BRB are indicated. (Figure from Díaz-Coránguez, M., et al.2017)

1.4 Tight Junctions (TJ)

In the BRB, the very tight control of solute and fluid flux across the endothelium is conferred by a well-developed tight junction complex. Evidence of TJ complexity in these tissues was demonstrated in studies of freeze fracture sections and electron microscopy, which unveiled a dense network of branch points on tight junction strands [38]. In ultrathin sections of epithelial cells, TJs appear as contact points of close apposition, or ‘‘kissing points”, where the two lipid bilayers of each neighboring cell are almost indistinguishable; these are located specifically at the most apical side of the polarized lateral membrane [39]. In contrast, in endothelial barriers, these same contact points are localized at several points along the paracellular space, between cells and at cell-cell contacts that form the capillary lumen [40]. The molecular mechanisms that regulate the difference in polarization between epithelial and endothelial cells have not yet been determined.

Tight junctions serve two main functions: a gate function that restricts the passage of molecules through the paracellular space, and a fence function that confers cell polarity by preventing movement of lipids and proteins between the apical and basolateral plasma membrane [39, 41, 42]. Additional roles of tight junctions in several cell-signaling processes such as cell proliferation, gene expression, and differentiation, have also been described [43-45].

At a molecular level, the tight junctions consist of over 40 proteins, which can be categorized as:1) transmembrane proteins, including the tetraspanin families of claudin and MARVEL (MAL and related proteins for vesicle trafficking and membrane link) proteins, and the single span proteins from the junctional adhesion molecules (JAM) family; or 2) cytoplasmic scaffold proteins, including members of the membrane-associated guanylate kinase homologue (MAGUK) family like zonula occludens (ZO), and other platform proteins such as afadin (AF6)

and cingulin [46-48].

1.4.1 Claudins

The claudin family consists of tetraspan transmembrane proteins that play a crucial role in paracellular transport by forming ion selective barriers and pores [49, 50]. Claudins range between 20-34 kDa and possess cytoplasmic intracellular NH_2- and COOH- termini, in addition to two extracellular loops [51]. Mutational analyses have revealed that amino acid charges on the first extracellular loop of claudins define the ion selective property of these proteins, while the second extracellular loop is involved in claudin-claudin interactions [52-55]. In addition, the carboxy-terminus of claudins interacts with the first of three PDZ domains on the scaffolding protein ZO-1 [56]. This allows the connection between transmembrane proteins and the actin cytoskeleton, and controls the localization of claudins at cell contacts.

Claudins expressed on the plasma membrane of the same cell can polymerize by cis-interactions into homomeric or heteromeric strands. Homomeric interactions occur between the same type of claudin, for example claudin-3 binds to claudin-3. Heteromeric interactions occur between different claudin types, for example claudin-3 binds claudin-1 [57]. Claudins in adjacent cells (trans-interaction) can also interact with other claudins in a homotypic (same type of claudin) or heterotypic (different claudin) fashion. Expression of different claudin isoforms yields tissue specific barrier properties. Indeed, claudins are subdivided into sealing claudins and pore-forming claudins that are ion-specific paracellular channels [58]. Moreover, overexpression of claudin in non-tight junction-forming cells like fibroblasts, leads to formation of a tight junction-like network [51, 59], supporting the important role of claudins in tight junction formation between adjacent cells.

There are 27 known mammalian claudin members, 26 of which are found in humans [60, 61]. Measurements of mRNA in mouse retinas from P18 show expression of several claudins, including claudin-1-5, -7, 9-14, 16-17, -19, -20, -22 and -23. Claudin-5 is the most abundant of the isoforms, and it localizes at the tight junctions of retinal vessels, together with claudin-1 and -2 [62]. Claudins-1-5, -12, -22 and -23 are regulated in retinal development. During early to mid-development, all the claudins mentioned above increase in expression, especially at P15, coinciding with the formation of the iBRB in retinal capillaries. After this point, their expression decreases, except for claudin-22. Moreover, after oxygen-induced retinopathy at P15 though P21, claudin-2 and -5 are overexpressed [62], suggesting that claudins regulate the barrier function of retinal endothelial cells. In accordance with the high levels of claudin-5 in both the BBB and BRB, claudin-5-deficient mice die within 10 hours after birth due to BBB disruption. While these mice show no abnormal development or morphology of blood vessels and no abnormal bleeding or edema, they do have a BBB leaky towards small molecules < 800 Da [63]. No BRB defects have been reported in mice lacking claudin-5. However, ongoing studies focusing on the BRB and the BBB in pathologies that model diabetes, ischemia, and strokes have associated loss of claudin-5 with an increase in permeability [64, 65], supporting the important role of claudin-5 in BRB. Claudin-1 deficient mice die within the first day of birth due to disruption of the skin barrier, however, no BBB or BRB alteration has been reported [51, 66]. Nevertheless, some studies suggest that claudin-1 is expressed in the retinal vasculature of adult mice, and its content decreases in both streptozotocin (STZ) induced diabetic rats [67], and a model of experimental autoimmune uveoretinitis (EAU) [68].

Not all retinal claudins are restricted to blood vessels. In contrast to BBB studies, in the BRB, there are no reports related to claudin-3 changes in retinal vasculature associated with

altered permeability. In fact, claudin-3 in the retina is expressed in the retinal ganglion cell layer (RGC) [62]. Likewise, other claudin isoforms were found in non-endothelial retinal tissues. Claudin-4 and -23 are localized at the RGC layer, claudin-4 and -12 are expressed in the outer plexiform layer (OPL), and claudin-23 was found in the inner nuclear layer (INL) [62]. The roles of these claudins in the retinal tissue have not been studied yet. Together, these data suggest that claudins, particularly claudin-5, are important in the regulation of the CNS barriers. However, additional claudin isoforms that have the potential to regulate BRB properties require further investigation.

1.4.2 MARVEL Proteins

MARVEL (MAL and related proteins for vesicle trafficking and membrane link) proteins contain a conserved four-transmembrane MARVEL domain. The MARVEL proteins are characterized by their association with the cell's plasma membrane and their involvement in vesicle trafficking [69]. The tight junction-associated MARVEL protein members involved in TJs are part of the TJ-associated MARVEL protein (TAMP) comprised of occludin (MARVELD1), tricellulin (MARVELD2), and MARVELD3 [70].

1.4.2.1 Occludin

Occludin (MARVELD1), a ~60kD membrane protein, was first identified as a component of TJ from chick liver junctional fractions [71]. Hydrophilicity plots and cDNA sequence analyses showed that occludin is a tetraspan transmembrane protein that has two extracellular loops and cytoplasmic NH_2 and COOH termini [71, 72]. The N-terminus of occludin interacts with Itch, an E3-ubiquitin-protein ligase that regulates occludin degradation [73] and endocytosis [74]. The distal C-terminus of occludin forms a coiled-coil region that binds to the scaffold proteins ZO-1,

specifically to the guanylate kinase like (GUK) domain of ZO-1 [75, 76], ZO-2 [77], and ZO-3 [78].

Occludin expression correlates with barrier properties. Overexpression of occludin in Madin-Darby Canine kidney cells (MDCK) causes an increase in trans-epithelial resistance but surprisingly not a decrease in solute flux. Truncation of the carboxyl tail causes an increase in permeability and tight junction disorganization [79-81]. Likewise, in the BBB and BRB, high levels of occludin expression are associated with increased barrier properties of vascular beds [82].

Occludin was once thought to be the main sealing tight junction protein; however, current research suggests this protein contributes to regulation of barrier properties, rather than acting directly as a structural protein in TJs. Mutations in occludin have recently been associated with microcephaly (small head size), brain calcification, polymicrogyria (excessive folding of the brain cortex), lack of motor development, reduced vision, and renal involvement in some families [83-85]. Knockout of occludin in mice has shown that occludin is not required for tight junction formation or basal intestinal epithelial barrier properties [86, 87]. These animals did, however, express several abnormalities such as brain calcification, male sterility, inability for female mice to nurse, and gastric epithelial hyperplasia [87, 88].

Recent studies show that occludin has a more complex function than originally thought, including the regulation of cell signaling, tight junction protein trafficking and cell growth. In these studies, specific occludin phosphosites and their role in barrier regulation and cell signaling have been identified [89, 90]. For example, phosphorylation of occludin at the threonine residues T403 and T404 by PKCη enhances TJ assembly and maintenance in epithelial cells [91]. In contrast, c-Src phosphorylation of occludin at the tyrosine residues Y398 and Y402 prevents its

association with ZO-1, leading to tight junction destabilization in epithelial cells [92]. In Caco-2 cells, phosphorylation of occludin at residue S408 by kinase CK2 causes occludin-occludin interactions, disassociation of ZO-1, and an increase of small cation paracellular flux via claudins -1 and 2-based pores [93].

In retinal endothelial cells and an ischemia reperfusion model, the activation of the vascular endothelial growth factor receptor 2 (VEGFR2) by VEGF induces occludin phosphorylation at Ser490, and promotes ZO-1 and claudin-5 endocytosis and endothelial permeability [65]. Previous studies in BREC and in rats showed that S490 occludin phosphorylation by PKCβ leads to occludin ubiquitination, endocytosis and degradation, along with an increase in retinal endothelial permeability [74, 94]. Collectively, these studies reveal that post-translational modifications of occludin regulate barrier properties in retinal endothelial cells, through TJ protein endocytosis. The TJ protein occludin, while not required for junction assembly, appears to act as a regulator of barrier properties.

Additionally, recent work revealed a role for occludin in cell growth regulation. Phospho-specific antibodies detected a surprising population of occludin in centrosomes, along with an increase in Ser490 phosphorylation during mitosis [95, 96]. Mutation of Ser490 to alanine retarded MDCK cell growth and prevented both VEGF-induced proliferation and tube formation in cell culture and neovascularization *in vivo* [96]. A second phosphorylation site, located in the coiled-coil domain, also contributes to proliferation and tight junction formation. Recent studies reveal that MDCK epithelial cells undergo post-contact proliferation, which is necessary for proper epithelial maturation and tight junction formation. Inhibition of Ser471 phosphorylation by either an alanine mutation or inhibition of the G-protein regulated kinase that targets this site, prevents this epithelial maturation and blocks tight junction formation, with no effect on

adherens junction formation [97]. Together, these data show the complex role of occludin in barrier regulation, cell growth, angiogenesis, and permeability transport regulation.

1.4.2.2 Tricellulin

Tricellulin (MARVELD2) is a ~64kDa transmembrane protein localized at the tricellular contacts (TCs), region where the corners of three epithelial or endothelial cells meet [98, 99]. Like occludin, tricellulin has a long C-terminus tail but they only share about a 32% homology [100]. Interestingly, tricellulin-deficient mice as well as occludin-deficient mice develop hearing loss [100-102].

A closer look at tricellulin organization in both cells and animals shows that loss of occludin alters tricellulin localization [101, 103]. In the absence or downregulation of occludin, tricellulin was observed to localize at bicellular tight junctions rather than at tricellular tight junctions. These results might suggest that in the absence of occludin, tricellulin can compensate for occludin in the formation of bicellular tight junctions.

Overexpression of tricellulin in fibroblasts shows that tricellulin is localized throughout the plasma membrane and does not concentrate at cell-cell contacts like claudins. However, when claudin-1 or -3 are overexpressed in fibroblasts tricellulin localize at cell-cell contacts [103]. These data indicate that claudins and occludin play a regulatory role in tricellulin's organization at the tricellular tight junctions. Additionally, studies in epithelial cells show that the angulin family proteins comprised of angulin-1/lipolysis-stimulated lipoprotein receptor (LSR), angulin-2/immunoglobulin-like domain-containing receptor (ILDR1), and angulin-3/ILDR2 recruit tricellulin to the TCs [104].

While the majority of the studies on tricellulin have been in epithelial cells, work done by the Furuse lab revealed that tricellulin is present in the endothelial cells of the BBB and iBRB,

but not in other tissues composed of endothelial cells [99]. This observation suggests the importance of angulins and tricelllulin in the BBB and BRB.

1.4.2.3 MARVELD3

MARVELD3, the third member of the MARVEL family, is also a tetraspan protein but lacks the carboxyl tail found in occludin and tricellulin [105]. The role of MARVEL D3 in the BBB and BRB remains unclear.

1.4.3 Junctional-Associated Adhesion Molecules (JAMs)

JAMs are single-span proteins that belong to the immunoglobulin superfamily because they contain at least one IgG domain at their extracellular N-terminus [106, 107]. The cytoplasmic tails of JAMs contain a PDZ binding sequence that interacts with the PDZ domain of ZO-1. Like the second extracellular loop of claudins, the extracellular domain of JAMs can associate with JAMs from adjacent cells (trans-interaction) or in the same cell (cis-interactions) in a homophilic (same type of JAM) or heterophilic (different type of JAM) manner [108, 109]. In contrast to claudins, JAMs do not form tight junction strands, instead, they facilitate junctional assembly.

JAMs are the first TJ proteins to appear during epithelial junction assembly. JAM-A co-localizes with AF-6 and Par3 at the intercellular junctions of the RPE. Their expression in fibroblasts promotes ZO-1, AF6, and occludin localization at cell-cell contacts, leading to barrier formation [109, 110].

In the cerebral and retinal endothelium, JAM-A is the predominant JAM isoform [111, 112]. The exact role JAMs play in the regulation of paracellular barrier and transport of the BBB and BRB remain unclear; however, recent studies suggest a role of JAM in the movement of leukocytes through the wall of blood vessels, diapedesis. JAM-A expression on monocytes

facilitates its movement across the BBB [113], while JAM-A knockout and endothelial specific JAM-A deficient mice, exhibit impaired neutrophil transmigration [114]. Further, although JAM-C and JAM-B are expressed at the junctions of the RPE, JAM-C deficient animals showed increased JAM-A expression and enhanced retinal vascularization [115, 116], suggesting a role for JAMs in retinal angiogenesis.

Together, these data indicate that JAMs contribute to several mechanisms, including cell migration, immune cell infiltration and angiogenesis in the BBB and BRB. However, further studies are needed to determine the exact role of the different JAMs in the BBB and BRB formation and maintenance.

1.4.4 Zonula Occludens (ZO)

Zonula occludens (ZO) are large (>200 kDa) scaffold proteins that connect transmembrane proteins with the cytoskeleton and play an important role in tight junction organization. ZOs form part of the MAGUK family, and there are 3 isoforms: ZO-1, -2, and -3 [78, 117, 118].

ZO proteins contain three PDZ domains which allow the interaction between proteins that have a PDZ domain and the interaction for proteins with a PDZ binding motif domain like claudins and JAMs [56, 75, 119]. Further, occludin interacts with a Src homology 3, guanylate kinase GUK homology domain [76]. ZO proteins serve as links between the junctional complexes and the cytoskeleton by their ability to bind actin, α-catenin, and afadin (AF6) [120-122], thus promoting TJ protein assembly at cell-cell contacts.

ZOs play a critical role in tight junction formation. In the absence of all ZO isoforms, formation of TJs is impaired and claudins fail to polymerize, but no effects on the adherens junction are observed [123, 124]. Additionally, ZO-1 deficient mice are embryonic lethal and

express defects in the vasculature and neural tube development [125]. Several studies focusing on pathologies disrupting the BBB and the BRB have revealed that loss/reduction of ZO-1 correlates with an increase in paracellular permeability [65, 126], thus supporting ZO-1 as a marker of leakiness of endothelial barriers. ZO-2 and ZO-3 are also expressed in BBB and BRB; however, their specific roles in endothelial barriers have not been addressed yet.

1.4.5 Adherens Junctions (AJs)

AJs play a critical role in cell-cell adhesion, cell polarity, contact inhibition, and paracellular transport regulation. The AJ of the iBRB includes vascular endothelial (VE)-cadherin of the cadherin superfamily. VE-cadherin is a transmembrane Ca^{2+}-dependent cell adhesion protein with a conserved cytoplasmic tail that binds to β-catenin. *In vivo* studies of transgenic mice deficient in VE-cadherin, which exhibit embryonic lethality by E9.5, have demonstrated that VE-cadherin is required for proper lumen formation and maintenance of newly formed vessels [127]. VE-Cadherin has an intimate relation to VEGF receptor and is a major control point for regulation of barrier development, paracellular permeability and growth control (for complete reviews, see: [47, 128, 129]).

1.5 Pro-Barrier Mechanisms

Maintenance and regulation of the vascular endothelial cell junctional complex is critical for normal barrier function of barriers of the CNS that help maintain a proper neuronal environment. Studies focusing on the mechanisms of barrier formation, maintenance, and disruption have been of particular interest to understanding development of the BBB and the BRB and identifying a means for therapeutic intervention for diseases ranging from brain tumors and dementia to blinding eye diseases. Research has revealed increasingly that small guanosine triphosphatases (GTPases) play a critical role both in barrier formation and disruption. Recent

studies have shed light on a direct role for small GTPases in barrier properties, assembly of adherens and tight junctions and prevention of barrier loss caused by permeabilizing agents such as inflammatory cytokines and growth factors. The discovery of the EPAC-Rap1 pathway has revealed a molecular mechanism by which cAMP signaling can promote barrier properties in the BBB and BRB and restore barrier properties after barrier breakdown.

1.5.1 Small GTPases

Small GTPases, like Rap1 and RhoA, have been identified as key regulators of both barrier formation and barrier disruption that promote signal transduction pathways that alter the junctional complex and regulate vascular permeability [130-132]. Small GTPases are hydrolase enzymes that bind and, over time, hydrolyze guanosine triphosphate (GTP) into guanosine diphosphate (GDP). These small GTPases serve as molecular switches that cycle between an active GTP-bound state and an inactive GDP-bound state. When in the GTP-bound form, GTPases undergo a conformational switch, which allows them to relay signals in the cell via interacting with and activating specific effector proteins [133]. Further, the activity of small GTPases is regulated by additional proteins, including guanine nucleotide exchange factors (GEFs) and GTPase-activating proteins (GAPs). GEFs promote signaling activity of small GTPases by facilitating the release of bound GDP, thereby allowing GTP to bind, while GAPs promote the hydrolysis of bound GTP, thus inactivating downstream signaling transduction. Additionally, guanosine nucleotide dissociation inhibitors (GDIs) regulate the activity of small GTPases by sequestering GDP-bound small GTPases in the cytoplasm and protecting them from degradation [134]. Small GTPases, including RhoA, Rac1, and Cdc42, can participate in both barriergenesis and barrier loss in response to a variety of extracellular cues and their

corresponding GEFs and GAPs. Recent research has helped to elucidate the role of small GTPases in barrier properties in the BBB and BRB.

1.5.1.1 The Ras Superfamily of Small GTPases

The Ras superfamily of small GTPases is composed of more than 154 proteins that are divided into the following 6 main families: Rheb, Ran, Arf, Rho, Ras, and Rab [135, 136]. Each GTPase family has a unique role in cell signaling. Broadly considering the Ras superfamily, the Ras homolog enriched in brain (Rheb) regulates the mTOR pathway. The Ras-like nuclear (Ran) GTPase family is the most abundant in the cell and is involved in nuclear transport of both RNA and proteins. The ADP-ribosylation factor (Arf) GTPase family contributes a role in vesicular transport. Further, the Ras-like proteins in the brain (Rab) GTPase family, like the Arf GTPases, regulate vesicle trafficking, including endocytosis and exocytosis. The Ras homologous (Rho) GTPase sub-family is involved in regulating cytoskeletal dynamics in cell shape and cell migration. The Ras sarcoma (Ras) GTPase family contributes to several cell signaling pathways such as transcription, cell differentiation, proliferation, and oncogenesis. For complete reviews, see refs [136-139].

GTPases are involved in both endothelial barrier formation and disruption. Rho GTPase family members, such as Cdc42 and Rac1, promote endothelial barrier properties and are associated with downregulation of RhoA [132, 140, 141]. On the other hand, hyperactivation of RhoA and its downstream effectors, Rho-associated kinases (ROCK1 and ROCK2), and phosphorylation of myosin-regulatory light chain-2 (MLC2) are associated with endothelial barrier disruption [142-144]. Moreover, the Ras GTPase family member, Rap1 and its GEF, EPAC, are involved in several cellular adhesion mechanisms such as cell-cell adhesion and cell-

extracellular matrix (ECM) adhesion [145]. Importantly, the interaction of EPAC1-Rap1 signaling with endothelial specific rasip1 promotes endothelial barrier function [131, 146].

1.5.1.2 Rho GTPases in Endothelial Barrier Regulation

Rho GTPases are a family of small GTPases (~20 – 25kD) involved in regulating cytoskeletal dynamics. Three of these Rho GTPases are Cdc42 (Cell division control protein 42), Rac1 (Ras-related C3 botulinum toxin substrate 1), and RhoA (Ras homolog gene family member A) [147]. Broadly, Cdc42 promotes filopodia formation and Rac1 regulates lamellipodia formation, both protrusive actin-based structures, whereas RhoA regulates stress fiber formation and other actomyosin contractile arrays [148]. Each of these Rho GTPases is ubiquitously expressed and possesses distinct functions in the assembly and homeostasis of endothelial cell-cell junctions, which are determined by tight spatiotemporal regulation of their activation state by GEFs and GAPs.

Factors such as tumor necrosis factor alpha (TNF-α), thrombin, vascular endothelial growth factor (VEGF), and other vasoactive agents lead to activation of RhoA and there is broad consensus that RhoA activation contributes to barrier disruption [149, 150]. Activation of RhoA in endothelial cells causes the formation of stress fibers, which are associated with disruption of the inter-endothelial junctions, thus increasing paracellular flux (Figure 1.4.A) [151, 152]. Rho GTPases also regulate the inter-endothelial junctions that form barriers of the CNS. Retinas under ischemic conditions in diabetic retinopathy express elevated levels of VEGF, which contributes to retinal vascular permeability. Studies in retinal endothelial cells, show that VEGF induces activation of RhoA and its downstream effectors (Rho-associated kinases) ROCK1 and ROCK2 [153]. *In vivo* studies of diabetic rat models show hyperactivation of RhoA and

localization of RhoA and ROCK at the vascular retinal endothelial cells [154]. These data demonstrate the relevance of hyperactivation of RhoA in barrier disruption.

However, RhoA has a dual role and has been reported to be important in AJ assembly [155]. Further, RhoA may contribute to both barrier loss and barrier induction dependent on the location of RhoA and the associated GEF. An elegant study using live imaging reveals that RhoA may contribute to TJ assembly associated with p114RhoGEF and TJ disassembly associated with GEF-H1 depending on the location of the RhoA being activated [156].

Other members of the Rho GTPases also demonstrate dual roles in junction assembly and disassembly. Cdc42 and Rac1 have an important role in regulating the assembly of endothelial and epithelial cell junctions [157, 158]. Activation of Cdc42 promotes binding to IQGAP1, a scaffold protein that binds β-catenin and actin, leading to assembly of adherens junctions in cells [159-161]. However, in endothelial cells, some studies reveal that VEGF activation of Rac1 promotes internalization of the vascular endothelial cadherin, VE-cadherin, leading to an increase in paracellular flux [162, 163].

Together these data show the complexity and multifunctional roles that the Rho GTPases have in regulating the junctional complex and paracellular flux of endothelial cells, in both the peripheral vasculature and CNS barriers. Activation of RhoA may contribute to junction assembly based on the location of RhoA in the cell, and the specific GEF involved in its activation.

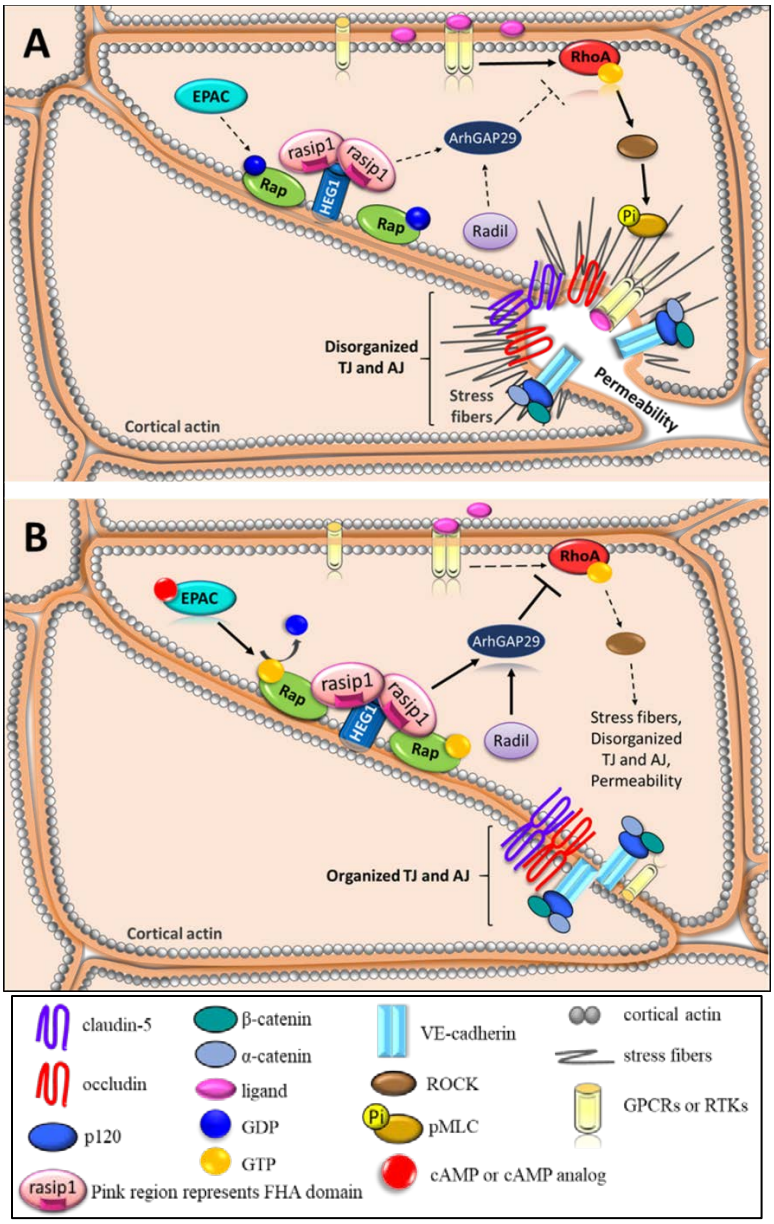

Figure 1.5 Small GTPases in Endothelial Barrier Regulation. Schematic, as seen from above, represents disorganized junctional complex versus organized junctional complex. **A)** Pro-inflammatory cytokines or growth factors bind and activate their corresponding GPCRs or RTKs and activate the RhoA/ROCK/pMLC signaling pathway which promotes formation of stress fibers and disrupts junctions causing an increase in paracellular permeability. **B)** Activation of EPAC via cAMP or cAMP analog activates Rap by promoting GTP exchange. Rasip1 localizes to the junctional complex by binging HEG1 and interacting with active Rap at the cell border. Rasip1 can dimerize via its RA domain and bind two Rap molecules at the plasma membrane. The active Rap-rasip1 complex and radil activates ArhGAP29, which inhibits RhoA activity and prevents loss of barrier. Downregulation of RhoA reduces stress fiber formation. **Abbreviations: ROCK: Rho-associated kinases, pMLC: Phospho Myosin light chain, p120: catenin p120, ligand: can be pro-inflammatory cytokine or growth factor, GPCR: G-protein-coupled receptors, RTKs: Receptor Tyrosine Kinases, FHA: Forkhead-associated domain, HEG1: Heart of Glass 1, RA: Ras-associated domain, TJ: Tight Junctions, AJ: Adherens Junctions.** (Figure from Ramos and Antonetti, 2017)

However, both inflammatory factors and growth factors regulate RhoA activity to promote breaks in the junctional complex and increase paracellular permeability.

1.6 Cyclic AMP Second Messenger for Barrier Regulation

The second messenger cyclic adenosine monophosphate (cAMP) plays an important role in multiple cell signaling pathways. Activation of G-protein-coupled receptors (GPCRs) leads to the activation of adenylyl cyclase which catalyzes ATP into cAMP. The effectors of cAMP include the classical protein kinase A (PKA) and cyclic nucleotide gated ion channels. In 1998, the Bos lab discovered an additional cAMP downstream target called exchange-protein-directly activated by cAMP (EPAC) that had a binding domain for the Rap1 small GTPase [164, 165].

1.6.1 EPAC, a GEF for Rap

The EPACs are guanine-nucleotide-exchange factors (GEFs), which activate Rap small GTPase proteins. Two isoforms of EPACs exist in mammals, the broadly expressed EPAC1 (RapGEF3 in human), and EPAC2 (RapGEF4 in human), which is expressed in the brain, kidney, and pancreas (Figure

1.6.A) [145]. The EPACs are multidomain proteins consisting of a C-terminal catalytic region and an N-terminal regulatory region [166]. The C-terminal catalytic region contains the following domains: the cell division cycle 25 (CDC25), homology domain (CDC25HD) which has the GEF activity specific for Rap; a protein interaction motif called Ras-associated (RA) domain; and a Ras exchange motif (REM), which is a region found in Ras and Rap GEFs involved in stabilization of the active GEF conformation [167]. The N-terminal regulatory region contains a Dishevelled, Egl-10, Pleckstrin (DEP) domain, which is involved in membrane attachment and the cyclic-nucleotide-binding (CNB) domain to which cAMP binds [164]. EPAC2 has an additional cAMP-binding domain, CNB, on its N-terminus [168]. EPACs have a

cAMP-binding site similar in sequence to the cAMP-binding domain from PKA and are also activated by cAMP [164]. When cAMP binds to the EPAC regulatory region, it allows the auto-inhibitory inactive state to change to an active state and bind to the small GTPases in the Rap family (Figure 1.6.B). Once EPAC is bound to Rap, it can exchange GDP for GTP, thus activating the Rap proteins (Figure 1.6.C) [169].

Gene deletion studies revealed a role for EPAC in mouse metabolism and behavior. Interestingly, *in vivo* studies show that global EPAC1 knockout is not lethal; however, the global EPAC knockout mice express a variety of phenotypes. Kai et al. show that the EPAC1 null mice have B-cell dysfunction, impaired glucose tolerance, obesity, and insulin resistance [170]. On the contrary, Yan et al. show that their EPAC1 null mice are resistant to high-fat diet-induced obesity, hyperleptinemia, and glucose intolerant [171]. In a 2012 study, EPAC1 and EPAC2 null animals were generated, as well as double knockout EPAC1/2 mice [172]. In the animals with a single isoform EPAC1 or EPAC2 gene deletion, no abnormalities were observed; however, in the double knockout mice, severe deficits of spatial learning and social interactions were observed.

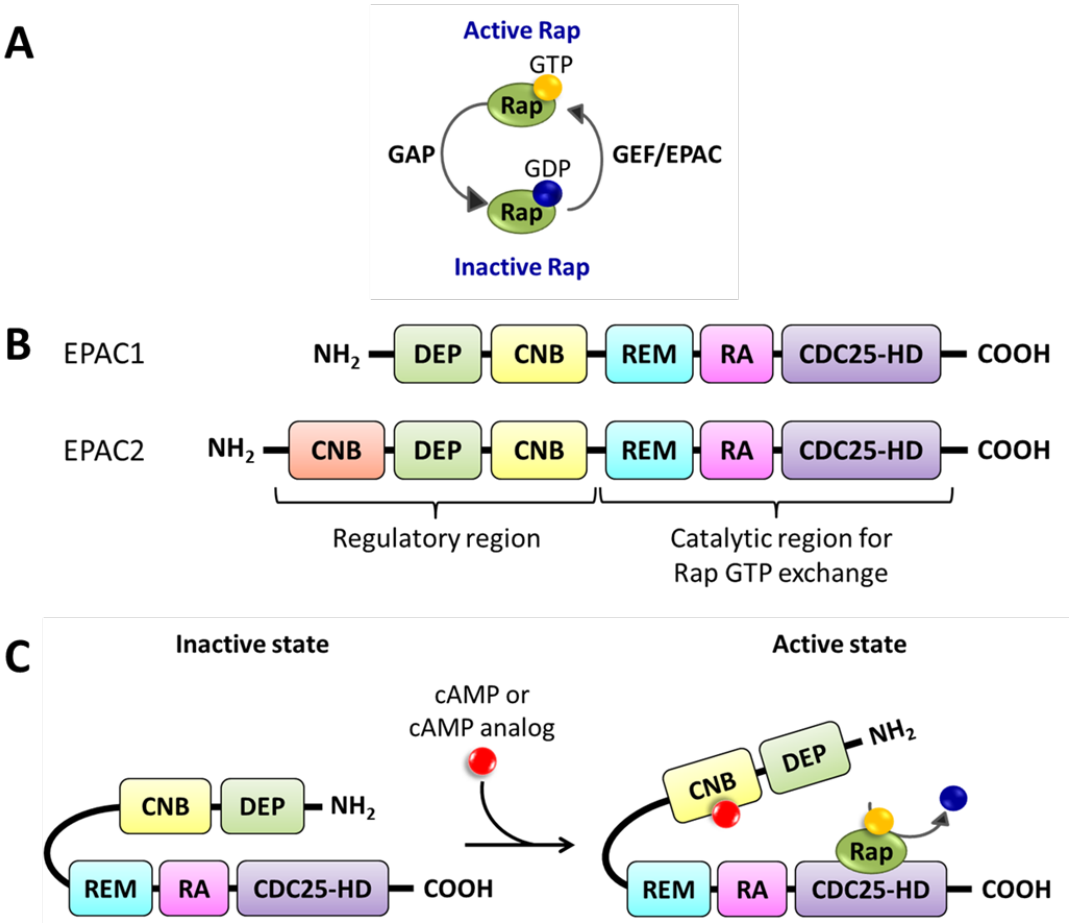

Figure 1.6 EPAC Structure and Activation via cAMP. **A)** Rap proteins are GTPases that hydrolyze GTP into GDP. GAPs increase the rate of GTP hydrolysis leading to GDP bound Rap, the inactive state. On the other hand, GEFs, such as EPAC, facilitate the exchange of GDP for GTP promoting the GTP bound Rap, the active state. **B)** EPAC has two known isoform proteins, EPAC1 and EPAC2, encoded in separate human genes, RAPGEF3 on chromosome 12 and RAPGEF4 on chromosome 2, respectively. EPAC's catalytic region contains the CDC25-HD, RA, and REM domains. The regulatory region contains the CNB and DEP domains. The EPAC2 protein contains an additional CNB region. **C)** EPAC exists in an autoinhibitory inactive state with the regulatory region suppressing the guanine nucleotide exchange (GEF) function of the catalytic region. The binding of cAMP to the CNB domain, located in the regulatory region, promotes a conformational change from an inactive to an activate state. The active EPAC binds Rap GTPases and facilitates the exchange between GDP to GTP. **Abbreviations: EPAC: exchange factor directly activated by cAMP, GAP: GTPase-activating proteins, GEF: guanine nucleotide exchange factors, RAPGEF: Rap guanine nucleotide exchange factor, CDC25-HD: cell division cycle 25 homology domain, RA: Ras-associated domain, REM: Ras exchange motif, DEP: Disheveled, Egl-10, and Pleckstrin domain, CNB: cyclic nucleotide-binding domain.** (Figure from Ramos and Antonetti, 2017)

1.6.2 The Role of Rap1 in Endothelial Cell Barrier

The Ras-related protein 1 (Rap1) is a small GTPase in the Ras family, known for its role in cell adhesion and cell junction regulation. Vertebrates express two highly homologous Rap1 isoform proteins, Rap1a and Rap1b, which are encoded by different genes [173]. Additionally, they express Rap2, which has approximately a 60% sequence homology to Rap1 [174, 175]. Rap2 has three isoforms (Rap2a, Rap2b, and Rap2c) and their distinct functions have not been well studied [176]. Rap1 activation is regulated by several Rap1-specific GEFs. These are CD-GEF1, C3G, PDZ-GEF1, and the EPACs discussed above [136, 177].

Rap1 gene deletion studies reveal that Rap contributes to a number of cell functions in vascular endothelial cells, including vasculogenesis and angiogenesis. Rap1 promotes VEGF receptor (VEGFR2) activation and is required for angiogenesis by a mechanism involving the integrin αvβ3 [178]. Rap1a and b isoforms can compensate for one another but recent work has also shown that the isoforms have distinct functions [179-181]. To study the differences of the Rap1 isoforms, mouse knockouts of each Rap1 isoform were generated. Mice with Rap1a knockout are viable and have no size difference in comparison to wild type mice. These animals exhibited defective leukocyte adhesion, altered myeloid cell function, and partial embryonic lethality [179, 182].

Global Rap1b knockout in mice leads to about 80% embryonic lethality between embryonic (E) day 13.5 and 18.5. This suggests that Rap1b is not necessary for vasculogenesis, which occurs from E7.5 to E10.0, but rather, it is necessary for further maturation of the vasculature [183]. Post-mortem analysis revealed that Rap1b null mice manifested abdominal, vascular and cranial hemorrhage due to a platelet defect. The Rap1b viable mice were smaller in

size and exhibited prolonged bleedings during tail bleeds [184]. Further studies of the Rap1b null mice identified defective angiogenesis, which led to a retardation in retinal neovascularization. Additionally, lung endothelial cells from the Rap1b null mice demonstrated defective endothelial migration and proliferation, due to impaired MAPK signaling. The lung endothelial cells from Rap1b null mice have a decreased response to growth factors VEGF and basic fibroblast growth factor (bFGF) [180].

Double Rap1a and Rap1b knockout leads to complete embryonic lethality by E10.5. The endothelial and hemangioblast specific double Rap1a and b knockout achieved by expression of Cre under Tie2 is completely lethal by E15.5. These animals expressed a leaky vasculature and engorged perineural vessels [181]. Interestingly, mice are viable with at least one allele of Rap1b but not with just one allele of Rap1a. These data together suggest that the Rap proteins are not required for early gastrulation development but are required for further development of the embryo. The data also suggest that Rap1b contributes a critical role in endothelial vasculature in comparison to Rap1a.

1.6.3 EPAC-Rap1 Signaling Pathway in Endothelial Cell Barrier Induction

Investigations on the cellular role of the EPAC-Rap1 signaling pathway have been facilitated by the development of cAMP analogs specific for EPAC, allowing for discrimination between PKA-independent cellular mechanisms and EPAC-dependent mechanisms. Popular EPAC selective cyclic AMP analogs used in cell culture and *in vivo* are 8-(4-chloro-phenylthio)-2´-O-methyladenosine-3´,5´-cyclic monophosphate (8-pCPT-2´-O-Me-cAMP) and the improved membrane permeable 8-pCPT-2´-O-Me-cAMP-AM, which contains an acetoxymethyl group (AM) to mask the negative charge from the phosphate group [185, 186]. These studies have elucidated the role of EPAC in integrin-mediated cell adhesion, E-cadherin-mediated cell

adhesion, and cell signaling. Studies performed using human umbilical vein endothelial cells (HUVEC) show that EPAC activation leads to the recruitment of VE-cadherin to the cell border and formation of long, linear and continuous adherens junctions [187]. This VE-cadherin-mediated junctional organization in HUVEC results in a decrease in solute flux [188]. Additional observations of EPAC activation included reduction of stress fiber formation and defined cortical actin at the cell periphery. Interestingly, actin rearrangements after EPAC activation are not VE-cadherin mediated [188, 189].

Activation of EPAC in endothelial cells requires Rap activity for barrier induction. Addition of 8-pCPT-2´-O-Me-cAMP for EPAC stimulation leads to activation of Rap1 associated with enhanced endothelial barrier properties and induces a continuous and linear distribution of VE-cadherin in both HUVEC and rat mesenteric vessels [189, 190]. The effect of EPAC activation on barrier properties requires Rap1 activity as silencing of Rap1 in HUVEC blocked 8-pCPT-2´-O-Me-cAMP-induced barrier function, as measured by trans electrical resistance [191]. Cullere et al. revealed that Rap1 localizes at the cell-cell junctions and inhibition of endogenous Rap1 disrupts the junctional complex [187]. Additionally, afadin (AF-6), a scaffold protein that binds to actin filaments and adhesion proteins, localizes at the cell periphery after EPAC activation and may serve as a molecular link between EPAC/Rap1 and the junctional complex [192, 193].

The EPAC-Rap1 pathway can prevent the action of permeabilizing agents on vascular endothelial cells. Activation of EPAC blocks thrombin-induced permeability by down regulating RhoA activity [187]. In HUVEC, EPAC1 activation reverses the transendothelial resistance decrease caused by both TNF-α and the transforming growth factor (TGF-β). Additionally, knockdown of EPAC1 alone induced a decrease in transendothelial resistance [194]. Moreover,

in vivo studies of the mesenteric microvasculature show that activation of the EPAC-Rap1 pathway via 8-pCPT-2´-O-Me-cAMP attenuates platelet-activating factor (PAF)-induced permeability as well as prevents PAF-induced VE-cadherin disorganization [190].

1.6.4 Active Rap1 Binds to Rasip1 in Endothelial Cells

In 2004, Mitin and colleagues identified ras-interacting protein 1 (rasip1) as a potential effector of Ras through a yeast two-hybrid screen. They showed that rasip1 contains a Ras-associating (RA) domain at the N terminus, which has a high sequence homology to AF-6, a known Ras/Rap effector as well as a scaffold intermediate protein that links the cytoskeleton to cell-cell junctions [195]. Additionally, rasip1 possesses a proline rich region like the Src homology 3 (SH3) domain binding motifs and a dilute (DIL) domain which is found in myosin V proteins involved in cargo loading during vesicle trafficking [195, 196]. Rasip1 expression is restricted to the vascular endothelium [197]. Rasip1 was identified as an endothelial-specific gene in an endothelial cell-specific transcriptome analysis of publicly available microarrays [198] and both whole mount embryo *in situ* hybridization and immunofluorescence reveals Rasip1 expression is restricted to the vascular endothelium [131, 199].

Xu et al. performed *in vivo* studies showing that rasip1 is restricted to the vascular endothelial cells of both mice and frogs and has an important role in vasculogenesis and angiogenesis. In mice, rasip1 is first observed at E7.0 in the parietal yolk sac and its expression is observed all the way until adulthood, implying that rasip1 is important in vasculogenesis and vessel maintenance [199]. Moreover, rasip1 interaction with GTPases in peripheral vessel endothelial cells regulates tubulogenesis and lumen formation. In this study, rasip1 null mice failed to form lumens in all blood vessels and were embryonic lethal at E10.5 displaying growth retardation, hemorrhage, and widespread edema [197]. Confocal microscopy of angioblasts

showed disruption in cell polarity due to mislocalization of Par3 and failure of junctional protein localization at the cord periphery. Additionally, Xu and colleagues showed that rasip1 and Rho GTPase-activating protein 29 (ArhGAP29) regulate endothelial cell architecture and tube formation. Endothelial cells depleted of either rasip1 or ArhGAP29 show increased activity of RhoA/ROCK/myosin II and decreased Cdc42 and Rac1 activity [197]. This was the first observation describing rasip1 as a downregulator of Rho signaling. Recently, rasip1 conditional gene deletion at different developmental time points [200] showed that rasip1 is essential for vessel formation and maintenance at different embryonic time points. Additionally, rasip1 is required for angiogenesis. Retinas of rasip1 null mice at P6 show a decrease in vessel growth, impaired lumen formation, and poorly organized capillary plexus [200].

An important contribution in understanding the function of rasip1 in endothelial cells was the identification of rasip1 as a Rap1-effector involved in endothelial barrier properties [146]. Activation of EPAC activates Rap1, and active Rap1 interacts with rasip1. Rasip1, together with ras-associated and dilute domain-containing protein (radil), recruit ArhGAP29, which in turn downregulates RhoA activity (Figure 1.4.B) [146]. Wilson et al, revealed that rasip1 mediates vascular endothelial junction stability through EPAC1-Rap1 signaling *in vivo*. Rasip1 null mice demonstrate embryonic lethality at E10.5 and the embryos displayed collapsed vessels, multifocal hemorrhage, edema, and smaller vessels [201]. One unique observation Wilson and colleagues made was that rasip1 null mice formed primitive vessel tubes that allowed the circulation of erythrocytes, but due to impaired cell-cell adhesion, these early vessels collapsed. They also observed no difference in cell motility between rasip1-deficient endothelial cells and controls.

HUVEC siRNA experiments further support a role of rasip1 in regulating vascular permeability. Additionally, rasip1 localizes at the cell borders, promotes cortical actin assembly, and interacts with Rap1 in an EPAC1-dependent manner. Knockdown of either Rap1 or EPAC1 in HUVEC prevents rasip1 localization at the cell borders and knockdown of either rasip1, EPAC1, or Rap1 leads to disorganization of F-actin at the periphery of cells. Together these data provide strong evidence for the role of EPAC1-Rap1-rasip1 signaling in regulating endothelial permeability.

Rasip1 transiently localizes to endothelial cell-cell junctions in a Rap-mediated manner [201]. A recent study showed that the localization of rasip1 to the endothelial cell-cell junctions occurs by anchoring to Heart of Glass 1 (HEG1), a transmembrane receptor involved in cardiovascular development [202]. Silencing HEG1 reveals that HEG1 is required for rasip1 localization at cell junctions. Mutational studies identified 9 amino acids (aa) from 1327-1335 in HEG1 that bind to rasip1 at the Forkhead-associate domain (FHA), aa 266 – 550. Deletion or mutations in FHA or HEG1's 9 aa region inhibits the interaction between rasip1 and HEG1 and prevents rasip1 inhibition of Rho signaling [202]. Furthermore, HEG1 knockdown, like rasip1 knockdown, shows an increase in Rho signaling activity and HEG1 rescue assays inhibit Rho signaling. These data suggest that HEG1 facilitates the translocation of rasip1 to cell junctions where it can bind to active Rap1 and downregulate Rho signaling (Figure 1.4.B).

Protein crystallography studies and modeling suggest that rasip1 forms a dimer and each Ras-associated (RA) domain can bind to one molecule of either Rap or Ras [203]. Therefore, a rasip1 dimer could bind to two Rap proteins (Figure 1.4.B) [203]. An interesting concept by Rehmann and Bos suggests that rasip1 and radil could potentially dimerize with each other since both proteins show a 30% sequence homology in the their RA domain [202, 204]. They propose

that the potential dimerization between rasip1 and radil could explain how ArhGAP29 is recruited since both radil and ArhGAP29 possess a PDZ domain and previous studies have shown coimmunoprecipitation of radil and ArhGAP29 [205].

1.7 Objectives

It is clear from the studies described above that the small GTPase, Rap1, and the GEF, EPAC, contribute to barrier properties in endothelial cells. However, the role of the EPAC-Rap1 signaling pathway in barriers of the CNS has not been examined in detail. The goal of this thesis is to investigate the ability of the EPAC-Rap1 signaling pathway to restore barrier properties and block permeability induced by permeabilizing agents, as well as to identify novel targets downstream of VEGF signaling. Therapeutically targeting small GTPases may yield specific opportunities to restore barrier properties of the BBB and BRB, preventing or limiting disease pathology for a host of diseases that involve brain or retinal edema. This dissertation contains two data chapters, followed by a conclusion and future directions chapter. The content of each data chapter is briefly outlined below.

Chapter 2: *EPAC-Rap1 Signaling Restores the Blood-Retinal Barrier after Vascular Endothelial Growth Factor*

In this chapter, the hypothesis that activation of the EPAC-Rap1 signaling pathway antagonizes VEGF signaling and restores barrier properties in retinal vascular endothelial cells is addressed. Here, I demonstrate that activation of EPAC via the cAMP analog 8-pCPT-2´-O-Me-cAMP-AM can block, and importantly reverse, VEGF and TNF-α-induced permeability in retinal endothelial cells and *in vivo* in the retina. Silencing of the Rap1b isoform induces an increase in basal endothelial cell permeability. Further, VEGF does not have an additive increase in permeability, suggesting that VEGF signaling may act, in part, through inhibition of the Rap1

pathway. Immunofluorescence staining of tight junctions (ZO-1, occludin, and claudin-5) shows that activation of EPAC prevents the VEGF-induction of tight junction barrier disorganization that is associated with VEGF-induced permeability. The combined *in vitro* and *in vivo* data suggest that EPAC-Rap1 signaling plays an important role in regulating endothelial paracellular flux by recruiting, organizing, and stabilizing the inter-endothelial adherens junctions and tight junctions.

Chapter 3: *Elucidating the molecular mechanism of aPKC regulation of VEGF-induced retinal vascular endothelial permeability*

In this chapter, I address the hypothesis that VEGF regulates retinal endothelial permeability at least in part via protein phosphorylation changes downstream of aPKC. Mass spectrometry-based phosphoproteomics were utilized to analyze phosphorylation changes induced by VEGF and reversed by an aPKC inhibitor. In these studies, 1,724 proteins were identified and of these 107 phosphoproteins showed a 25% phosphorylation change and were repeated in more than one mass spectrometry analysis. Bioinformatics analysis of the 107 phosphoproteins identified a protein-protein interactive subnetwork consisting of EPAC, rasip1, and Rap1.

CHAPTER 2

EPAC-Rap1 Signaling in Blood-Retinal Barrier Maintenance and Restoration*

2.1 Abstract

Increased retinal vascular permeability contributes to macular edema, a leading cause of vision loss in eye pathologies such as diabetic retinopathy (DR), age-related macular degeneration (AMD), and central retinal vein occlusions. Pathological changes in vascular permeability are driven by growth factors such as vascular endothelial growth factor (VEGF) and pro-inflammatory cytokines such as tumor necrosis factor-α (TNF-α). Understanding pro-barrier mechanisms that block vascular permeability and restore the blood-retinal barrier (BRB) may lead to novel therapies. The cAMP-dependent guanine nucleotide exchange factor, EPAC, promotes exchange of GTP of the small GTPase, Rap1. Rap1 enhances barrier properties in human umbilical endothelial cells by recruiting Rasip1, which inhibits RhoA and promotes adherens junction assembly. In this study, we hypothesized that the EPAC-Rap1 signaling pathway regulates the tight junction complex of the blood-retinal barrier and can restore barrier properties after cytokine induced permeability. Here, we show that stimulating EPAC or Rap1 activation can prevent and reverse VEGF and/or TNF-α induced permeability in cell culture and *in vivo*.

**Note: This chapter has been submitted to JBC for publication and it is currently under review.*

In addition, activation of EPAC inhibits VEGF receptor (VEGFR) signaling through the Ras/MEK/Erk pathway. We show that Rap1B knockdown or an antagonist for EPAC increases endothelial permeability and VEGF has no additive effect, suggesting a common pathway. Additionally, GTP-bound Rap1 promotes tight junction assembly and loss of Rap1B leads to loss of junctional border organization. Collectively, our results indicate that the EPAC-Rap1 pathway helps maintain basal barrier properties in the retinal vascular endothelium, and activation of the EPAC-Rap1 pathway represents a potential therapeutic strategy to restore the BRB.

2.2 Introduction

The retinal vasculature provides oxygen and nutrients to the inner retina and forms the inner blood-retinal barrier (iBRB) that helps maintain the retinal environment, allowing for proper neural function [25]. The BRB maintains strict regulation of vascular permeability through a continuous endothelium lacking fenestrations, has limited transcellular vesicles, and controls the flux through the intercellular spaces between endothelial cells through the formation of a well-developed junctional complex [41, 42].

Tight junctions (TJs) promote endothelial cell barrier properties by restricting the passage of molecules through the intercellular space (gate function) and conferring cell polarity by preventing lateral diffusion of lipids and proteins in the plasma membrane (fence function) [35]. Over 40 proteins make up the TJs that are subdivided into transmembrane and scaffolding proteins [129]. Important retinal endothelial cell transmembrane proteins include, but are not limited to, occludin and claudin-5 along with scaffolding proteins zonulae occludentes such as ZO-1, 2 and 3, which connect the TJ to the actin cytoskeleton. Eye pathologies that result from

elevated levels of permeabilizing agents such as vascular endothelial growth factor (VEGF) and pro-inflammatory cytokines like TNF-α exhibit increased retinal vascular permeability, which occurs at least in part by disrupting TJ organization [23]. TJ disruption may be mediated by VEGF-induced occludin phosphorylation [89], or TNF-α-induced reduction in claudin-5 and ZO-1 expression [206] as well as currently uncharacterized mechanisms. Current medical therapies for macular edema involve intraocular injection of anti-VEGF agents, which demonstrate good effectiveness in approximately half of treated patients [207].

The second messenger 3´, 5´-cyclic adenosine monophosphate (cAMP) regulates several cell signaling pathways including barrier properties in endothelial cells [208, 209]. In addition to the well-studied cAMP effector protein kinase A (PKA) an additional cAMP effector was identified, named exchange-protein-directly activated by cAMP (EPAC) [164]. This exchange factor targets the small GTPase, Ras-associated protein (Rap), promoting exchange of GDP for GTP and activation of Rap [210]. Mammals express two isoforms of the EPAC protein, EPAC1 (RapGEF3), which is widely expressed, and EPAC2 (RapGEF4), which is prominently expressed in the brain and adrenal gland [211]. The Rap proteins are small GTPases in the Ras family involved in several cell-signaling mechanisms. Mammals express two Rap proteins from separate genes, Rap1 and Rap2, which share approximately 60% protein sequence homology [174, 175]. Rap1 is further divided into two highly homologous isoforms, Rap1A and Rap1B, which are encoded by different genes [173]. Rap2 has three isoforms (Rap2A, Rap2B, and Rap2C) and their functions have not been well characterized [176]. Vascular development requires Rap1 proteins, as vasculature conditional gene deletion of both Rap1A and Rap1B leads to complete embryonic lethality by E15.5 [181]. Interestingly, mice with Rap1A deleted and only one Rap1B allele are viable, whereas mice with Rap1B deleted and only one Rap1A allele are

not, suggesting a critical role for Rap1B in endothelial vasculature [181]. Active Rap1 proteins are known for their role in cell adhesion in leukocytes [184] and cell adherens junction regulation [212]. However, the relation of Rap to TJs is not well understood.

The development of EPAC-specific cAMP analogs, such as 8-(4-chloro-phenylthio)-2´-O-methyladenosine-3´,5´-cyclic monophosphate (8-CPT-2′-O-Me-cAMP) and the improved membrane permeable 8-pCPT-2´-O-Me-cAMP-AM (8CPT-AM), which contains an acetoxymethyl group (AM) to mask the negative charge from the phosphate group, has allowed investigation of the cAMP-EPAC-Rap1 pathway independent of PKA signaling. Studies focusing on the activation of EPAC-Rap1 signaling in endothelial cells such as human umbilical vein endothelial cells (HUVEC) have identified a role for EPAC/Rap in regulating barrier properties through cortical actin increase at the endothelial junctions [189], recruitment of junctional proteins such as VE-cadherin [213], and inhibition of the small GTPase, RhoA, known to be involved in permeability [187]. More recently it has been demonstrated that the interaction of Rap1 with the endothelial-specific effector, ras-interacting protein 1 (rasip1), promotes endothelial barrier function by recruiting Rho GTPase-activating protein 29, ArhGAP29, downregulating the activity of RhoA [146, 201]. However, very little is known about the role of the EPAC-Rap1 signaling pathway in endothelial cells that form barriers of the CNS such as the BRB.

In the present study, we demonstrate a role for EPAC-Rap1 signaling pathway in retinal vascular endothelial cells. We show Rap1B confers basal barrier properties to retinal endothelial cells and that pharmacologic activation of the EPAC-Rap1 pathway can prevent and restore BRB properties after both growth factor- and inflammatory factor-induced permeability. Further,

activation of EPAC-Rap1 signaling is shown to promote TJ organization and reduce paracellular permeability.

2.3 Methods

2.3.1 Reagents: The following reagents were purchased from Tocris Bioscience: the cAMP analog 8-pCPT-2-O-Me-cAMP-AM (8CPT-AM) specific for EPAC (catalog #4853), EPAC2 inhibitor (HJC 0350) 2,4-Dimethyl-1-[(2,4,6-trimethylphenyl) sulfonyl]-1H-pyrrole (catalog #4844), and EPAC inhibitor (ESI 09) α-[(2-(3-Chlorophenyl) hydrazinylidene]-5-(1,1-dimethylethyl)-β-oxo-3-isoxazolepropanenitrile (catalog #4773). Recombinant human VEGF165 was from R&D Systems (Minneapolis, MN).

2.3.2 Antibodies (Ab): The following antibodies were used for western blotting. Purchased from Cell Signaling: AKT rabbit polyclonal (pAb) (catalog #9272), phospho-AKT (Ser473) rabbit monoclonal (mAb) (catalog #4060), phospho-CREB (Ser133) rabbit mAb (catalog #9198). CREB rabbit mAb (catalog #9197), VEGFR2 rabbit mAb (catalog #2479), phospho-VEGFR2 (Tyr1175) rabbit mAb (catalog #3770), Erk1/2 rabbit pAb (catalog #9102), phospho-Erk1/2 (T202/Y204) mouse (catalog #9106L) and β-actin mouse mAb (catalog #3700). EPAC rabbit pAb (catalog #sc-25632) was purchased from Santa Cruz Biotechnology (SCBT) (Santa Cruz, CA, USA). The following were used in tissue and cell staining: Rap1A mouse mAb (catalog #sc-373968) SCBT, CA, IB4, Hoescht. ZO-1 rat (catalog #MABT11, Millipore, USA), Claudin-5 rabbit (catalog #34-1600, Invitrogen, USA), and Occludin mouse 488 Alexa (catalog #331588, Lifetech, USA).

2.3.3 *In vivo* Permeability Assays: For the Evans Blue permeability assay, male Long-Evans rats (Charles River Laboratories, Wilmington, MA, USA) weighing 200g-250g were housed in accordance with the guidelines of the institutional animal care and use committee (IACUC) and

consistent with ARVO Statement for the Use of Animals in Ophthalmic and Visual Research. The IACUC approved all animal procedures. Rats were anaesthetized with intramuscular injection of ketamine and xylazine (66.7 mg/kg and 6.7 mg/kg of body weight, respectively). A 32-gauge needle was used to create a hole for an intravitreal injection (2 μL/eye) using a 5 μl Hamilton syringe. The experimental animal groups received an intravitreal injection of VEGF (50ng) and TNF-α (10ng) together, or VEGF/TNF-α/8CPT-AM either at 10μM (355ng) or 50μM (1.78μg) simultaneously. The animals recovered for 3 hours and were then anaesthetized again for the permeability assay as described by our group previously [214]. For studies using ischemia reperfusion to induce vascular permeability and retinal sterile inflammatory response, mice underwent ischemia on their left retina by increasing the intraocular pressure in the anterior chamber with PBS in order to block the blood supply from the retinal artery for 90 min followed by natural reperfusion, as described previously [65].

2.3.4 Solute Flux Assay: Primary bovine retinal endothelial cells (BREC) were isolated and grown in culture as previously described [215] to model the vascular endothelial blood-retinal barrier *in vitro* [216]. BREC were seeded on 0.4 μm pore transwells filters (Corning Costar, Acton, MA, USA) coated with 1μg/cm^2 fibronectin. BREC were grown to confluence in MCDB-131 medium, supplemented with 10% fetal bovine serum (FBS), 22.5μg/mL endothelial cell growth factor, 120μg/mL heparin, 0.01mL/mL antibiotic/antimycotic. Then cell culture media was changed to stepdown media, MCDB-131 supplemented with 1% FBS, 0.01 mL/mL antibiotic/antimycotic, and 100 nmol/L hydrocortisone, for 48 hours prior to experiment. For experiments with TNF-α treatment, no hydrocortisone was in the stepdown media. The cells were treated with VEGF (50ng/mL) for 30 minutes, and/or with TNF-α (10ng/mL) or 8CPT-AM (1μM unless otherwise stated) for indicated time. Cell monolayer permeability to 70 kDa

rhodamine isothiocyanate (RITC) dextran (Sigma-Aldrich Corp., St. Louis, MO, USA) was calculated by measuring the rate of flux of the substrate over a 4 hour time course followed by calculating the diffusive permeability (Po) across the monolayer [28].

$$Po = [(F_L/\Delta t)V_A]/(F_A A)$$

Where *P*o is in cm/s, F_L is basolateral fluorescence, F_A is apical fluorescence, Δ**t** is the change in time, *A* is the surface area of the filter and V_A is the volume of the basolateral chamber.

2.3.5 Transendothelial Electrical Resistance (TEER) Assay: Cell monolayer ion flux was measured by electrical resistance using an electrical cell-substrate impedance sensing (ECIS)-ZΘ system at 4000 Hz (Applied Biophysics, Troy, NY). BRECs were seeded on 8-wells 8W10E$^+$ ECIS plates containing gold electrodes. Cells were left to grow overnight or until 90% confluent followed by media changed to stepdown media for 48 hours. After 48 hours of stepdown the monolayers of cells were treated with compounds of interest.

2.3.6 GTP Bound Rap1 Pull-down and Detection Assay: Pull-down for active Rap1 based on capture using the GST linked peptide of the downstream Rap1 effector Ral guanine nucleotide dissociation stimulator (RalGDS) Rho binding domain (RBD) kit was purchased from (Thermo Scientific, Rockford, IL, USA) (kit cat #16120) and used per manufacturer instructions. Cells were lysed with 500 µL of 1X lysis/binding/wash buffer provided in kit, centrifuged at 16,000 x g for 15 minutes at 4°C and supernatant was transferred onto spin cup collection tube containing Glutathione Resin. GST-RalGDS-Rap binding domain (RBD) fusion protein (20 µg/spin cup) was added to the supernatant and incubated for 1 hour with gentle rocking at 4°C. Samples were then centrifuged at 6,000 x g for 30 seconds, washed 3 times, and eluted with 50 µL of 2X reducing sample buffer (1-part β-mercaptoethanol to 20 parts 2X SDS Sample Buffer; Thermo Scientific, Rockford, IL, USA). Eluted samples, 25 µL, and total cell lysates, 30µg, were loaded

onto NuPAGE SDS gels for western blot analysis. Captured GTP-bound Rap1, as well as total Rap1 protein in lysate was detected using the anti-Rap1 rabbit mAb provided by the GTP-Rap1 Pull-down kit (Thermo Scientific).

2.3.7 Immunofluorescent (IF) Staining: For IF staining and imaging, BREC were fixed with 1% paraformaldehyde for 10 minutes at room temperature (RT). The cells were permeabilized with 0.2% Triton X-100 followed by blocking with 10% milk in 0.1% Triton X-100 for 1 hour at RT. Cells were stained with primary antibodies for 2 days at 4°C. Cells were washed, then stained with secondary antibodies overnight at 4°C. Cells were imaged with Leica confocal microscope (TCS SP5; Wetzlar, Germany).

2.3.8 Western Blot: Cell lysates, 30µg of protein, were loaded into each well of NuPAGE SDS gels (Life Technologies, Carlsbad, CA) and separated by electrophoresis. After nitrocellulose membrane transfer, membranes were blocked in 2% ECL Prime Blocking Reagent and incubated with primary antibodies overnight at 4°C. Secondary antibodies IgG conjugated with HRP were detected with Lumigen ECL ultra chemiluminescent reagent (Lumigen, Inc, TMA-100; Southfield, MI, USA).

2.3.9 Viability Assay: To measure viability of cells, the CellTiter-Fluor Cell Viability assay was used according to manufacturer's protocol (Promega, Madison, WI, USA). The fluorescent signal proportional to the number of living cells is generated by the cell-permeant peptide substrate (glycyl-phenylalanyl-aminofluorocoumarin; GF-AFC) which is cleaved by live cell protease activity. Cells were grown on 96-well plate until they reached confluency and then changed to step down media for 48 hours. VEGF (50ng/mL), DMSO (50%), ESI 09, HJC 0350, or vehicle were diluted in media, applied to the cells at a final volume of 100µL and incubated for 1 hour. The CellTiter-Fluor Reagent was added in an equal volume, mixed briefly using

orbital shaker, and incubated for 30 minutes at 37°C. Fluorescence was measured after 1.5 hours using a fluorometer ($355nm_{Ex}/520nm_{Em}$).

2.3.10 Gene Expression Knockdown Experiments: Composite and individual Rap1B siRNAs specific for bovine (sc-270595, sc-270595A (Rap1B-1 siRNA), sc-270595B, and sc-270595C; Santa Cruz, CA, USA) were purchased from SCBT. BRECs were transiently transfected with 100nM of either Rap1B siRNA or scramble siRNA (siGENOME Non-Targeting siRNA#1, D-001210-01-05; Dharmacon GE Healthcare, USA) using the nucleofection technique (Lonza). Briefly, cells were trypsinized and $5x10^5$ cells were used per nucleofection. Nucleofection solution and supplement solution were used to resuspend the cell pellet in a final volume 100µL. The cell suspension was mixed with 100nM of siRNAs in cuvette and nucleofection carried out per manufacturer instructions (setting S-05; Amaxa Biosystems). Cell were diluted with 0.5 mL MCDB-131 media and added onto 6-well plates containing 1.5mL of media. Nucleofected cells were gently mixed in a total of 2 mL media then 0.5 mL of cell suspension were plated directly onto fibronectin-coated 0.4 µm pore transwell filters. After 4 hours, the media was replaced with fresh MCDB-131 media. Confluent cells were then changed to step down media for 48 hours and treated with compounds of interest followed by *in vitro* Solute Flux assay as described above.

2.4 Results

2.4.1 Activation of EPAC Prevents VEGF and TNF-α-Induced Permeability and Reverses Ischemia Reperfusion-Induced Permeability *In Vivo*. Activation of the EPAC-Rap1 signaling pathway via the EPAC specific cAMP analog, 8-CPT-2′-O-Me-cAMP, regulates barrier properties in endothelial cells such as HUVEC, pulmonary endothelial cells and in rat mesenteric microvasculature [187, 188, 190]. However, little is known about the role of EPAC-Rap1 signaling in the endothelial cells of the BRB or the relation of EPAC-Rap1 signaling to vascular permeabilizing factors such as VEGF and TNF-α. Long-Evans rats were utilized to determine if pharmacological activation of the EPAC-Rap1 signaling pathway prevents retinal vascular permeability *in vivo*. First, to determine the localization of Rap1 expression in retinas, immunofluorescent staining of rat retinas was performed using an anti-Rap1 antibody, which binds both the Rap1A and B isoforms; retinas were co-stained with IB4 to identify blood vessels. Rap1 was located only in the capillary vessels and colocalizes with IB4 staining (Figure 2.1.A). Next, VEGF and TNF-α were intravitreally co-injected into Long-Evans, rats and 3 hours later, Evan's blue was administered through the femoral vein to assess Evan's blue dye accumulation in the retina tissue as a measure of retinal vascular permeability. VEGF and TNF-α increased retinal vascular permeability by two-fold in comparison to control (Figure 1B). The retinas that were intravitreally co-injected with either 10μM or 50μM of 8CPT-AM, along with both VEGF and TNF-α, had no significant increase in retinal vascular permeability compared to controls, showing that 8CPT-AM treatment blocks VEGF/TNF-α-induced permeability (Figure 2.1.B). To determine if activation of the EPAC-Rap1 signaling pathway can restore barrier properties to the retinal vasculature, an ischemia reperfusion model was used. In rodent models, ischemia reperfusion (IR) rapidly induces a VEGF dependent increase in retinal vascular permeability,

which persists for at least 48 hours and leads to expression of a host of inflammatory factors [65]. IR was induced in mice and 48 hours later, 8CPT-AM was administered intravitreally and retinal vessel permeability was compared to vehicle-injected control eyes. The 100µM 8CPT-AM concentration used for intravitreal injection was a dose shown to activate EPAC independent of PKA activation in retinal pigment epithelium (RPE) and choroid [185, 217] and was shown to not increase PKA activity (Figure 2.S1.A). Animals with ischemia displayed a 2-fold increase in retinal vascular permeability (Figure 2.1.C) as previously observed in rat [65]. Mice that received intravitreal injection of 100µM 8CPT-AM after ischemia showed a reversal of ischemia-induced retinal vascular permeability by measuring accumulation of FITC-BSA (Figure 2.1.C) or 70kDa Dextran-Texas Red in the retina, (Figure 2.S1.B).

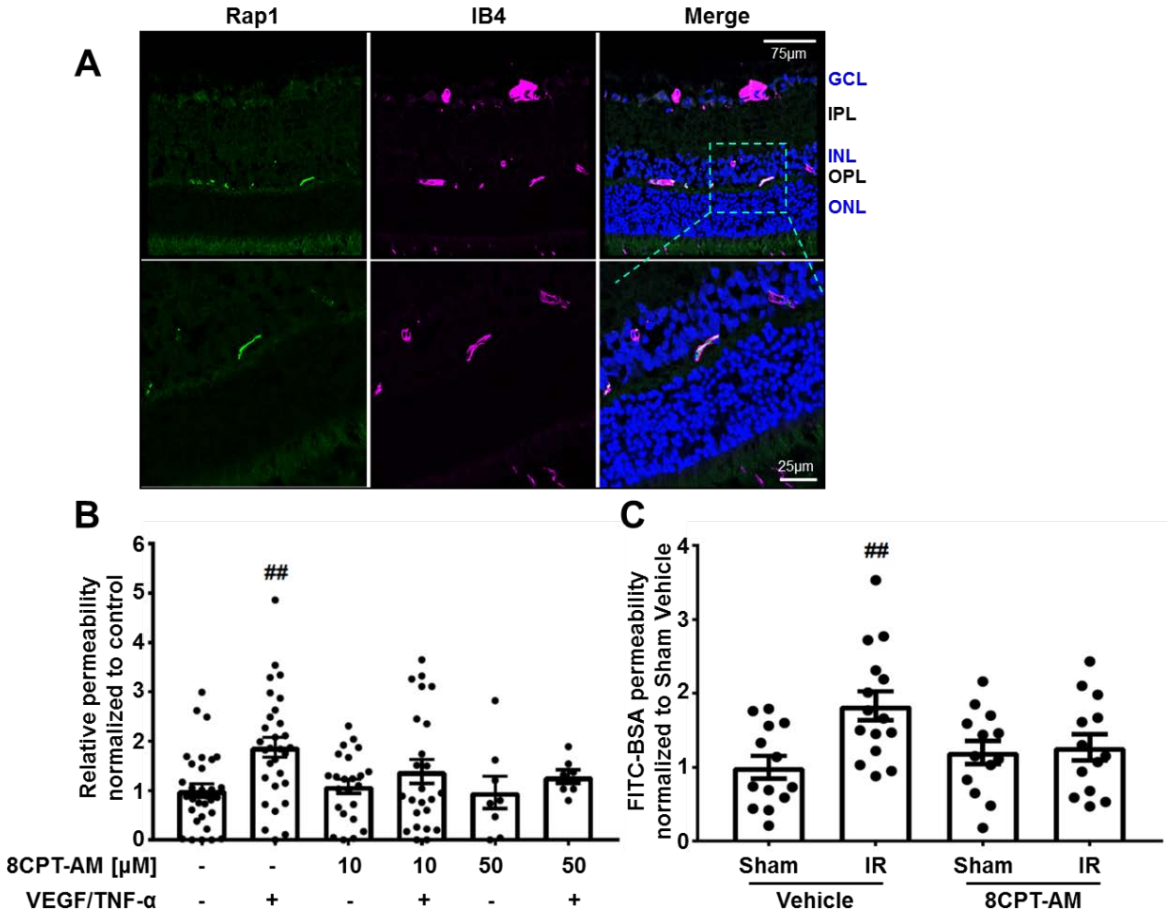

Figure 2.1 Cyclic AMP Analog, 8CPT-AM, Regulates Retinal Vascular Permeability. **A.** Rap1 is found in the capillary plexus of the retina. Immunofluorescence analysis was utilized to detect the presence of Rap1 (green) in rat retina. IB4 vascular marker (purple) and Hoechst nuclear stain was used. Ganglion cell layer (GCL), inner nuclear layer (INL), outer plexiform layer (OPL), outer nuclear layer (ONL). Scale bar 75μm and 25μm for zoom image. **B.** 8CPT-AM blocks retinal vascular permeability. Long-Evans rats received intravitreal co-injection of VEGF (50ng) and TNF-α (10ng) or 8CPT-AM at 355ng (an estimated vitreous concentration of 10μM) or 1.78μg (estimated 50μM) with VEGF and TNF-α and compared with vehicle control. After 3 hours, rats received a femoral vein injection of Evans Blue and retinal dye accumulation was determined. **C.** 8CPT-AM reverses ischemia reperfusion-induced permeability. Retinal ischemia in mice was achieved by increasing intraocular pressure with PBS delivered to the anterior chamber to prevent blood flow for 90 min followed by natural reperfusion. 48 hours later vehicle or 8CPT-AM at 278ng (estimated vitreous concentration of 100μM) was delivered by intravitreal injection and FITC-BSA dye accumulation was determined. Results are expressed as the mean relative to the control $\pm$ S.E.M., Bonferroni post hoc test $^{\#\#}p < 0.01$ compared to control.

2.4.2 Activation of the EPAC-Rap1 Pathway Prevents and Reverses VEGF or TNF-α

Induced Endothelial Permeability. The EPAC-Rap1 signaling pathway in VEGF- or TNF-α-induced endothelial permeability was examined in primary culture of bovine retinal endothelial cells (BREC). Western blotting reveals that EPAC and Rap1 proteins are expressed in BREC, (Figure 2.2.A). To validate that 8CPT-AMactivates the EPAC-Rap1 signaling pathway in these cells, we used the active Rap1 capture assay, which captures active, GTP-bound Rap1 through binding to a GST-linked peptide for the downstream Rap1 effector RalGDS. Confluent monolayers of BREC were treated with VEGF, or first pretreated with 8CPT-AM then VEGF or 8CPT-AMalone, and compared to controls. BREC treated with 8CPT-AM (1μM) showed a significant 2.5-fold increase in Rap1 bound to GTP. One hour of VEGF had no apparent effect on Rap1 GTP loading with or without 8CPT-AM (Figure 2.2.B-2.C). To determine if longer exposure of VEGF affected the ability of 8CPT-AM to induce Rap1 GTP loading, BREC were stimulated with VEGF for 24 hours followed by 30 minutes of 8CPT-AM (1μM). Longer exposure of VEGF had no effect on Rap1 GTP loading and again 8CPT-AM alone or after VEGF induced a significant 2-3-fold increase in Rap1 activation (Figure 2.S2.A-S2.B). Additionally, a VEGF time response was performed to determine if VEGF directly affected active Rap1 levels in confluent BREC, but no differences in comparison to control were observed (Figure 2.S2.C-S2.D).

Having established the ability of 8CPT-AM to activate EPAC/Rap in BREC, we tested whether activation of EPAC increases endothelial barrier properties and reverses permeability after VEGF or TNF-α. A dose response of 8CPT-AM was performed in BREC both with and without VEGF, and permeability to 70kDa RITC dextran was measured. 8CPT-AM at concentrations of 2μM, 1μM, and 0.5μM significantly reduced basal permeability in comparison

to control (Figure 2.2.D). To determine if 8CPT-AM was capable of blocking VEGF-induced retinal endothelial permeability, BREC were treated with varying doses of 8CPT-AM for 30 minutes prior to VEGF (50ng/mL) and solute flux was measured beginning 30 minutes after VEGF addition. 8CPT-AM at the concentrations of 2μM, 1μM, and 0.5μM completely blocked VEGF-induced permeability (Figure 2.2.E). Based on these results, 1μM 8CPT-AM was used for all additional experiments unless otherwise stated.

To verify that 1μM 8CPT-AM was specifically activating the EPAC signaling pathway independently of PKA signaling, we quantified phosphorylation of CREB, a downstream PKA target. BREC were stimulated for 1 hour with either 1μM or 100μM 8CPT-AM, or with 100μM forskolin (FSK) as a positive control to elevate cAMP (Figure 2.2.F). Cells were lysed and prepared for western blot. The BREC treated with FSK or with 100μM of 8CPT-AM had a 2-fold increase in phosphorylation of CREB, but 1μM of 8CPT-AM did not increase phosphorylation of CREB (Figure 2.2.F) and quantified in (Figure 2.2.G).

To address the question of whether activation of the EPAC-Rap1 signaling pathway can reverse permeability, we pretreated BREC with VEGF or TNF-α followed by 8CPT-AM and measured permeability to 70kDa RITC dextran using the solute flux assay. BREC were stimulated with VEGF alone, 8CPT-AM alone, pretreatment with 8CPT-AM 30 minutes prior to VEGF (pre-8CPT), or treatment with VEGF 30 minutes prior to 8CPT-AM treatment (post-8CPT). As shown previously in (Figure 2.2.E), 8CPT-AM pretreatment (pre-8CPT) significantly blocks VEGF-induced permeability (Figure 2.3.A), and TNF-α-induced permeability (Figure 2.3.B). Importantly, post-treatment with 8CPT-AM (post-8CPT) reverses VEGF-induced permeability (Figure 2.3.A). The combination of VEGF and TNF-α induces an additive 3-fold increase in endothelial permeability (Figure 2.3.C), and pretreatment with 8CPT-AM

significantly prevents combined VEGF/TNF-α-induced permeability as well as reverses the effects of both VEGF/TNF-α (Figure 2.3.C).

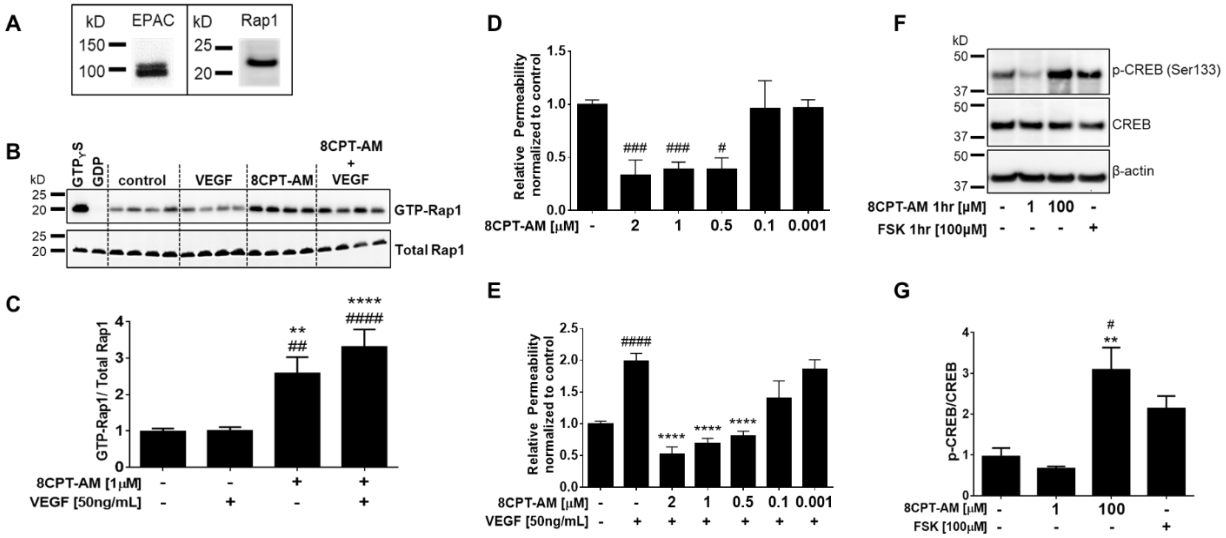

Figure 2.2 8CPT-AM Rap1 Activation Prevents VEGF-Induced Permeability of BREC. **A.** Western blot analysis from BREC lysates shows the presence of the GEF EPAC1 and small G-protein Rap1. **B.** GTP bound Rap1 was determined by capture assay using GST-RalGDS RBD. 8CPT-AM (1μM) was added 30 min prior to VEGF (50ng/mL) for a total time of 1.5 hours. Assay controls GTP□S and GDP were added to lysates before capture. Quantification shown in **C** with a total n≥ 11. **D.** Solute flux assay was used to test permeability to 70kDa RITC dextran after 8CPT-AM at varying concentrations on BREC n≥ 6 **E.** 8CPT-AM prevents VEGF-induced permeability. BREC stimulated with 8CPT-AM at doses indicated given 30 minutes prior to VEGF addition. Doses from 0.5μM to 2μM blocked VEGF-induced permeability. Average P_o values for control were $7.1x10^{-7}$ and VEGF were $1.4x10^{-6}$(cm/s), total of n≥ 8. **F.** Low dose 8CPT-AM does not activate the PKA pathway. 8CPT-AM at 1μM was added to BREC for 1 hour and no increase in CREB phosphorylation was observed. Incubation of 8CPT-AM or Forskolin (FSK) at 100μM for 1 hour increased CREB phosphorylation. **G.** Quantification shown in **F** with a total n≥3. All results are expressed as the mean ± S.E.M. relative to the control. One-way ANOVA and Bonferroni post hoc test $^{\#}p < 0.05$; $^{\#\#}p < 0.01$; $^{\#\#\#}p < 0.001$; $^{\#\#\#\#}p < 0.0001$ compared to control in **C**, **D**, **E**, and **G**. $^{**}p < 0.01$; $^{****}p < 0.0001$ compared to VEGF in **C** and **E** or 8CPT-AM (1μM) in **G**.

Permeability to ions was also determined as a measure of paracellular permeability by measuring the transendothelial electrical resistance (TEER) in BREC monolayer using the ECIS system. The BREC cells were either pretreated or post-treated with 8CPT-AM (2µM) and the monolayer's resistance was measured for 5 hours. BREC treated with VEGF display a 40% decrease in TEER compared to control (Figure 2.3.D). BREC pretreated with 8CPT-AM block VEGF from decreasing TEER, and BREC post-treated with 8CPT-AM reverse the effects of VEGF and increase TEER levels to control (Figure 2.3.D). To determine how long the 8CPT-AM effect on VEGF reduction is maintained, we measured TEER for 24 hours. 8CPT-AM at 1µM was statistically different from VEGF for 8 hours (Figure 2.S3.A) and a higher dose of 8CPT-AM (5µM) was statistically different from VEGF for 16 hours (Figure 2.S3.B).

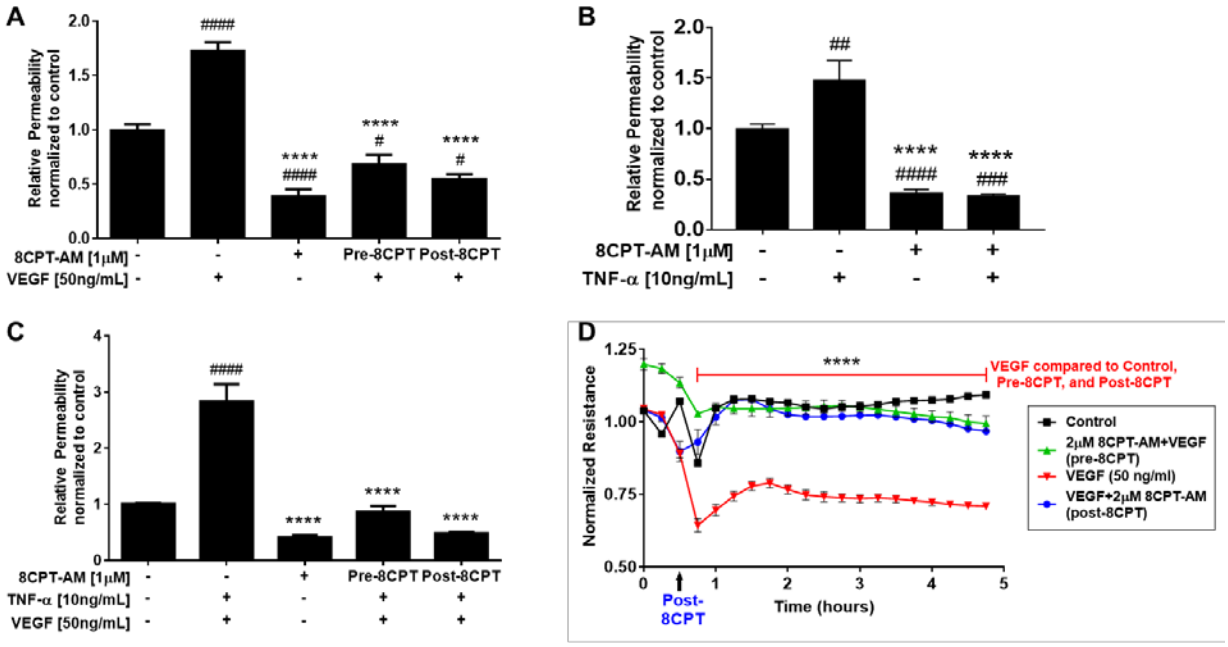

Figure 2.3 8CPT-AM Blocks and Reverses Permeability Induced by VEGF and TNF-α. **A.** BREC were stimulated with VEGF (50ng/mL) or/and 8CPT-AM (1μM). Pre-8CPT: BREC were stimulated with 8CPT-AM 30 min before VEGF treatment. Post-8CPT: BREC were treated with 8CPT-AM 30 min after VEGF. 70kDa RITC-dextran was added 30 min after the last treatment. Average P_o values for control and VEGF were $9.7x10^{-7}$ and $1.7x10^{-6}$(cm/s) respectively $n \geq 6$. **B.** BREC were pretreated for 30 min before stimulated with TNF-α (10ng/mL) and 70kDa RITC-dextran was added 1h later. Average P_o values for control and TNF-α were $1.1x10^{-6}$ and $1.7x10^{-6}$(cm/s) $n \geq 12$. **C.** BREC were stimulated with TNF-α (10ng/mL) for 1 hour followed by VEGF for 30 minutes. Pre-8CPT: (1μM) was added 30 min before TNF-α+VEGF or Post-8CPT: (1μM) was added 1.5 hours after TNF-α+VEGF. 70kDa RITC-dextran was added 30 min after the last treatment. Average P_o values for control were $7.5x10^{-7}$ and for TNF-α+VEGF were $1.9x10^{-6}$(cm/s) $n \geq 15$. Results are expressed as the mean relative to the control ± S.E.M. One-way ANOVA $^{\#}p < 0.05$; $^{\#\#}p < 0.005$; $^{\#\#\#}p < 0.001$; $^{\#\#\#\#}p < 0.0001$ compared to control. $^{****}p < 0.0001$ compared to VEGF, TNF-α, or VEGF+TNF-α in **A**, **B**, and **C** respectively. **D.** BREC were seeded on 8W10E+ arrays and TEER was measured every hour on the ECIS Z-theta instrument. 8CPT-AM (2μM) added 30 min prior to VEGF increases resistance and prevents VEGF-induced TEER loss for up to 6 hours. 8CPT-AM post-VEGF restores endothelial barrier after VEGF-induced ion permeability. Data represents the mean ± S.E.M. with analysis by two-way ANOVA Bonferroni post hoc test $^{****}p < 0.0001$ compared to VEGF, n = 3/group.

2.4.3 8CPT-AM Prevents and Reverses VEGF-Induced Tight Junction Disorganization. To assess the role of 8CPT-AM in junctional complex organization we performed immunofluorescence staining of BREC TJs. Cells were treated with VEGF (50ng/mL) for 1 hour, 8CPT-AM (1μM) alone for 90 minutes, pretreated with 8CPT-AM for 30 minutes followed by 1 hour of VEGF, or treated with VEGF for an hour prior to 30 minutes of 8CPT-AM. VEGF induced significant disorganization, with large invaginations (arrows) and junctional border breaks (arrowheads) in all 3 TJ proteins analyzed (ZO-1, occludin, and claudin-5) (Figure 2.4.A) and as previously reported [216]. 8CPT-AM alone induced a significantly more linear and continuous organization of all 3 TJ proteins at the junctions in comparison to control as assessed by scoring in a blinded fashion (Figure 2.4.A). 8CPT-AM pretreatment blocked and post-treatment reversed VEGF induction of TJ disorganization (Figure 2.4.A). It is notable that the increased cytoplasmic staining for both occludin and claudin-5 after VEGF treatment was not lost with 8CPT-AM post-treatment but the border organization was dramatically increased. To determine if 8CPT-AM or VEGF was causing a change in total TJ protein levels, we performed western blotting of the TJ proteins ZO-1, occludin, and claudin-5 after the same treatment with VEGF for 1 hour, 8CPT-AM for 90 minutes, or 8CPT-AM+VEGF. TJ proteins ZO-1, occludin, and claudin-5 (Figure 2.4.B-4.E) and adherens junction protein VE-cadherin (Figure 2.S4.A) showed no total protein changes in this short time course, suggesting that EPAC-Rap1 activation promotes TJ assembly at the border.

2.4.4 8CPT-AM Attenuates VEGF Signaling. The mechanistic connection between 8CPT-AM and VEGF signaling was investigated by western blotting for phosphorylation of signal transduction proteins known to function downstream of VEGF. BREC were treated with VEGF (50ng/mL) for 15 minutes, 8CPT-AM (1μM) alone for 45 minutes, or pretreated with 8CPT-AM

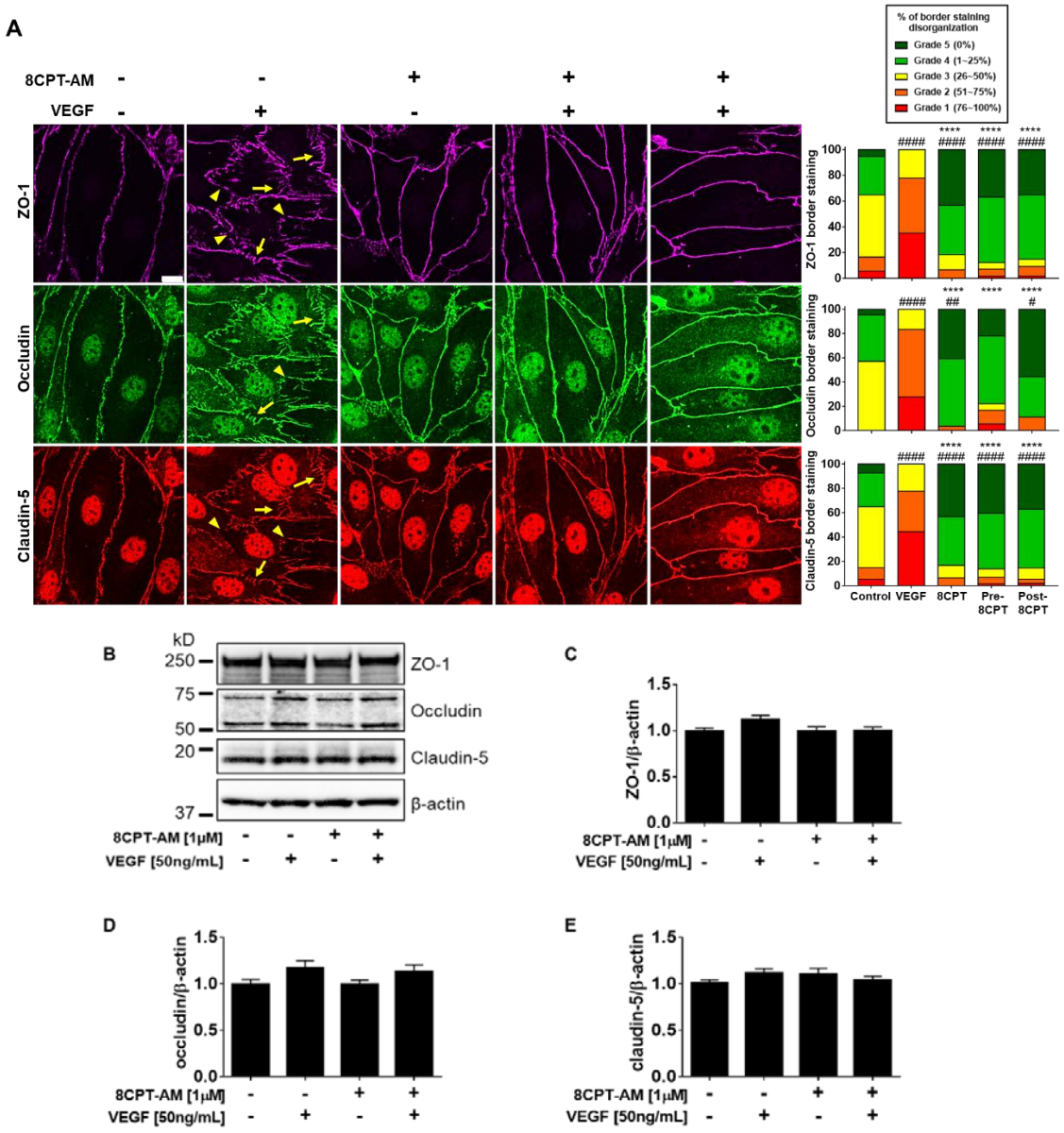

Figure 2.4 8CPT-AM Prevents and Reverses VEGF-Induced Tight Junction Disorganization. **A.** Immunofluorescence staining of TJ proteins ZO-1, occludin, and claudin-5 was performed to assess their organization after the addition of 8CPT-AM (1μM) for 30 minutes and/or VEGF (50ng/mL) for 1 hour. Yellow arrows show loss of linear organization (invaginations), and yellow arrowheads show border breaks or gaps between adjacent cells. Histograms show scoring of TJ proteins as percent organization. ZO-1, occludin and claudin-5 border staining were quantified by semi-quantitative ranking score system based on a graded scale from 1 to 5: Grade 1 for near complete disorganization of border staining 0% to 25%, Grade 2 for 25% to 50% continuous border staining, Grade 3 for 50% to 75% continuous border staining, Grade 4 for 75% to 100% continuous border, and Grade 5 completely continuous border. **B.** Changes in TJ total protein expression with VEGF or 8CPT-AM were measured using western blot **C- E**. No changes in ZO-1, occludin, and claudin-5 expression were observed in any of the experimental conditions. Results are expressed as the mean relative to the control n≥ 4 with analysis by One-Way ANOVA and Bonferroni post hoc test, $^{\#}p < 0.01$; $^{\#\#}p < 0.005$; $^{\#\#\#\#}p < 0.0001$ or **** compared to VEGF.

for 30 minutes followed by VEGF for 15 minutes and compared to control cells. VEGF caused a significant increase in phosphorylation of both VEGFR2 (Tyr 1175) and Erk1/2 (Figure 2.5A-5D). 8CPT-AM alone caused a 50% decrease in both Erk1 and Erk2 basal phosphorylation in comparison to control (Figure 2.5C-D). No phosphorylation changes were observed in VEGFR2 between control and 8CPT-AM (Figure 2.5.B). However, pretreatment of 8CPT-AM significantly reduced the phosphorylation of both VEGFR2 (Tyr 1175) and Erk-1/2 in comparison to VEGF alone (Figure 2.5.B-D). This effect was specific, as both VEGF and 8CPT-AM promote an additive increase in AKT (Ser 473) phosphorylation (Figure 2.5.E).

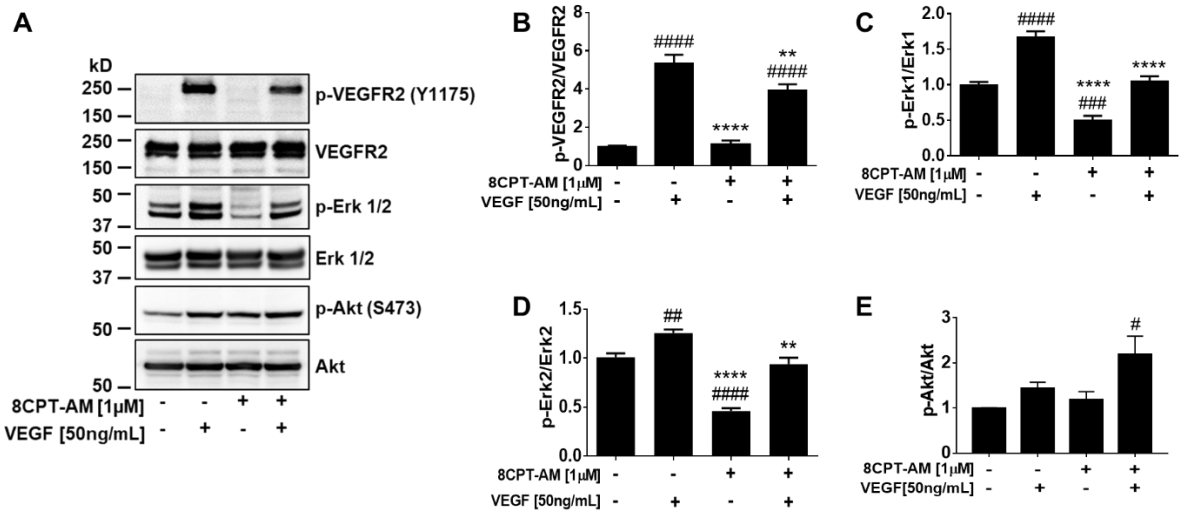

Figure 2.5 8CPT-AM Attenuates VEGF-Erk1/2 Signal Transduction. A. Immunoblotting was used to detect phospho-Tyr 1175 and total VEGFR2, Phospho and total Erk ½, and phosphor-Ser 473 and total AKT changes in BREC pre-treated with 8CPT-AM (1 μM) for 30 minutes followed by 15 minutes of VEGF (50ng/mL). **B.** VEGFR2 Y1175 phosphorylation was reduced by 8CPT-AM when added prior to VEGF $n \geq 12$. **C.** 8CPT-AM decreased Erk1 and **D.** Erk2 phosphorylation $n \geq 10$. **E.** Both VEGF and 8CPT-AM increase AKT phosphorylation $n \geq 4$. Values are means $\pm$ S.E.M. $^{\#\#\#\#}p < 0.0001$ or $^{\#\#\#}p < 0.001$ or $^{\#}p < 0.05$ compared to control and $^{****}p < 0.0001$ or $^{**}p < 0.01$ compared to VEGF.

2.4.5 Inhibition of EPAC2 Increases Basal Permeability and Blocks 8CPT-AM Induction of Barrier Properties. To determine whether EPAC2 contributes to regulating basal permeability properties, the EPAC2 specific inhibitor, HJC0350, was used in a dose response solute flux assay. BREC were incubated with different HJC0350 concentrations for a total time of 45 minutes. HJC0350 at 5µM and 10µM caused approximately a 2-fold permeability increase, (Figure 2.6). Inhibition of EPAC2 with HJC0350 at 5µM and 10µM blocked 8CPT-AM (1µM) from decreasing basal permeability. To determine potential cytotoxicity of HJC0350, a viability assay was performed. Viability of BREC treated with HJC0350, ESI 09 (an inhibitor of both EPAC1 and EPAC2), DMSO (50% as a positive control for BREC cytotoxicity), and VEGF (50ng/mL) were tested for 1.5 hours using the CellTiter-Fluor Cell Viability assay. VEGF, HJC0350 (0.1-50 µM), and ESI 09 (1-10 µM) did not cause cell death (Figure 2.S5), whereas 50% DMSO caused ~75% cell death, and 30µM ESI 09 caused 33% cell death (Figure 2.S5).

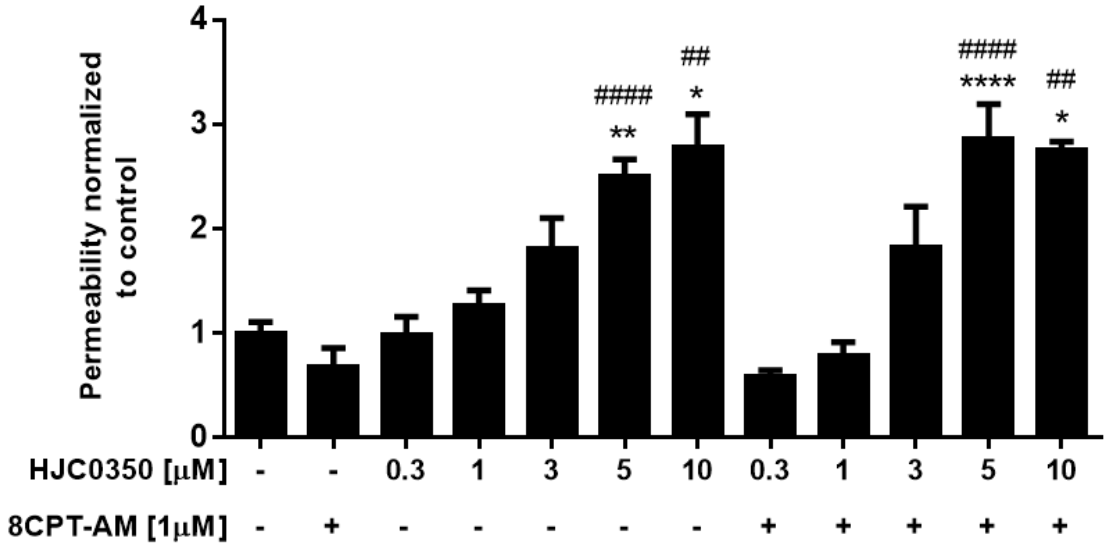

Figure 2.6 EPAC 2 Antagonist Increases Basal Permeability and Blocks 8CPT-AM Effect. Solute flux assay was used to test EPAC2 antagonist, HJC0350, at different concentrations on BREC. HJC0350 5μM to 10μM had a significant increase in basal permeability and blocked 8CPT-AM barrier induction. Average P_o values for control and HJC0350 were $2.2x10^{-7}$ and $4.4x10^{-7}$(cm/s). Results are expressed as the mean $\pm$ S.E.M. relative to the control with a total of $n \geq 3$, $^{\#\#\#\#}p < 0.0001$ or $^{\#\#}p < 0.001$ compared to control and $^{****}p < 0.0001$; $^{**}p < 0.01$; $^{*}p < 0.05$ compared to 8CPT-AM.

2.4.6 Rap1B Isoform Regulates Basal Permeability and Tight Junction Organization.

Mammals possess two isoforms of EPAC proteins, EPAC1 and EPAC2, and two isoforms of Rap1 proteins, Rap1A and Rap1B [145, 173]. To determine if BREC express these isoforms of EPAC and Rap1, we designed primers for each isoform and performed PCR. BREC express mRNA for both Rap1A and Rap1B isoforms, as well as EPAC1 and EPAC2 isoforms (Figure 2.7.A). Specific bovine Rap1B siRNAs were used to knockdown Rap1B in BREC. A composite of 3 Rap1B specific siRNAs (transfected at 100nM) caused a 66% Rap1 knockdown in BREC, as assessed by western blot (Figure 2.7.B). Note that the antibody detects both Rap1A and B, as no isoform-specific antibody was available. To determine the role of Rap1B in basal endothelial permeability, we silenced the Rap1B gene in BREC and measured permeability using the 70kD solute flux assay. BREC with scramble siRNA behaved comparably to wild type BREC in response to both VEGF and 8CPT-AM (Figure 2.7.C). BREC with Rap1B knockdown demonstrated a 2-fold increase in basal permeability comparable to VEGF treatment (Figure 2.7.C); notably this response was also comparable to addition of the EPAC2 antagonist (Figure 2.6). VEGF addition to BREC with Rap1B knockdown had no additional change in permeability. BREC with Rap1B knockdown had a significant decrease in basal permeability in the presence of 8CPT-AM, which could be due to the presence of Rap1A or Rap2 isoforms or failure of complete Rap1B knockdown (Figure 2.7.C). To ensure specificity of the composite Rap1B siRNA, the 3 siRNAs were tested individually and one of the siRNAs (Rap1B-1 siRNA) was found to yield a 58% knockdown of Rap1 expression (Figure 2.S6.A) comparable to the composite Rap1B siRNA. Rap1B-1 siRNA at 100nM again led to a significant increase in basal permeability in comparison to scramble siRNA control (Figure 2.7.D).

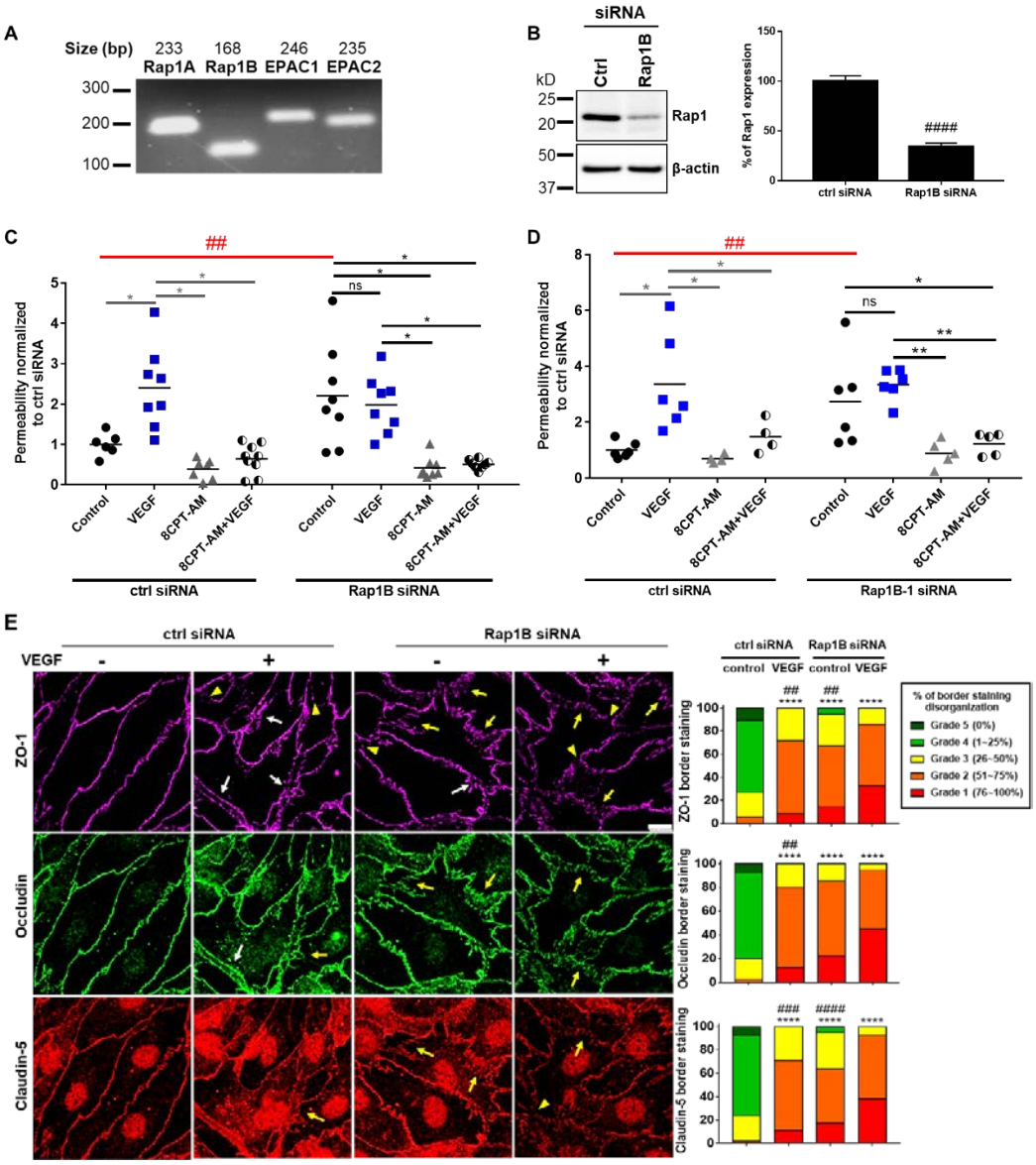

Figure 2.7 Rap1B Contributes to Basal Permeability and Tight Junction Organization. A. Both Rap1 (Rap1A and Rap1B) and EPAC (EPAC1 and EPAC2) isoforms were found to be present in BREC by PCR. **B.** Western blot shows that composite Rap1B (100nM) siRNA results in a 66% knockdown, Student's t-test $^{\#\#\#\#}p < 0.0001$, $n \geq 9$. **C.** Solute flux assay was used to test permeability in BREC with Rap1B knockdown. Scramble and Rap1B siRNA at 100nM were used in BREC. Average P_o values for scramble control and Rap1B siRNA control were $2.4x10^{-7}$ and $5.4x10^{-7}$(cm/s). **D.** Solute flux assay was used to test permeability in BREC with individual Rap1B-1 siRNA. Scramble and Rap1B-1 siRNA at 100nM were used in BREC. Average P_o values for scramble control and Rap1B-1 siRNA control were $9.0x10^{-8}$ and $2.3x10^{-7}$(cm/s). **E.** Immunofluorescence staining of TJ proteins ZO-1, occludin, and claudin-5 was performed to assess the organization of TJ proteins after Rap1B knockdown with and without VEGF (50ng/mL) for 1 hour. Scale bar, 10µm. Histograms of scoring TJ show % organization of TJs. All results are expressed as the mean relative to the scramble control with a total of $n \geq 4$. ZO-1, occludin, and claudin-5 border staining were assessed by semi-quantitative ranking score system based on scale grade 1 to 5. Immunofluorescence results are expressed as the mean relative to the scramble control $n \geq 4$ with analysis by One-Way ANOVA and Bonferroni post hoc test, $^{****}p < 0.0001$ compared to scramble control and $^{\#\#}p < 0.05$; $^{\#\#\#}p < 0.001$; $^{\#\#\#\#}p < 0.0001$ compared to Rap1B siRNA VEGF. Permeability results are expressed as the mean $\pm$ S.E.M. relative to the scramble control two-way ANOVA analysis and Bonferroni post hoc test $^{*}p < 0.1$ and $^{\#\#}p < 0.01$ comparison between scramble and Rap1B or Rap1B-1 siRNA controls.

occludin, and claudin-5. Scramble siRNA had no effect on basal organization, and BREC treated with VEGF for 1 hour showed disorganization of all three TJ proteins (Figure 2.7.E). BREC with Rap1B knockdown showed a significant percentage of TJ disorganization in comparison to scramble siRNA control with invaginations (arrows) gaps (arrowheads) and regions of border separation between cells (white arrows) (Figure 2.7.E). The combination of VEGF and Rap1B knockdown showed an even greater effect on TJ disorganization in comparison to scramble siRNA with VEGF. Similar to the solute flux assay results, BREC with Rap1B knockdown treated with 8CPT-AM alone or with 8CPT-AM plus VEGF for 1 hour showed increased organization of the TJs at the cell border (Figure 2.S6.B). These results are likely due to the remaining Rap protein available to respond to 8CPT-AM.

2.5 Discussion

The present study provides compelling evidence that activation of the EPAC-Rap1 signaling pathway via the cAMP analog, 8CPT-AM, promotes barrier properties in retinal vascular endothelial cells. Previous research on the role of EPAC-Rap1 signaling in barrier properties has focused on HUVEC and epithelial cells [138, 165]. In this work, we demonstrate that the GEF, EPAC2, and the small GTPase, Rap1B, regulate basal retinal endothelial barrier properties and contribute to the TJ complex organization. We demonstrate that activation of EPAC-Rap1 blocks permeability induced by VEGF and TNF-α both in cells and *in vivo*. Importantly, activation of EPAC-Rap1 reverses permeability induced by these cytokines in cell culture and reverses retinal vascular permeability induced by ischemia reperfusion *in vivo*. 8CPT-AM activation of EPAC-Rap1 regulates TJ organization and reverses the effect of TJ disorganization by VEGF, which likely contributes to the control of endothelial barrier properties. We further show that 8CPT-AM specifically attenuates the VEGF-Erk signaling

pathway. Together these data indicate that EPAC-Rap1 signaling contributes to basal barrier properties and TJ organization of retinal endothelial cells and activating this pathway can restore barrier properties of the BRB.

Previous studies support a role for activation of the EPAC-Rap1 signaling pathway in blocking permeability induced by permeabilizing agents. *In vivo* studies show that activation of the EPAC-Rap1 signaling pathway attenuates platelet-activating factor (PAF)-induced permeability in the mesenteric microvasculature [190] and inhibits VEGF-induced dermis vascular permeability [189]. Activation of the EPAC-Rap1 signaling pathway also has been shown to block thrombin-induced permeability in HUVEC [187]. Additionally, activation of the EPAC-Rap1 pathway restores barrier properties in endothelial cells and in blood vessels. For example, activation of EPAC-Rap1 reverses TEER decrease caused by TNF-α and transforming growth factor (TGF-β) in HUVEC [194]. Our study builds upon these previous reports demonstrating that activation of EPAC-Rap1 reversed IR-induced permeability *in vivo* and reversed VEGF- and TNF-α-induced permeability in BREC and *in vivo*. Together these data show pharmacologic activation of EPAC-Rap1 signaling promotes and restores the BRB.

The EPAC1 and EPAC2 protein isoforms are both expressed in the retina [218]. In the endothelium, EPAC1, but not EPAC2, is expressed in HUVEC [188]. EPAC2 has been detected in human pulmonary aortic endothelial cells (HPAECs) [187], and we show that EPAC2 mRNA is present in BREC. EPAC1 is known for its involvement in regulating cell-cell junctions and endothelial barrier properties [165, 188], and EPAC2 has been observed in modulating neuronal activity [219]. Here, we show that EPAC2, in addition to EPAC1, plays a role in retinal endothelial barrier. In BREC, when EPAC2 is inhibited, basal permeability is increased and 8CPT-AM cannot restore the barrier. In a previous study, it was observed that ischemic

retinopathy in EPAC2-deficient mice induced a more severe retinal edema and a larger expression of aquaporin AQP4 surrounding the blood vessels in the inner BRB in comparison to the EPAC1-deficient mice [220]. The EPAC2 and EPAC1-decificient mice, without ischemic retinopathy, appeared relatively normal in comparison to the wild type mice. Future studies may address the role of EPAC2 in BRB properties after cytokine challenge or diabetes.

The Rap1B isoform contributes a major role in endothelial barrier regulation, vasculogenesis, and angiogenesis [180, 181]. Even though the Rap1 isoform proteins have a high protein sequence homology, mice gene deletion studies of the individual Rap1 isoforms show different viability outcomes. The Rap1A null mice were viable and had no size difference in comparison to wild type mice. On the other hand, the Rap1B null mice show an 80% embryonic lethality between embryonic (E) day 13.5 and 18.5 [179, 182]. Global or endothelial specific double Rap1A and Rap1B gene deletion is completely embryonic lethal and mice die within E10.5 to E15.5 [181]. Post-mortem analysis revealed that Rap1B and double Rap1A and Rap1B null mice manifested vascular hemorrhage [181, 184]. The Rap1B null viable mice exhibited defective angiogenesis, which led to a retardation in retinal neovascularization [184]. Consistent with these studies, we reveal that silencing the Rap1B protein in BREC was sufficient to induce an increase in endothelial permeability and disruption of the TJs. However, addition of 8CPT-AM decreased solute flux and promoted TJ organization at the cell periphery in BREC with Rap1B knockdown. These data are unsurprising Rap1A as well as Rap2A/B/C, or residual Rap1B from incomplete knockdown, may compensate with the pharmacologic dose of 8CPT-AM and EPAC activation.

Activation of the EPAC-Rap1 pathway contributes to endothelium barrier properties through junction complex maintenance [221] and down regulation of small G-protein RhoA,

known to be involved in permeability [131]. EPAC activation in HUVEC leads to the recruitment of VE-cadherin to the cell border and formation of long linear and continuous adherens junctions [187]. VE-cadherin-mediated junctional organization in HUVEC results in a decrease in solute flux [188]. Additional observations of EPAC-Rap1 activation include reduction of actin stress fiber formation, and maintenance of VE-cadherin and cortical actin at the cell periphery [187]. Here, we show for the first time in BREC that EPAC-Rap1 signaling protects TJ organization of the proteins ZO-1, occludin, and claudin-5. EPAC-Rap1 signaling blocks and reverses VEGF-induced TJ invaginations, gap formations, and TJ border breaks. As it has been observed with VE-cadherin organization [187, 188], we also observed that 8CPT-AM alone increases the recruitment and continuous linear organization of TJ at the cell border but does not increase TJ protein expression.

The mechanism by which activation of EPAC-Rap1 recruits and maintains TJ proteins at the cell borders of BREC remains to be fully understood. However, studies in endothelial cells show that organization and stabilization of the adherens junctional complex proteins may occur through the recruitment and interaction of afadin (AF-6) and Krev interaction trapped 1 (Krit1) with active Rap1 [192, 222]. In human pulmonary artery endothelial cells (HPAEC), activation of Rap1 promotes colocalization of AF-6 with both VE-cadherin and ZO-1 and interaction between AF-6 and p120-catenin [192]. In HUVEC active Rap1 recruits Krit1 to the cell-cell junctions, which interacts with β-catenin, p120-catenin, and AF-6 but not with ZO-1 [222]. Therefore, additional studies are necessary to determine if EPAC-Rap1 activation mediates TJ recruitment and organization in BREC via AF-6.

Permeabilizing agents such as VEGF, TNF-α, and thrombin all activate RhoA [154, 187, 192]. Activation of RhoA induces stress fiber formations associated with junctional complex

alterations and formation of intercellular gaps resulting in increased permeability [223]. Inhibition of RhoA downstream targets such as RhoA/Rho kinase (ROCK) blocks permeability [154]. In HUVEC, activation of EPAC-Rap1 signaling reduced permeability induced by permeabilizing agents by down regulating RhoA activity [187]. Studies in HUVEC show that active Rap1 interacts with rasip1 and together with Rap associating with DIL domain (radil), recruits Rho GTPase-activating protein 29 (ArhGAP29), which down-regulates RhoA activity [146]. Recently, it has been observed that rasip1 and radil are recruited to the cell membrane via the transmembrane protein heart of glass 1 (HEG1) [202]. An interesting finding from this group showed that interaction of Rap1-rasip1 and rasip1-radil-ArhGAP29 was not affected by HEG1 knockdown. Immunofluorescent studies show that rasip1 has a perinuclear localization [195] but moves to the cell border during nascent junction formation after a calcium switch assay [201]. Together these data suggest that rasip1 serves a dual function, to interact with radil and ArhGAP29 to suppress RhoA activity and localizing to the cell border through HEG1 where it regulates recruitment and stabilization of junctional proteins, for mechanism schematic refer to [224].

Studies of the outer retina show that Rap1 activation promotes barrier integrity in the retinal pigment epithelium (RPE) and inhibits choroidal neovascularization [217, 225]. In a retinal epithelial cell line (ARPE-19) Rap1 knockdown led to mislocalization of cadherins and a decrease in transepithelial electrical resistance (TER) [225] in a Rap1A specific manner [217]. Studies in RPE show that Rap1A regulates barrier integrity by modulating the interaction of β-catenin and IQGAP, a scaffold protein involved in actin cytoskeleton and cell-cell adhesion regulation [226, 227]. This barrier stabilization inhibits choroidal endothelial cells transmigration [217, 228]. The results from the ARPE-19 cells and *in vivo* studies indicate that the Rap1A

isoform is the major contributor to RPE barrier integrity in contrast to the role of Rap1B in retinal vascular endothelial barrier properties observed here. These data suggest that individual Rap1 isoforms control barrier properties in a cell specific manner.

Rap1 signaling regulates several cell processes including suppression of the Ras-Raf-Erk signaling pathway [229]. The extracellular signal-regulated kinase (Erk1/2) is involved in several cell pathways including but not limited to cell proliferation, cell survival, and migration [230]. In retinal endothelial cells, binding of VEGF to the VEGFR2 induces an increase in Erk1/2 signaling. We showed that in BREC, activation of EPAC-Rap1 signaling attenuates the Erk1/2 signaling and reduces the phosphorylation of the VEGFR2 on Tyr 1175. Previous studies have shown VEGFR2 activation leads to activation of the kinase, PKCβ, which phosphorylates occludin, promoting ubiquitination and leading to endocytosis of occludin and other junctional proteins, resulting in permeability [65, 74, 94]. Even though 8CPT-AM addition blocks VEGF-induced permeability, 8CPT-AM does not attenuate phosphorylation of (S490) occludin (data not shown). 8CPT-AM treatment does block or prevent the internalization of junctional proteins suggesting either dominance of the junctional assembly pathway or inhibition of junctional internalization at a separate step.

In conclusion, activation of the EPAC-Rap1 pathway, specifically the EPAC2 and Rap1B isoforms, contributes to both basal permeability and shows promise as a therapeutic strategy to restore barrier properties after VEGF or inflammatory cytokine induced permeability.

2.6 Supplement Data

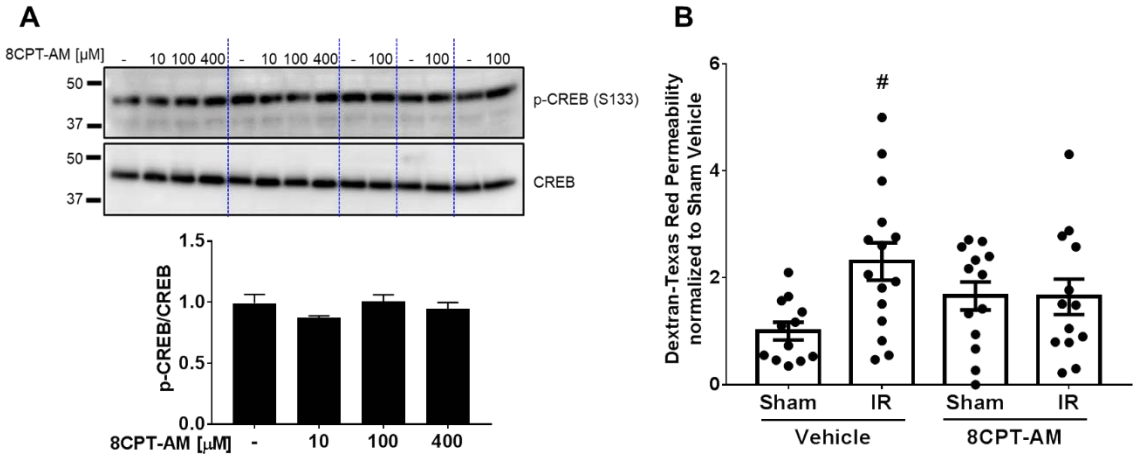

Figure 2.S1 8CPT-AM Reverses Ischemia Reperfusion-Induced Permeability. A. 8CPT-AM was intravitreally injected in mice at various concentrations to determine if the PKA pathway is activated. The different doses of 8CPT-AM did not cause a difference in CREB phosphorylation in comparison to control, $n \geq 2$. **B.** Retinal ischemia in mice was achieved by increasing intraocular pressure with PBS delivered to the anterior chamber to prevent blood flow for 90 min. 48 hours later vehicle or 8CPT-AM at 100µM (278ng) was delivered by intravitreal injection and permeability was determined by measuring accumulation of 70kDa Dextran-Texas Red in the retina. Results are expressed as the mean relative to the control $\pm$ S.E.M., Bonferroni's post hoc test $^{\#}p < 0.05$ compared to vehicle sham.

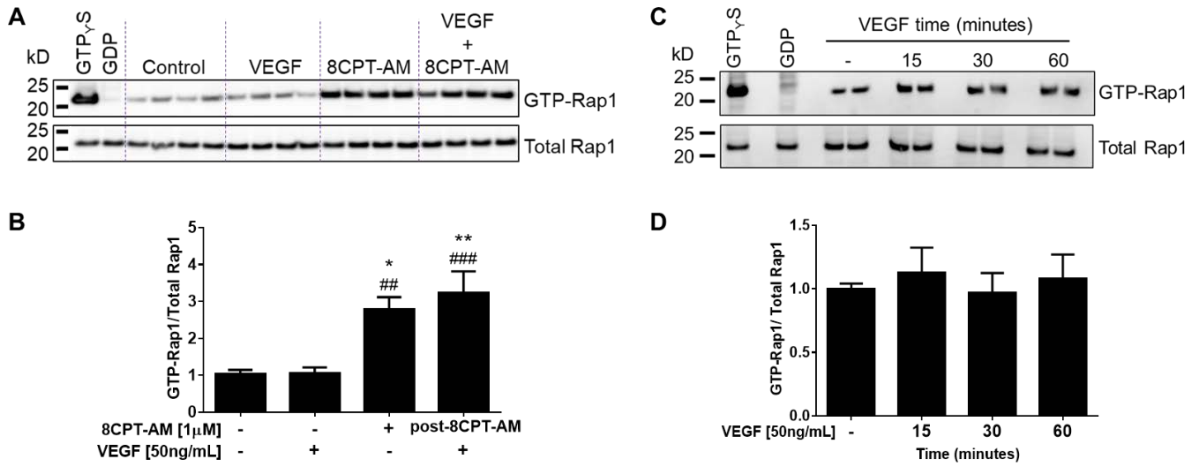

Figure 2.S2 VEGF Does Not Alter Basal GTP-Bound Rap1 Levels in BREC. **A.** GTP bound Rap1 was determined by GTP-bound Rap1 capture assay using GST-RalGDS RBD. VEGF (50ng/mL) was added for 24 hours prior to 8CPT-AM (1μM) for 30 minutes. Quantification shown in **B.** with a total n≥ 8. **C.** VEGF time course, 15 to 60 minutes, was performed on BREC. GTP-bound Rap1 levels were determined using the capture assay and quantification shown in **D.**

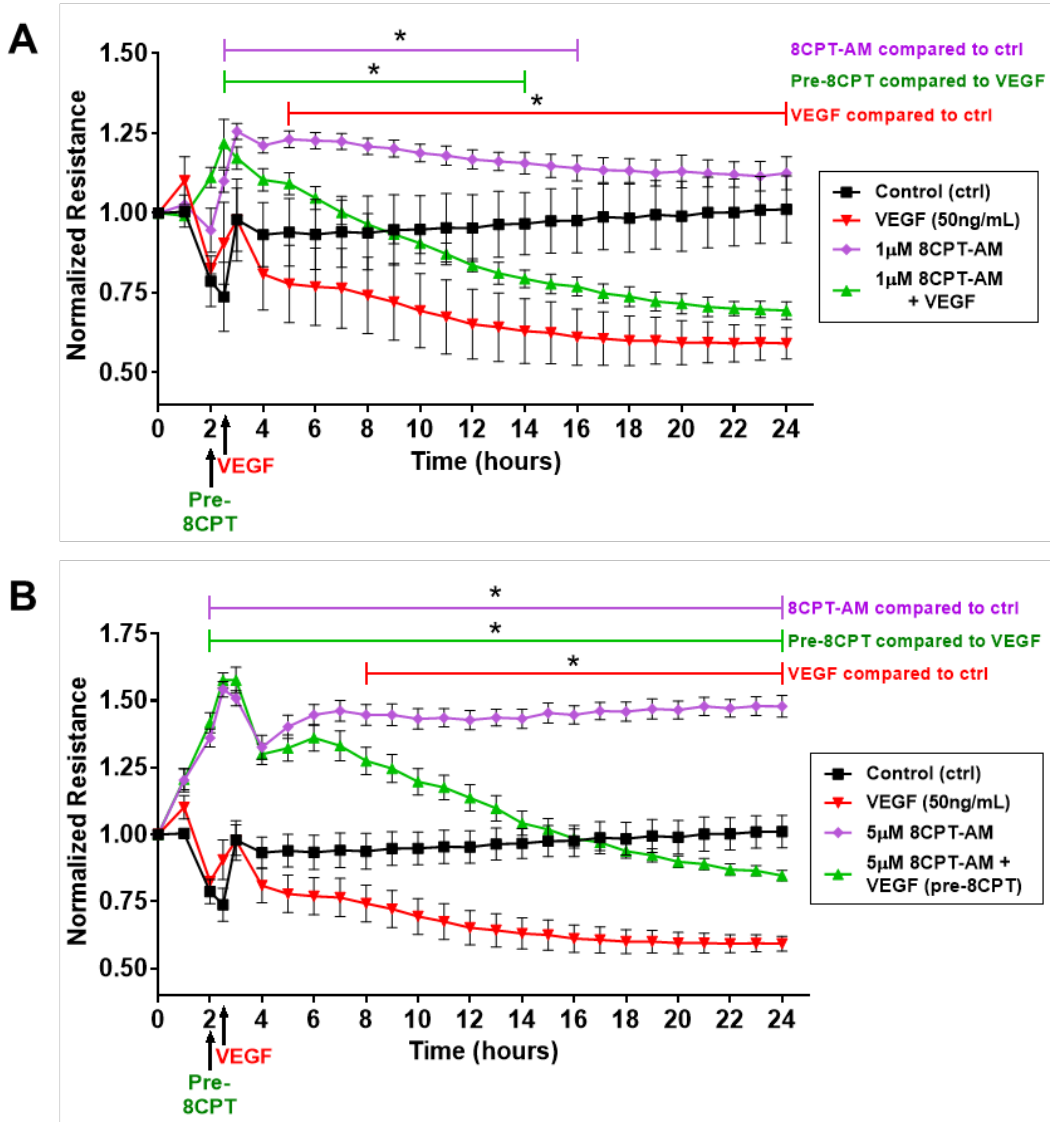

Figure 2.S3 Higher Concentration of 8CPT-AM Maintains a High Resistance in BREC. BREC were seeded on 8W10E+ arrays and TEER was measured continually every hour on the ECIS Z-theta instrument. 8CPT-AM at the different concentrations 1µM and 5µM maintained BREC TEER statistically significant higher than controls. **A.** 8CPT-AM (1µM) pre-treatment is significantly different from VEGF treatment in BREC for 14 hr ($^{*}p<0.0001$). **B.** 8CPT-AM (5µM) pre-treatment is significantly different from VEGF for at least 24 hr ($^{*}p<0.0001$).

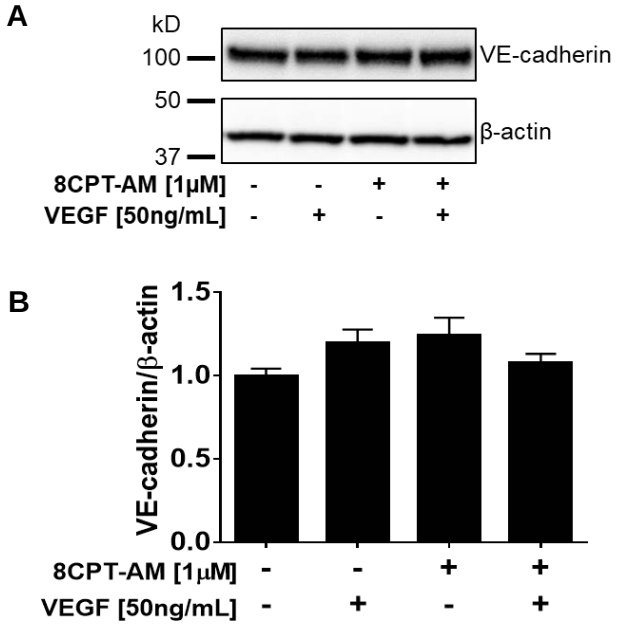

Figure 2.S4 8CPT-AM Does Not Alter VE-Cadherin Protein Expression. Changes in VE-cadherin total protein expression with VEGF or 8CPT-AM were measured using western blot. No changes in VE-cadherin expression were observed in any of the experimental conditions. Results are expressed as the mean relative to the control $\pm$ S.E.M., $n \geq 4$ per group with analysis by One-Way ANOVA with Bonferroni post hoc test.

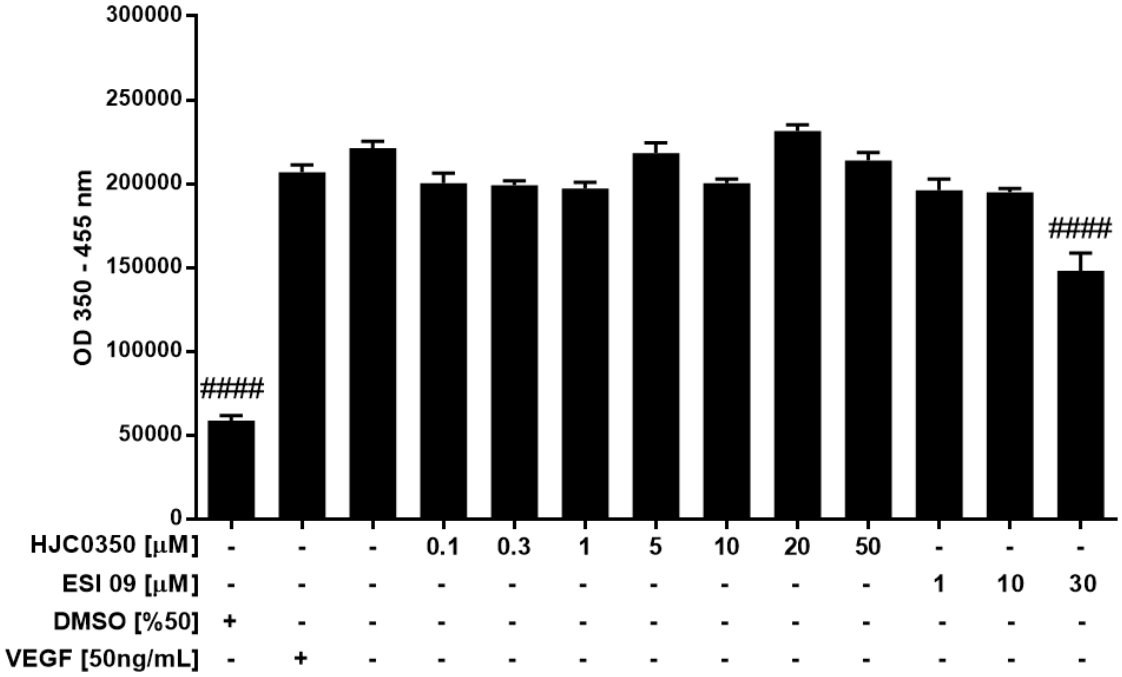

Figure 2.S5 EPAC 2 Inhibitor, HJC0350, is Not Cytotoxic to BREC. BREC were incubated for 1.5 hours with 50% DMSO, VEGF (50ng/mL) and different concentrations of HJC0350 and ESI 09, an EPAC1 and EPAC2 inhibitor. The viability of cells was measured with a fluorogenic, cell-permeant, peptide substrate (GF-AFC). Results are expressed as the mean relative to the control with a total of $n \geq 4$ one-way ANOVA analysis and Bonferroni post-test $^{\#\#\#\#}P<0.0001$.

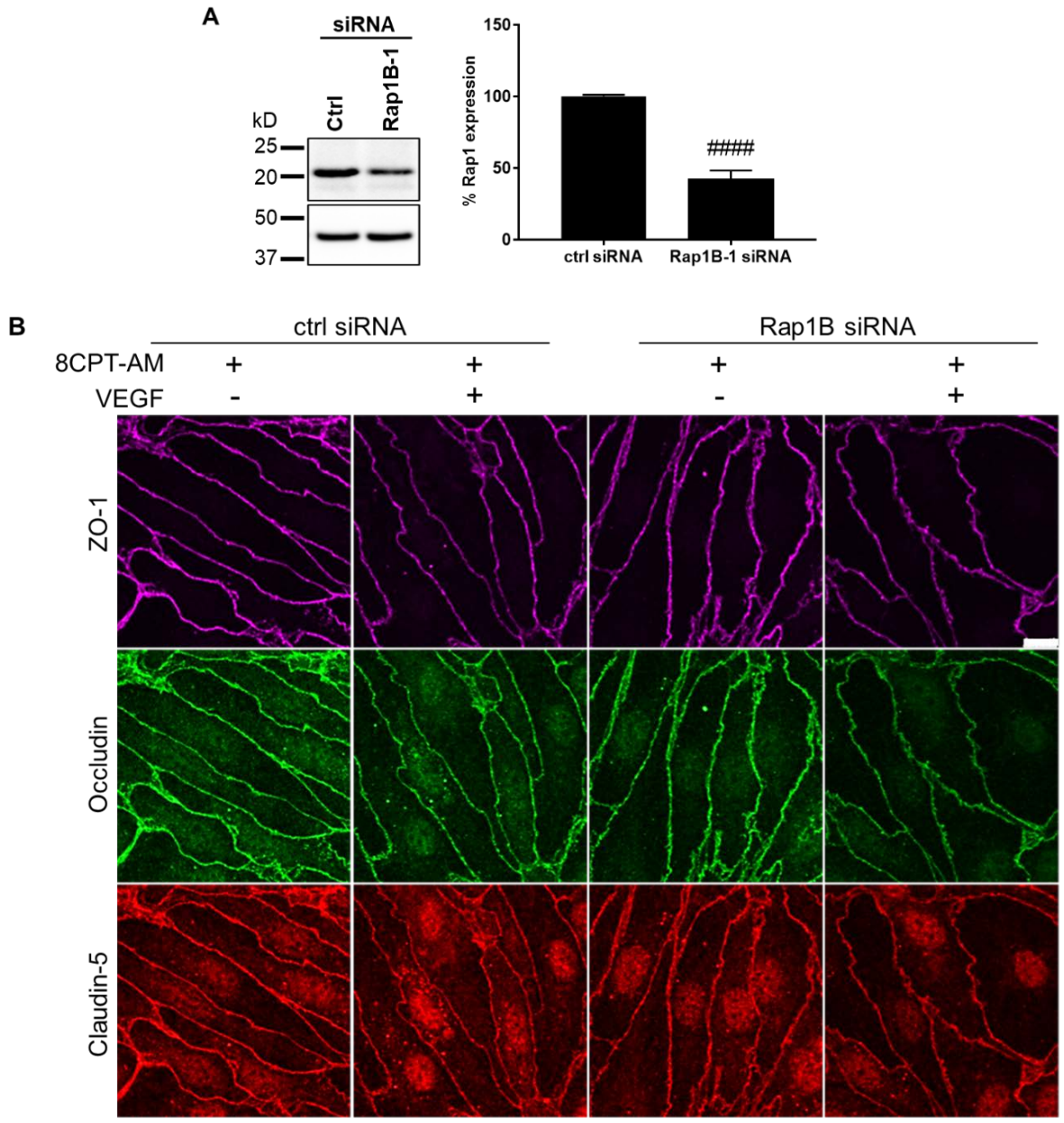

Figure 2.S6 8CPT-AM Restores Tight Junction Organization in Rap1B Knockdown BREC. A. Western blot shows a 58% Rap1 knockdown with 100nM Rap1B-1 siRNA, Student's t-test $^{\#\#\#\#}p < 0.0001$, $n \geq 6$. **B.** Immunofluorescence staining of TJ proteins ZO-1, occludin, and claudin-5 was performed to assess the organization of TJ proteins after Rap1B knockdown and treated with 8CPT-AM for a total time of 1.5 hours or VEGF (50ng/mL) for 1 hour. Scale bar, 10µm.

CHAPTER 3

Elucidating the Molecular Mechanism of aPKC Regulation of VEGF-Induced Retinal Vascular Endothelial Permeability

3.1 Abstract

VEGF signaling contributes to the pathology of eye diseases such as diabetic retinopathy (DR) by altering retinal vascular permeability. In VEGF signaling, both classical Protein Kinase C (cPKC) and atypical Protein Kinase C (aPKC) are activated. Recent studies have shown that inhibitors of aPKC isoforms zeta (ζ) and lambda (λ) block both VEGF and proinflammatory cytokine TNF-α-induced permeability. Moreover, studies in our lab have identified small molecule inhibitors specific for aPKC that prevent BRB breakdown. Remarkably, our data showed that these drugs effectively block both VEGF and TNFα-induced permeability, both in vitro and in vivo. However, the molecular mechanism by which aPKC regulates permeability remains unknown. The purpose of the present study is to identify downstream substrates of aPKC that are activated in the presence of VEGF and that induce changes to the retinal vascular permeability that result in loss of the BRB. To further explore the mechanism of VEGF-aPKC signaling, mass-spectrometry was used to identify phosphorylation changes regulated by VEGF and aPKC. Analysis of the phosphoproteome in primary retinal endothelial cell culture identified 1,724 proteins. From these 1,724 proteins, 107 proteins showed a 25% phosphorylation change in response to VEGF and were repeated in more than one mass spectrometry analysis. Protein interaction networks were developed using Cytoscape, an open source software for visualizing

protein interactions. We identified a subnetwork consisting of the endothelial specific ras interacting protein, rasip1, and small GTPase proteins EPAC1 and Rap1. For future studies, we will focus on the role of aPKC and the EPAC-Rap1-rasip1 pathway to better understand the mechanisms involved in retinal vascular permeability. This research has the potential to provide strong mechanistic support for the use of aPKC inhibitors to treat retinal vascular permeability in a host of diseases, including DR.

3.2 Introduction

Elevated growth factors such as vascular endothelial growth factor (VEGF) and pro-inflammatory cytokines drive pathological changes in the permeability state of the blood-retinal barrier (BRB) during diseases like diabetic retinopathy [231]. Diabetic retinopathy (DR) is an eye complication that causes damage to all the cells of the retina. DR is a complication of prolonged diabetes that affects people with both type 1 and type 2 diabetes, and is the leading cause of vision loss in people with diabetes [232]. An estimate of more than 200 million people have diabetes worldwide and about one third of these individuals show signs of DR [233]. It is estimated that by 2030, the prevalence of diabetes will double worldwide. This means that in the United States alone, an estimated 55 million Americans will have diabetes and 18 million will show signs of DR, costing the country more than $600 billion [234]. Available treatments for DR include photocoagulation, corticosteroids, and the most recently developed anti-VEGF therapies, which improve vision in about 40% of patients [232, 235]. However, these treatments have secondary complications, are invasive, inefficient, and are administered in later stages of the disease pathology, when vision has already been severely compromised. Thus, understanding the mechanisms involved in regulating retinal endothelial permeability will allow us to develop early detection methods, prevention techniques, and additional treatments against DR.

The VEGF family is comprised of several cytokines and receptors, which are fundamental in angiogenesis, vasculogenesis, endothelial cell biology, and vascular permeability. Mammals possess five VEGF isoforms: VEGF-A, -B, -C, -D, and PIGF (placenta growth factor) [236]. Additionally, several of these isoforms have splice variants, for example, VEGF-A has nine. The VEGF ligands bind with varying affinities to receptor tyrosine kinases (RTKs) called VEGF receptors (VEGFR) [237]. The VEGFRs consist of VEGFR1, also known as Fms-like tyrosine kinase-1 (Flt-1); VEGFR2, also known as fetal liver kinase-1(Flk-1) or kinase insert domain containing receptor (KDR) in human; and VEGFR3, also known as Fms-related tyrosine kinase 4 (FLT-4) [238]. The various VEGF isoforms and receptors have distinct roles. The most widely studied VEGFs are VEGF-A and its splice variant VEGF-A (165), both of which signal via the VEGFR2 to promote angiogenesis.

In the vitreous of patients with leaky retinal blood vessels, elevated levels of VEGF and other pro-inflammatory cytokines are observed [239-241]. VEGF is known to drive both proliferation and vascular permeability. Ischemia in diabetic retinas causes an upregulation of chemokines that activate macrophages and microglia. Activated macrophages secrete angiogenic factors such as TNF-α, which can increase new vessel formation [242]. In addition, upregulation of TNF-α and macrophages can induce endothelial cells to release chemokines, such as monocyte chemoattractant protein-1 (MCP-1), VEGF, and interleukin-8 (IL-8) [243]. Another contributor to hypoxic conditions is the hypoxia inducible factor-1α and β (HIF-1α/β) complex which translocates to the nucleus, binds to the hypoxia response element (HRE) and upregulates VEGF transcription [244, 245]. Elevated levels of VEGF then increase angiogenesis and vascular permeability through both transcellular and paracellular pathways.

Studies focusing on the role of VEGF signaling in DR have elucidated some of its pathophysiology. VEGF-A can signal through either VEGFR1 or VEGFR2. The predominant secreted isoform, VEGF-A(165), binds VEGFR2, triggering dimerization of the receptor and activation of the cytoplasmic domain tyrosine kinase catalytic activity, resulting in phosphorylation of the tyrosine (Y) residues [246]. This leads to activation of several downstream signaling pathways that regulate proliferation, migration, survival, angiogenesis, and permeability [247]. The VEGFR2 tyrosine phosphorylation sites studied thus far include, but are not limited to, Y951, Y1054, Y1059, Y1214, and Y1175. The phosphosites Y951, 1054, and 1059 are located in the receptor's kinase domain, while Y1214 and 1175 are found in the receptor's C-terminus [248]. Briefly, phosphorylation of Y951 serves as a binding site for proteins containing the Src Homology 2 (SH2) domain and has a role in regulating pathological angiogenesis through the binding of T cell-specific adapter molecule (TSAd) [249]. The autophosphorylation sites Y1054 and Y1059 are required for maximal kinase activity [250]. The autophosphorylation sites Y1214 and Y1175 serve as binding sites for SH2 domain proteins, which in turn activate several signal transduction pathways that regulate angiogenesis, vasculogenesis, cell proliferation, survival, and permeability [246].

Studies of VEGF signal transduction in endothelial cells have revealed that increase phosphorylation of tight junctional proteins like occludin and ZO-1 are associated with increased permeability [251]. In accordance with the above observations, diabetic mice show an increase in occludin phosphorylation, and VEGF intravitreal injection in rats increases ZO-1 phosphorylation in the retina [216, 251]. Studies in BREC show that VEGF signaling activates the protein kinase C beta, PKCβ, which phosphorylates occludin at serine (S) 490 [216]. This leads to ubiquitination and endocytosis of occludin, fragmentation of tight junctions, and

ultimately an increase in permeability [74]. Similarly, *in vivo* studies show that VEGF signaling induces PKCβ activation which phosphorylates S490 occludin [94]. Phosphorylation of S490 occludin is required for retinal neovascularization and retinal endothelial cell proliferation [96]. Additionally, recent studies have demonstrated that VEGF-induced permeability requires activation of atypical PKC (aPKC) [214], (Figure 3.1).

The serine/threonine protein kinases, PKCs, belong to the AGC kinase super family [252]. The PKC family is divided into 3 subfamilies: classical PKC (cPKC), novel PKC (nPKC), and atypical PKC (aPKC). The aPKC subfamily consists of two isoforms, zeta (ζ) and iota (ι), in humans, and lambda (λ) in mice. The classical PKCs, such as PKCβ, are activated by diacylglycerol **(**DAG) and calcium, while the novel PKCs are activated by DAG, but are insensitive to calcium. The aPKCs are insensitive to both calcium and DAG [253]. Rather, the aPKCs are activated via the phosphatidylinositol 3-kinase pathway (PI3K) pathway, which activates the PH domain-dependent kinase 1 (PDK1). PDK1 can directly phosphorylate aPKC at the C-terminus [253]. Phosphorylation of Thr410/Thr412 on PKCζ/ι by PDK1 liberates the pseudo-substrate domain, allowing autophosphorylation of Thr560/Thr555, which results in a fully active kinase [254]. For a complete review of the PKC family and subfamilies, refer to [252].

Our lab has developed small molecule inhibitors specific for aPKC that prevent BRB breakdown. Remarkably, our data showed that these drugs effectively block both VEGF and TNFα-induced permeability, both *in vitro* and *in vivo* [214]. However, the molecular mechanisms of these aPKC inhibitors remain unclear. Mass-spectrometry and iTRAQ labeling were used to identify and characterize the effectors of aPKC, which was activated in response to the presence of VEGF. The phosphoproteome performed using BREC, identified 1,724 unique

phosphoproteins and 107 phosphoproteins within the criteria of a ~25% phosphorylation change that were repeated in at least 2 out of 3 experiments. These studies suggest a molecular association between aPKC, small GTPases, and rasip1 in regulating VEGF-induced retinal vascular endothelial permeability.

3.3 Methods:

3.3.1 Reagents: Recombinant human VEGF165 was purchased from R&D Systems (Minneapolis, MN, USA). PKCζ/ι myristoylated pseudosubstrate inhibitor was purchased from Calbiochem (Gibbstown, NJ, USA). Small molecule aPKC inhibitors were purchased from ChemBridge Corporation (San Diego, CA, USA), Sigma-Aldrich (St. Louis, MO, USA) or synthesized by Apogee, Inc. (Hershey, PA, USA).

3.3.2 Cell Culture: Bovine retinal endothelial cells (BREC) were used for the mass spectrometry analysis. Briefly, BREC were grown on plates that were coated with 1ug/cm^2 fibronectin 30 minutes prior to seeding cells. BREC were grown to 95% confluence in MCDB-131 medium, supplemented with 10% fetal bovine serum (FBS), 22.5 µg/mL endothelial cell growth factor, 120 µg/mL heparin, 0.01 mL/mL antibiotic/antimycotic. Then, cell culture media was changed to stepdown media, MCDB-131 supplemented with 1% FBS, 0.01 mL/mL antibiotic/antimycotic, and 100 nmol/L hydrocortisone, for 48 hours prior to experiment. The experimental cell culture set ups were: a) Control, consisting of BREC cells with vehicles, b) BREC cells incubated with VEGF, c) BREC cells incubated with aPKC inhibitor 30 minutes prior to VEGF for 15 minutes, and d) BREC cells incubated with aPKC inhibitor only.

3.3.3 Mass Spectrometry Based Phosphoproteomics: The iTRAQ labeling, TiO_2 enrichment, and mass spectrometry procedures were conducted at Wayne University under the supervision of Dr. Paul. M. Stemmer. First, BREC were grown to confluence and stepdown for 48 hours, then

treated with VEGF, aPKC inhibitor (diMeO), or treated with both diMeO+VEGF. The cell lysate samples were labeled with isobaric tag for relative and absolute quantitation (iTRAQ), which is a non-radioactive isotope. Then, phosphorylated peptides were enriched with titanium dioxide (TiO_2). For protein quantification and identification, the matrix-assisted laser desorption/ionization (MALDI) time-of-flight (TOF) was used. This is a soft ionization and broad mass range technique which utilizes a laser energy absorbing matrix to create ions from macromolecules and minimize molecule fragmentation. The time of flight mass spectrometer separates the molecules based on the time it takes them to travel through the tube and reach the detector. The results from the mass-spectrometry were analyzed using the Scaffold proteome software versions 4 and PTM. Criteria for significant phosphorylation changes induced by VEGF were determined if the change was greater than 0.6 log base 2 relative to control and were repeated in at least 2 out of 3 experiments.

The mass spectrometry results are based on log base 2 (log_2)
Explanation $log_2(1) = 0$
$Log_2(1.5) = 0.6$
Our cut off at 0.25
$log_2(x) = 0.25 = 2^{0.25}$ = **1.189**

The formulas used on excel for the 2 different categories and 2 subcategories are the following:

Table 3.1 Excel Equations for Categories 1 and Subcategories 2
1A and 1B = IF(AND(V>0.25,V+I>0.25),"1A",IF(AND(V<-0.25,V+I<-0.25), "1B","""))
2A AND 2B = IF(AND(V>0.25, V/2>V+I), "2A", IF(AND(V<-0.25, V/2<V+I),"2B","""))
V=VEGF, V+I = VEGF + aPKC inhibitor

Table 3.2 Definitions of Categories

Categories	**Description**
1A	Phosphorylation increased with VEGF
1B	Phosphorylation decreased with VEGF
2A	Phosphorylation increased with VEGF and was reversed by aPKC inhibitor
2B	Phosphorylation decreased with VEGF and was reversed by aPKC inhibitor

3.3.4 Cytoscape Analysis: Cytoscape is an open source platform that allows for visual protein interaction network models. The plug-ins are software components that add specific features to the software being utilized. The plug-in used for visualizing protein-protein interactions using the mass spectrometry results was the Michigan Molecular Interaction (MiMI). The MiMI plug-in retrieves molecular interaction information from several databases, including BIND, DIP, HPRD, RefSeq, SwissProt, IPI and CCSB-HI1 and merges it into one location, the MiMI database [255]. The combination of Cytoscape and the MiMI plug-in allow the display of protein interaction network(s).

Western Blot: The western blot assay was performed as described previously in Chapter 2 Methods (Section 2.3.8, page #44).

***In Vivo* Permeability Assays:** The permeability assay was performed as described previously in Chapter 2 Methods (Section 2.3.3, page #41).

***In Vitro* Permeability Assay:** The permeability assay was performed as described previously in Chapter 2 Methods (Section 2.3.4, page #42).

3.3.5 Immunoprecipitation: Immunoprecipitation was utilized to detect the aPKC-pThr560 site and phosphoserine rasip1 in BREC treated with VEGF. The lysate was centrifuged at 14,000 × *g* for 10 min, and the supernatant was transferred to another microcentrifuge tube. 750 ug of protein was subjected to a preclear with 100 µl of 1:1 slurry of Protein G-SepharoseTM 4 Fast Flow (GE Healthcare) for 1 h. After brief micro-centrifugation the supernatant was incubated with either 5 ug aPKC Ab (C-20) or rasip1 Ab for 2 h. Protein G beads were added, followed by further incubation for 1 h. The beads were recovered by centrifugation at 1500 × *g* for 1 min and washed four times with 1 ml of lysis buffer. Proteins bound to Protein G were eluted by boiling in Laemmli buffer for 5 min then used to Western blot, as described above.

3.4 Results

3.4.1 VEGF-Induced Permeability Requires Activation of Atypical PKC. Permeability induced by VEGF signaling is known to activate PKCβ, which phosphorylates occludin and results in ubiquitination and endocytosis of occludin [216]. Inhibitors of PKCβ partially block VEGF-induced permeability, suggesting additional kinases are involved in VEGF-induced permeability. Recent studies show that in addition to PKCβ, aPKC are activated in the presence of VEGF [214]. Activation of aPKCs, PKCζ/ι, is determined by an increase in phosphorylation of the phosphosites pThr560/Thr555 and pThr410/Thr412 in PKCζ/ι. To determine if VEGF activates aPKC, a time response of VEGF was performed in rats. Rats were intravitreally injected with VEGF (50 ng/mL), and after 15 or 30 minutes, retinas were harvested and prepared for immunoblotting, (Figure 3.1.A). The data show that VEGF induces phosphorylation of pThr560/Thr555 PKCζ/ι in the retina after 15 minutes and 30 minutes (Figure 3.1.A) and pThr410/Thr412 PKCζ/ι (Figure 3.1.B). Similarly, BREC stimulated with VEGF show an increase in aPKC phosphorylation (Figure 3.1.C).

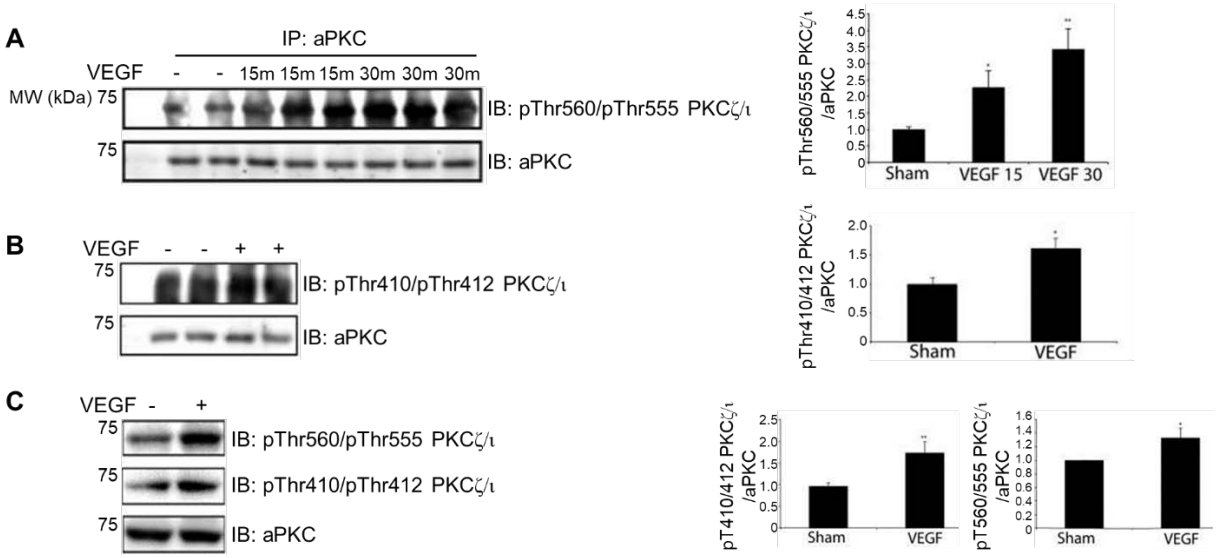

Figure 3.1. VEGF Signal Activates aPKC Both *In Vivo* and *In Vitro*. (A) VEGF was intravitreally injected for the indicated time and retinas were excised from Sprague-Dawley rats. aPKC was immunoprecipitated where indicated and immunoblotted for the autophosphorylation residue, pThr560/Thr555. **(B)** VEGF was intravitreally injected for 15 min and retinas were excised from Sprague-Dawley rats. aPKC was immunoprecipitated where indicated and immunoblotted for the pThr410/Thr412. Quantitation of the results (mean ± SEM) from three independent experiments and are expressed relative to the control with a total of n≥8. *, $p<0.05$, **$p<0.01$. **(C)** BREC were treated with VEGF (50 ng/mL) and lysates were subjected to immunoblotting for pThr410/Thr412 and pThr560/Thr555 PKCζ/ι, and aPKC. Quantitation of the results are expressed as the mean relative to the control, error bars represent ± SEM. n≥8. *, $p<0.05$, ** $p<0.01$. (Image adapted from Titchnell et al., 2012)

3.4.2 Inhibition of aPKC Blocks VEGF-Induced Permeability. Knockdown of aPKCi as well as expression of dominant negative aPKC and a peptide inhibitor to aPKC all block VEGF induced endothelial permeability [214]. The small molecule aPKC inhibitors were identified in a drug screen [214, 256] (Figure 3.2). Administration of VEGF intravitreally in rats induces a significant increase in retinal vascular permeability, but co-administration of VEGF and the aPKC inhibitor (aPKC-I-PD) blocks VEGF-induced permeability (Figure 3.3.A). Similarly, addition of VEGF on BREC increases permeability by 2.5-fold, and co-administration of VEGF and aPKC inhibitor (aPKC-PS) significantly blocks VEGF-induced permeability (Figure 3.3.B).

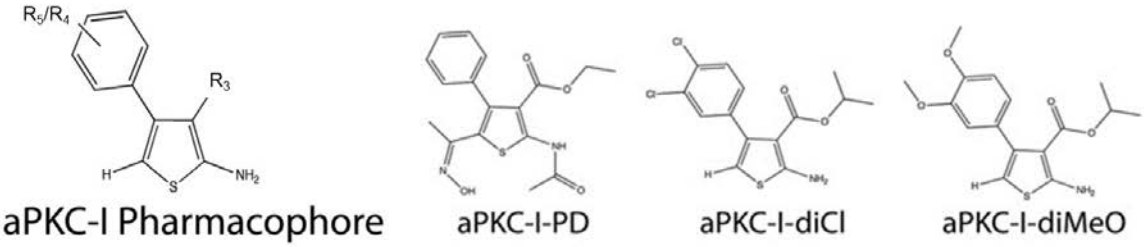

Figure 3.2 Identification of Small Molecule aPKC Inhibitors. An aPKC inhibitor pharmacophore (aPKC-I-Pharmacophore) depicts regions of substitutions R3, R4, and R5. Three drugs were identified and further studied: PD (pro-drug) (aPKC-I-PD), dichloro-substituted phenyl ring (aPKC-I-diCl), and dimethoxy-substituted phenyl-thiophene (aPKC-I-diMeO) (Figure from Titchenell et al., 2012).

3.4.3 1,724 Responsive Phosphoproteins Identified Downstream of VEGF Signaling. To identify effectors of aPKC downstream of VEGF signaling, mass spectrometry (MALDI-TOF) was used. BREC were set up into 4 experimental settings: 1) control, 2) VEGF, 3) VEGF+aPKC inhibitor (diMeO), and 4) diMeO alone. After harvesting the cells, labeling with iTRAQ and reducing the lysates with TiO_2, samples were subjected to MALDI-TOF mass spectrometry. From 3 separate mass spectrometry analyses, 1,724 unique phosphoproteins responsive to VEGF signaling were identified (Table 3.3.A). VEGF signaling induced both increases and decreases in phosphorylation. The proteins responsive to VEGF were divided into 2 main categories: 1A show a protein phosphorylation increase in the presence of VEGF and 1B show a protein phosphorylation decrease in the presence of VEGF. These categories were further subdivided into subcategories: 2A show proteins with phosphorylation increase in the presence of VEGF that was reversed by aPKC inhibitor and proteins in 2B show a phosphorylation decrease in the presence of VEGF that was reversed by aPKC inhibitor (Table 3.3.B).

To narrow our results, the total phosphoproteins in each of the 3 mass spectrometry analyses were compared to select proteins identified in more than one mass spectrometry analysis. We identified a total of 107 phosphoproteins that were present in more than one analysis and had a 25% phosphorylation change in the presence of VEGF. Like the results above, the results of the 107 phosphoproteins containing a total of 139 phosphosites, were arranged by categories (Table 3.4). In category 1A, 67 phosphosites were identified and from these 37 phosphosites were reversed in the presence of the aPKC inhibitor, subcategory 2A. In category 1B, 72 phosphosites were identified from which 47 were in category 2B.

3.4.4 Visual Protein-Protein Networks. Protein interactions of the 107 phosphoproteins were visualized using the Cytoscape bioinformatic tool and the plug-in MiMI. The input of the 107

phosphoproteins into Cytoscape gave us a large visual protein interaction network consisting of a total of 1,054 nodes and 21,069 Edges. The Nodes represent proteins and the Edges represent protein interactors (Figure 3.4). The use of Cytoscape allowed us to identify another subcategory of proteins that responded to VEGF signaling, those that had at least one site exhibiting increased phosphorylation and a site that showed a decreased in phosphorylation; these are represented by the color fuchsia. The octagon symbol represents phosphoproteinsin either category (1A or 1B) whose phosphorylation were reversed in the presence of the aPKC inhibitor.

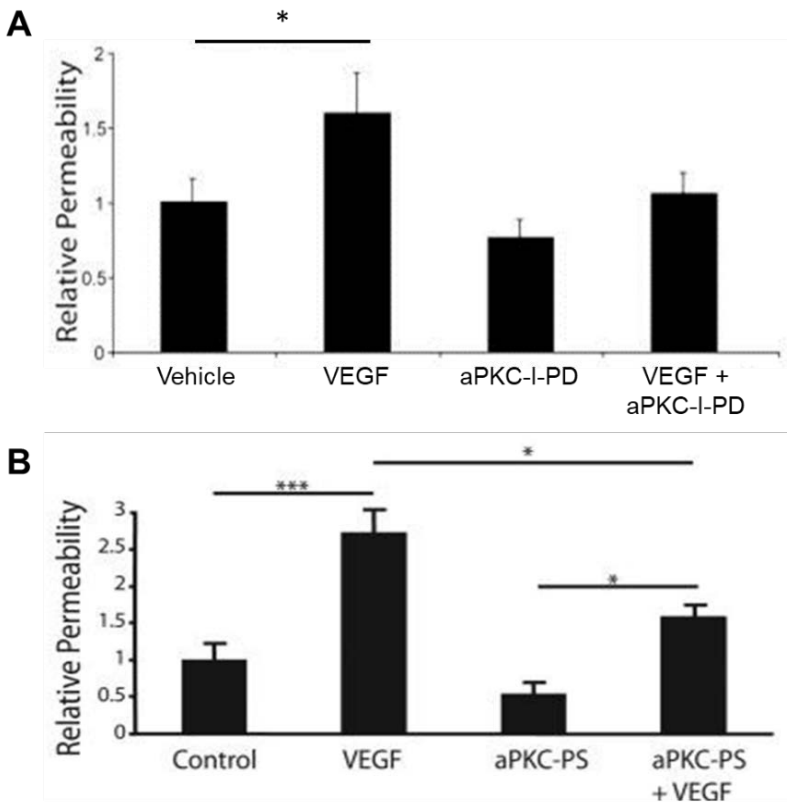

Figure 3.3. aPKC Inhibitors Block VEGF-Induced Permeability *In Vivo* and *In Vitro.* (A) aPKC-inhibitor blocks VEGF induction of retinal vascular permeability *in vivo.* Sprague-Dawley rats were injected intravitreally with (25 μM) aPKC-I-PD, aPKC inhibitor. After 3 hours, rats received a femoral vein injection of 45 mg/kg Evans blue. After 2 hours, animals were perfused with citrate/paraformaldehyde buffer for 2 min, retinas removed, dried and Evans blue extracted with formamide. Evans blue was quantified on a spectrophotometer and normalized to plasma levels measured pre-perfusion. Permeability was calculated and expressed as μl plasma/g dry weight/h circulation. The results are expressed as the mean relative to the control, error bars represent ± SEM. n≥8 per group, * $p<0.05$. **(B) aPKC peptide inhibitor blocks VEGF-induced permeability in endothelial cells.** BREC were grown to confluence on 0.4 μm Transwell filters then stepped-down for 24 h. BREC were treated for 30 min with 50 nM aPKC pseudo-substrate as a peptide inhibitor (aPKC-PS) prior to 30 min treatment with 50 ng/ml VEGF where indicated. Permeability of the monolayer to 70kDa RITC-Dextran was measured. n≥4. The results are expressed as the mean relative to the control, error bars represent ± SEM. ***, $p<0.001$; *, $p<0.05$. (Image adapted from Titchnell et al., 2012)

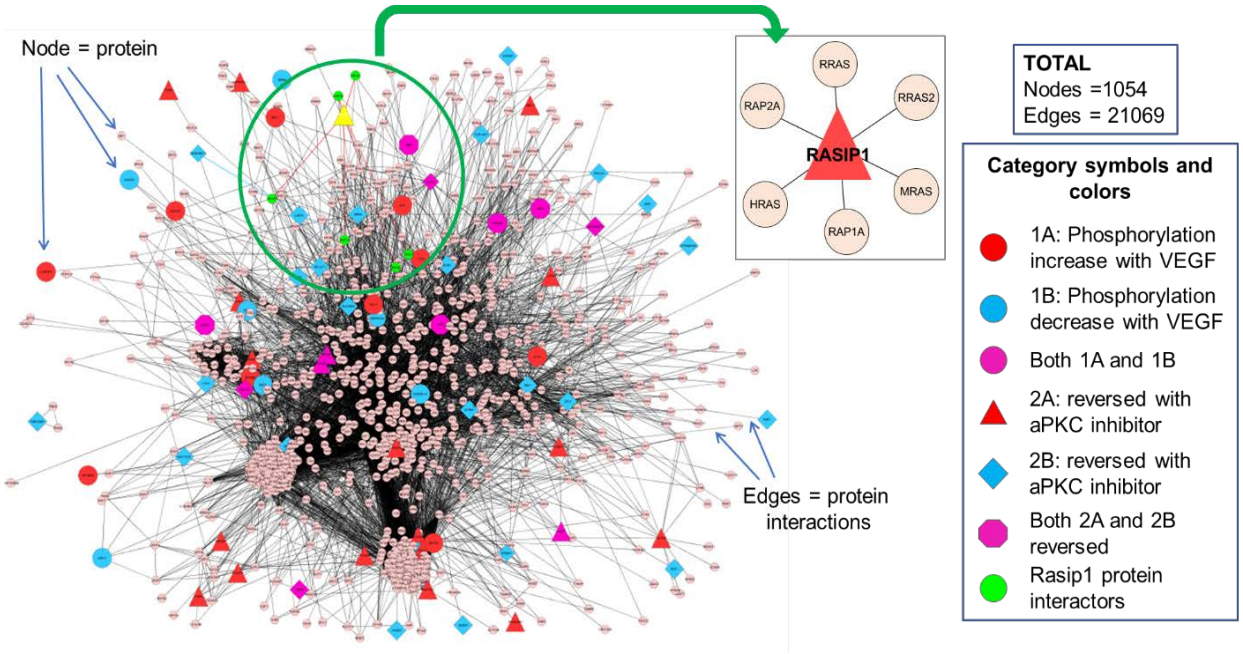

Figure 3.4 Visual Cytoscape Protein-Protein Interaction Network. Cytoscape was used to visualize protein interaction network of the 107 phosphoproteins. The nodes represent proteins comprise of the 107 phosphoproteins identified in Table 2, primary interactors which bind directly to our 107 proteins, and secondary interactors are proteins that interact with primary interactor proteins. Edges are the lines that connect 2 or more nodes and they depict protein interactions.

3.4.5 Rasip1 Protein Interaction Subnetwork.

To narrow our search within the large network, we used the plug-in named Enhance Search, which permits us to focus on one particular protein and identify its primary interactors. We applied this search to several of the 107 proteins with a major focus on the endothelial specific ras interacting protein 1 (rasip1). Rasip1 was of particular interest because it has been observed to play a significant role in vasculogenesis, lumenogenesis, and in endothelial cell barrier properties. Here, we observed that rasip1 interacts with 6 primary interactors which include Rap1A, Rap2A, and 4 isoforms of Ras. Additionally, secondary interactors of rasip1are EPAC1,

afadin, and SMARCA4, which are all from our 107-phosphoprotein list. Other secondary interactors of interest observed are ArhGAP29, EPAC2, RapGEF1 and 2, (Figure 3.5).

Total unique proteins obtained from all 3 mass spectrometry tests	1724		
(A) Experiments A-C	**Exp. A**	**Exp. B**	**Exp. C**
Total proteins	863	989	1164
Total Phosphosites	572	2322	1714
(B) Exp. A-C with 0.25 and -0.25 cut off based on $\log_2$ (1.189)			
1A: Protein phosphorylation increase in the presence of VEGF.	**132**	**296**	**177**
2A: Phosphorylation increase in the presence of VEGF was reversed by aPKC inhibitor.	73	114	115
1B: Protein phosphorylation decrease in the presence of VEGF.	**175**	**280**	**162**
2B: Phosphorylation decrease in the presence of VEGF was reversed by aPKC inhibitor.	106	179	110

Table 3.3 Mass Spectrometry Results (A) Three mass spectrometry analyses were performed, Exp. A through C. Each Exp. section shows the total proteins and the total phosphosites identified in each mass spectrometry analysis. **(B)** Phosphosites categories: Results are based on log base 2 ($\log_2$). Explanation: $\log_2(1) = 0$, $\text{Log}_2(1.5) = 0.6$, our cut off at 0.25; $\log_2(x) = 0.25 = 2^{0.25} = 1.189$. Definitions: Category 1A Phosphorylation increases in the presence of VEGF. Category 1B phosphorylation decreases in the presence of VEGF. Subcategories: Category 2A Phosphorylation increases in the presence of VEGF. Protein phosphorylation is reversed by aPKC inhibitor. Category 2B Phosphorylation decreases in the presence of VEGF. Protein phosphorylation is reversed by aPKC inhibitor.

107 phosphoproteins that overlap in Exp. A-C within the 0.25 and -0.25 criteria	Phosphosites
1A: Protein phosphorylation increase in the presence of VEGF	67
2A: Phosphorylation increase in the presence of VEGF. Protein phosphorylation reversed by aPKC inhibitor.	37
1B: Protein phosphorylation decrease in the presence of VEGF	72
2B: Phosphorylation decrease in the presence of VEGF. Protein phosphorylation reversed by aPKC inhibitor.	47
Total number of phosphosites	**139**

Table 3.4 Identification of 107 Phosphoproteins Repeated in Mass Spectrometry Analyses. Analysis of phosphoproteome in BREC identified 1,724 phosphoproteins responsive to VEGF. From these 1,724 phosphoproteins, 107 proteins had their phosphorylation reversed in the presence of the aPKC inhibitor. From these 107 phosphoproteins, 139 phosphosites were identified.

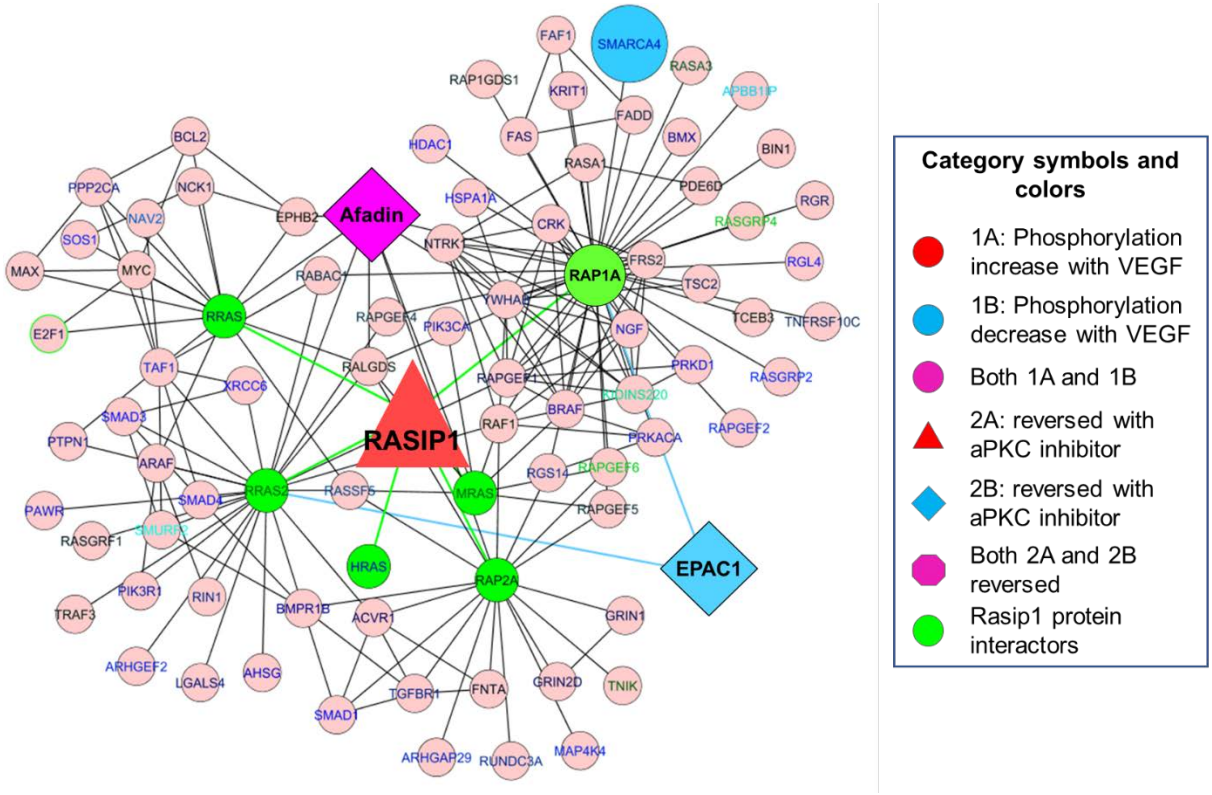

Figure 3.5 Visual Rasip1 Protein Interaction Subnetwork Obtained Through Cytoscape and MiMI Plugin. Cytoscape and plugin MiMI were used to visualize the protein-protein interaction network of rasip1. This analysis identified a subnetwork consisting of small GTPase proteins such as rasip1, EPAC, Rap1, and afadin.

3.4.5 Phosphosites Consistent in 2 or More Mass Spectrometry Results. The protein rasip1 shows an increase in phosphorylation at S419 in the presence of VEGF. Addition of the aPKC inhibitor shows a reversal of this phosphosite (Table 3.5.A). EPAC1 shows a decrease in phosphorylation on S864, which is reversed in the presence of the aPKC inhibitor. To determine if the rasip1 residue S419 is conserved among different species, we aligned the rasip1 bovine amino acid sequence 409-429. The sequence identity among species was above 90%; S419 was conserved in all 4 species (Table 3.6.B).

The phosphosite, S864, in EPAC is found within the RasGEF domain, and S419 in rasip1 is found within the FHA domain, (Figure 3.6.A). To determine if phosphorylation changes occur in rasip1 after VEGF addition we performed immunoprecipitation studies in BREC. Preliminary studies show that immunoprecipitated rasip1 from BREC lysates treated with VEGF has an increase in phosphoserine in comparison to control (Figure 3.6.B).

A

PROTEIN NAME	Phosphosites	Gene symbol	13 aa sequence	Category
rasip1	S419	RASIP1	SSARGG**S**PAPYVD	2A
rasip1	S419	RASIP1	SSARGG**S**PAPYVD	2A
EPAC1	S864	RAPGEF3	HSNVPL**S**PLRSRV	1B
EPAC1	S864	RAPGEF3	HSNVPL**S**PLRSRV	1B

B

	419	identity (%)
Bovine (409-429)	RGGNSSARGG**S**PAPYVDTFLN	Identity (%)
Human	RGGNSSGRGG**S**PAPYVDTFLN	97%
Mouse	RGGPSSSRGG**S**PAPYVDTFLN	93%
Rat	RGGPSSSRGG**S**PAPYVDTFLN	96%

Table 3.5 Rasip1 and EPAC Repeated Phosphosites Identified in the Mass Spectrometry. A. Rasip1 S419 was increased in the presence of VEGF and reversed with aPKC inhibitor (diMeO). EPAC1 S864 was decreased in the presence of VEGF and reversed in the presence of the aPKC inhibitor. These phosphosite changes were observed in two or more mass spectrometry results. **B.** Rasip1 bovine amino acid sequence from 409-429 were aligned with human, mouse, and rat rasip1 sequence and show a high sequence identity. The S419 is conserved in all 4 species.

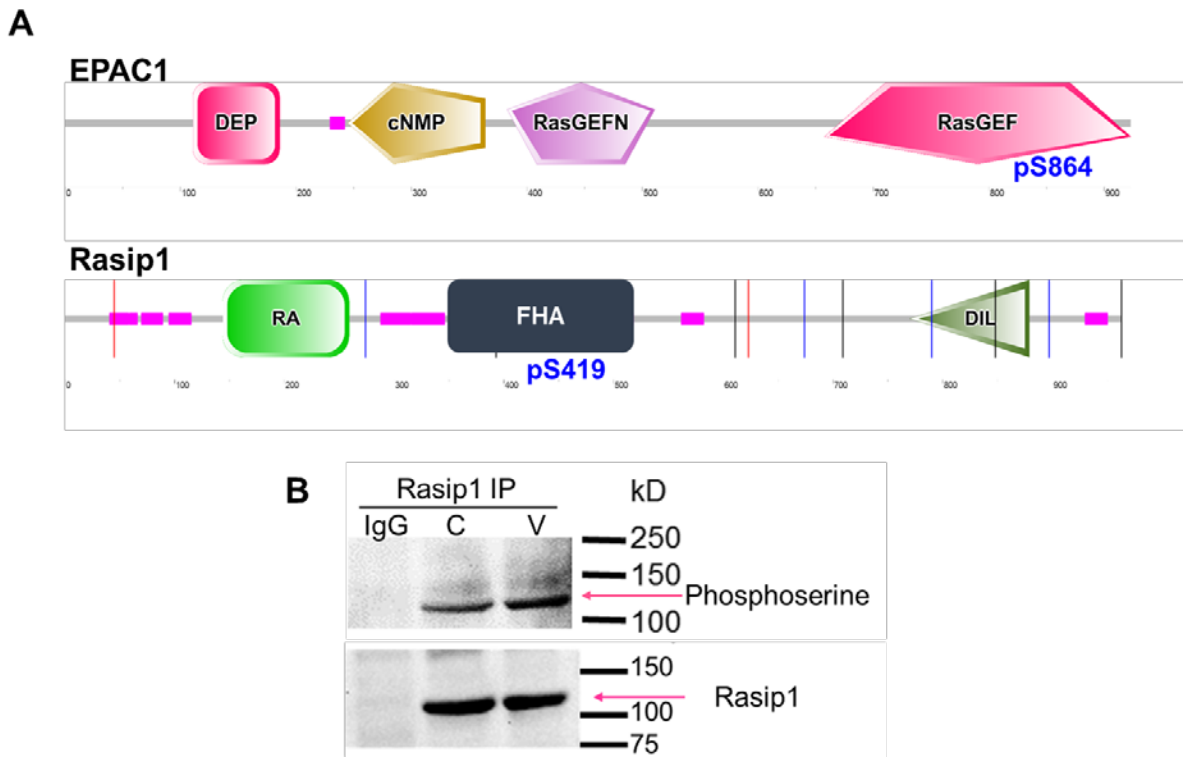

Figure 3.6 Locations of Phosphorylation Sites in EPAC1 and Rasip1 and IP of Phosphoserine-Rasip1. A. The S864 in EPAC1 is found on the RasGEF domain. The S419 in rasip1 is found in the Forkhead-associated (FHA) domain a.a. 334-539. **B.** Immunoprecipitation of rasip1 from BREC treated with VEGF 30 min and incubated with phosphoserine antibody, show an increase in serine phosphorylation. Rasip1 is 100 kD.

3.5 Discussion

The epidemic of diabetes in the United States and worldwide will lead to a higher incidence of diabetic retinopathy, demanding new means of early detection, prevention, and treatments. Diabetic macular edema remains the clinical outcome most closely linked to vision loss in DR. Therefore, it is imperative to understand and characterize the normal and aberrant mechanisms that regulate permeability in the BRB.

In the present study, we began to examine the mechanisms by which VEGF-aPKC signaling modulates retinal endothelial permeability. Here, we identified several phosphoproteins that responded to VEGF stimuli, and from these phosphoproteins, 107 were repeated in more than one mass spectrometry analysis. We identified specific phosphosites on both EPAC1 and rasip1 that were changed in the presence of VEGF and reversed in the presence of the aPKC inhibitor, suggesting that these changes in phosphorylation are regulated by aPKC activation. How these phosphorylation changes regulate the activity of either EPAC1 or rasip1 remains to be investigated. Moreover, the use of bioinformatic tools like Cytoscape and the plug-ins MiMI and Enhance Search identified several protein-protein interaction subnetworks, including one consisting of EPAC, rasip1, Rap1A, and afadin.

The proteins identified, EPAC, rasip1, Rap1A, and afadin, in the Cystocape-MiMI protein-protein interaction subnetworks validate our results from Chapter 2. As shown in Chapter 2, activation of the EPAC-Rap1 signaling pathway contributes to barrier properties of the BRB. Additionally, permeability induced by VEGF and/or TNF-α was blocked or reversed during EPAC-Rap1 signaling activation. Studies in HUVEC show that when active, Radil, a Rap1 effector, recruits the GTPase-activating protein, ArhGAP29, to the cell border. Here, it is responsible for downregulating small GTPase activity [205]. Activation of Rap1 recruits both

Radil and rasip1 to the cell border and rasip1 then binds to the Radil-ArhGAP29 complex and downregulate rhoA activity [146, 205]. The phosphorylation increase on rasip1-S419 under VEGF signaling led us to ask if VEGF decreased the interaction between Rap1 and rasip1. Preliminary co-immunoprecipitation studies showed that VEGF did not reduce Rap1-rasip1 interaction (data not shown). The mechanism of how VEGF inhibits rasip1 signaling remains unknown, but it is possible that since VEGF does not affect Rap1 and rasip1 interaction, it may affect rasip1-radil-ArhGAP29 interaction. This question should be addressed in the future via co-immunoprecipitation studies using rasip1 S419 point mutant constructs.

Another possibility as to how VEGF-induced phosphorylation of rasip1 inhibits its ability to help maintain the endothelial barrier is by blocking the interaction between rasip1 and the transmembrane protein Heart of Glass 1 (HEG1). Recently, de Kreuk et al., demonstrated that rasip1 moves to the cell border by binding to HEG1, and that loss of HEG1 prevents rasip1 localization at cell borders of HUVEC [202]. They also determined that the region Forkhead-associated (FHA) domain in rasip1, aa 334-539, is required to bind to HEG1. Interestingly, the phosphosite identified by our mass spectrometry, S419, falls within the FHA domain. Further studies will be required to determine if phosphorylation of rasip1-S419 affects rasip1 localization to the cell borders.

Overall, the mass spectrometry analyses identified 107 proteins that showed phosphorylation changes in the presence of VEGF and some of these phosphoproteins were reversed by the aPKC inhibitor. The subnetwork consisting of rasip1, EPAC, afadin, and Rap1A is only a small subset of the entire set of 107 phosphoproteins, and additional investigations should be performed on the additional proteins. These studies will facilitate our understanding of

the signal transduction mechanism of aPKC and rasip1 involved in retinal vascular permeability and potentially lead to new therapeutic options to control macular edema.

Chapter 4

Conclusions and Future Directions

Breakdown of the BRB occurs early in the development of DR, which contributes to the formation of lipid exudates, in addition to inducing hemorrhages, and macular edema [231, 257]. In ischemic diabetic retinas, permeability is observed, in addition to increased VEGF levels, new vessel formation, and inflammation [239]. Increased BRB permeability, combined with new vessel formation, angiogenesis, causes changes in the retina's homeostasis, resulting in neuronal cell death and ultimately vision loss [258]. Over the last three decades, investigations into DR have identified targets such as VEGF and mechanisms like inflammation that contribute to an increase in permeability. Identification of VEGF and its involvement in regulating angiogenesis led to the development of antibodies that block VEGF and the progression of angiogenesis [235, 259]. Additionally, administration of glucocorticoids shows a decrease in inflammation and edema, and improves visual acuity in patients [260, 261]. However, not all patients treated with anti-VEGF antibodies show improvement and glucocorticoid treatments are associated with secondary adverse complications, such as elevated intraocular pressure, glaucoma, and cataracts [262-264]. Therefore, additional investigation is required to identify new targets in DR, identify mechanisms that restore the BRB, and elucidate early DR mechanisms that will allow the development of early detection methods.

In this thesis, I investigated the mechanisms that regulate retinal endothelial barrier formation and maintenance. There were two main objectives in this thesis. The first objective,

addressed in Chapter 2, was to elucidate the role of the EPAC-Rap1 signaling pathway in barrier formation and maintenance. The second objective, in Chapter 3, was to identify novel VEGF targets and aPKC effectors involved in retinal vascular permeability. The summary of our findings and future directions are discussed in the section below.

Studies in endothelial cells, such as HUVEC, show that activation of the EPAC-Rap1 signaling pathway contributes to barrier properties. Administration of cAMP or cAMP analogs that specifically target EPAC, activate Rap1, which promotes endothelial barrier strengthening and shows a decrease in basal permeability [189, 201]. Additionally, activation of the EPAC-Rap1 signaling pathway has been observed to block permeability induced by platelet-activating factor (PAF) [190], TNF-α [187], and thrombin [187]. Mechanistically, activation of Rap1 recruits rasip1 to cell borders, rasip1 in turn binds to the Radil-ArhGAP29 complex and this interaction leads to downregulation of RhoA activity [146, 205]. Active RhoA is associated with VEGF, TNF-α, and thrombin-induced permeability [155]. When active, RhoA activates the Rho kinase, ROCK1/2, which stabilizes the phosphorylated state of myosin light chain (MLC) and promotes interaction between actin and myosin. These results in actin stress fiber formation and actomyosin contractility, which increases tension at cell junctions causing gaps [138, 265]. Inhibition of RhoA or ROCK ameliorates permeability [154, 266].

To our knowledge, the role of the EPAC-Rap1 signaling pathway in the retinal endothelial cells that form the iBRB, had not been investigated. Therefore, in Chapter 2, we investigated the role of the EPAC-Rap1 pathway in BREC and the retina. With the use of an improved cell membrane permeable cAMP analog, 8-pCPT-2´-O-Me-cAMP-AM (8CPT-AM), we investigated the role of the EPAC-Rap1 pathway in the BRB. Intravitreal administration of 8CPT-AM blocked VEGF+TNF-induced permeability in rats. In mice, activation of the EPAC-

Rap1 signaling pathway reversed IR-induced permeability. Similar to the results in HUVEC, we observed that activation of EPAC-Rap1 signaling decreased BREC basal permeability and blocked and reversed permeability induced by VEGF and TNF-α. These results suggest that the EPAC-Rap1 pathway contribute to the maintenance and restoration of the BRB.

Increase in retinal vascular permeability has been associated with disruptions to TJs, special cell-cell contacts which help regulate movement through the paracellular space. Studies in DR and VEGF-induced permeability show a reduction in the TJ protein occludin [267]. VEGF has been observed to cause phosphorylation of the TJ proteins occludin and ZO-1 [251, 268]. Mechanistically, VEGF signaling activates PKCβ, which phosphorylates occludin at S490. Phosphorylated occludin is followed by ubiquitination and endocytosis [216]. Additionally, TNF-α-induced permeability is associated with loss of ZO-1 and claudin-5 and discontinuous occludin staining at cell borders [206]. Therefore, we used immunofluorescent staining to evaluate the role of EPAC-Rap1 signaling on the TJ proteins ZO-1, claudin-5, and occludin in BREC. Our results show that under basal conditions, activation of EPAC-Rap1 signaling promotes continuous linear TJ staining at the cell borders. Additionally, activation of the EPAC-Rap1 signaling pathway blocks and reverses the TJ disruption induced by VEGF signaling. These data show that in BREC, the EPAC-Rap1 pathway confers barrier properties through stabilization and organization of the TJs at the cell borders. The specific mechanism of how activation of EPAC-Rap1 signaling regulates TJ assembly and stability at cell borders remains to be investigated. It is possible that TJ stability occurs through the scaffold protein afadin (AF-6), which is known to link junctional proteins to the cytoskeleton. In the presence of cAMP analogs, AF-6 staining has an increase in its continuity along cell-cell contacts [187], and it interacts with active Rap1, ve-cadherin and ZO-1 [269]. Additionally, active Rap1 is known to recruit KRIT-1

(CCM1), a junctional protein important in proper vascular function, which interacts with the AJ proteins p120-catenin and β-catenin. Loss of function mutations in KRIT1 result in vascular malfunctions [222]. Co-immunoprecipitation studies show that active Rap1 increases the interaction between KRIT-1 and AF-6 [222].

The results in Chapter 2 show for the first time that EPAC2 plays a role in regulating basal permeability. Inhibition of EPAC2 induces an increase in permeability that cannot be restored by 8CPT-AM treatment (a drug known to activate the EPAC pathway). Additionally, we show that Rap1B regulates basal permeability and the organization of TJs, which are disrupted in Rap1B knockdown BREC. However, addition of 8CPT-AM to Rap1B knockdown cells showed a decrease in permeability, blocked VEGF-induced permeability, and restored TJ organization at cell borders. We propose that additional Rap isoforms like the Rap2 and Rap1A are activated by 8CPT-AM and compensate for the lack of Rap1B. Further studies testing the roles of EPAC and Rap isoforms will allow us to identify specific differences in these isoforms and identify which ones contribute most to barrier formation and maintenance.

TNF-α signaling activates aPKC, which is associated with retinal endothelial permeability [270, 271]. Inhibitors towards aPKC block TNF-α-induced permeability [206]. Recently, it was found that VEGF-induced permeability also requires activation of aPKC [214]. Inhibitors that target aPKC block both TNF-α and VEGF-induced permeability, suggesting that aPKC represents a common node in both TNF-α and VEGF signaling. However, the specific mechanisms in VEGF-aPKC permeability are not known. In Chapter 3, our objective was to further investigate the mechanism of VEGF-aPKC pathway and identify aPKC effectors.

Our studies identified more than 1,700 unique phosphoproteins responsive to VEGF treatment from three independent mass spectrometry analyses. From the 1,724 proteins obtained,

107 phosphoproteins were observed in more than one analysis. We focused on the phosphosites that were changed with VEGF and reversed by the aPKC inhibitor, diMeO. We identified several of these proteins and focused on a subnetwork comprised of rasip1, Rap1A, EPAC, afadin, and the transcription factor, SMARCA4. We found that rasip1 is phosphorylated at S419 and EPAC is dephosphorylated at S864 in the presence of VEGF. The aPKC inhibitor reversed the phosphorylation changes induced by VEGF. The scaffold protein, afadin, showed both phosphorylation increases and decreases in the presence of VEGF, but only the decrease in phosphorylation induced by VEGF was reversed in the presence of the aPKC inhibitor.

The results from the mass spectrometry work open many possibilities for future studies. The most interesting is the analysis of rasip1-S419 and the construction of rasip1-S419 point mutants. Future studies will address the question of whether overexpression of rasip1-S419D leads to permeability and if rasip1-S419A prevents permeability. Additionally, our laboratory will investigate the mechanism of rasip1-S419. Currently, we know that active Rap1 recruits and binds rasip1, and binding to HEG1 localizes rasip1 at the cell membrane. Some questions to address would be if rasip1-S419D blocks interaction between rasip1 and HEG1 or the interaction with the radil-ArhGAP29 complex in BREC.

In conclusion, the studies presented in this thesis expand our knowledge on the role of EPAC-Rap1 signaling in promoting retinal endothelial barrier properties via TJs assembly at cell borders. We, also identified that EPAC2 and Rap1B contribute to basal endothelial barrier regulation. Rap1B regulates TJ cell border organization. We also identified several phosphoproteins responsive to aPKC. Inhibition of aPKC blocks both VEGF and TNF-α-induced permeability, thus aPKC effectors might represent common nodes between VEGF and TNF-α

signaling. Understanding the mechanisms that regulate barrier properties are of significance in developing novel ways to treat pathologies with leaky vessels.

References

1. Ehrlich, M., *Königthum und staatswesen der alten Hebräer : nach biblischen und talmudischen quellen bearbeitet*. 1885, Steinamanger: Gedruckt bei J. v. Bertalanffy. 120 p.
2. Saunders, N.R., et al., *The rights and wrongs of blood-brain barrier permeability studies: a walk through 100 years of history.* Front Neurosci, 2014. **8**: p. 404.
3. Palm, E., *On the occurrence in the retina of conditions corresponding to the blood-brain barrier.* Acta Ophthalmol (Copenh), 1947. **25**(1): p. 29-35.
4. Ashton, N. and J.G. Cunha-Vaz, *Effect of Histamine on the Permeability of the Ocular Vessels.* Arch Ophthalmol, 1965. **73**: p. 211-23.
5. Cunha-Vaz, J.G., M. Shakib, and N. Ashton, *Studies on the permeability of the blood-retinal barrier. I. On the existence, development, and site of a blood-retinal barrier.* Br J Ophthalmol, 1966. **50**(8): p. 441-53.
6. Antonetti, D.A., R. Klein, and T.W. Gardner, *Diabetic retinopathy.* N Engl J Med, 2012. **366**(13): p. 1227-39.
7. Hawkins, B.T. and T.P. Davis, *The blood-brain barrier/neurovascular unit in health and disease.* Pharmacol Rev, 2005. **57**(2): p. 173-85.
8. Zlokovic, B.V., *The blood-brain barrier in health and chronic neurodegenerative disorders.* Neuron, 2008. **57**(2): p. 178-201.
9. Nag, S., A. Kapadia, and D.J. Stewart, *Review: molecular pathogenesis of blood-brain barrier breakdown in acute brain injury.* Neuropathol Appl Neurobiol, 2011. **37**(1): p. 3-23.
10. Winkler, B.S., *Glycolytic and oxidative metabolism in relation to retinal function.* J Gen Physiol, 1981. **77**(6): p. 667-92.
11. Niven, J.E. and S.B. Laughlin, *Energy limitation as a selective pressure on the evolution of sensory systems.* J Exp Biol, 2008. **211**(Pt 11): p. 1792-804.
12. Yu, D.Y. and S.J. Cringle, *Oxygen distribution and consumption within the retina in vascularised and avascular retinas and in animal models of retinal disease.* Prog Retin Eye Res, 2001. **20**(2): p. 175-208.
13. Yao, H., et al., *The development of blood-retinal barrier during the interaction of astrocytes with vascular wall cells.* Neural Regen Res, 2014. **9**(10): p. 1047-54.
14. Wangsa-Wirawan, N.D. and R.A. Linsenmeier, *Retinal oxygen: fundamental and clinical aspects.* Arch Ophthalmol, 2003. **121**(4): p. 547-57.
15. Lutty, G.A., et al., *Development of the human choriocapillaris.* Eye (Lond), 2010. **24**(3): p. 408-15.
16. Hughes, S., H. Yang, and T. Chan-Ling, *Vascularization of the human fetal retina: roles of vasculogenesis and angiogenesis.* Invest Ophthalmol Vis Sci, 2000. **41**(5): p. 1217-28.
17. Penn, J.S., et al., *Vascular endothelial growth factor in eye disease.* Prog Retin Eye Res, 2008. **27**(4): p. 331-71.
18. del Toro, R., et al., *Identification and functional analysis of endothelial tip cell-enriched genes.* Blood, 2010. **116**(19): p. 4025-33.
19. Gerhardt, H., et al., *VEGF guides angiogenic sprouting utilizing endothelial tip cell filopodia.* J Cell Biol, 2003. **161**(6): p. 1163-77.
20. Siemerink, M.J., et al., *Endothelial tip cells in ocular angiogenesis: potential target for anti-angiogenesis therapy.* J Histochem Cytochem, 2013. **61**(2): p. 101-15.

21. Larrivee, B., et al., *Activation of the UNC5B receptor by Netrin-1 inhibits sprouting angiogenesis.* Genes Dev, 2007. **21**(19): p. 2433-47.
22. Patel-Hett, S. and P.A. D'Amore, *Signal transduction in vasculogenesis and developmental angiogenesis.* Int J Dev Biol, 2011. **55**(4-5): p. 353-63.
23. Frey, T. and D.A. Antonetti, *Alterations to the blood-retinal barrier in diabetes: cytokines and reactive oxygen species.* Antioxid Redox Signal, 2011. **15**(5): p. 1271-84.
24. Antonetti D.A, V.G.H.D., Lin C.M., *Vascular Permeability in Diabetic Retinopathy*, in *Diabetic Retinopathy*, E.J. Duh, Editor. 2008, Humana Press: Totowa, New Jersey.
25. Runkle, E.A. and D.A. Antonetti, *The blood-retinal barrier: structure and functional significance.* Methods Mol Biol, 2011. **686**: p. 133-48.
26. Anderson, J.M., C.M. Van Itallie, and A.S. Fanning, *Setting up a selective barrier at the apical junction complex.* Curr Opin Cell Biol, 2004. **16**(2): p. 140-5.
27. Facchini, L., A. Bellin, and E.F. Toro, *A mathematical model for filtration and macromolecule transport across capillary walls.* Microvasc Res, 2014. **94**: p. 52-63.
28. DeMaio, L., et al., *VEGF increases paracellular transport without altering the solvent-drag reflection coefficient.* Microvasc Res, 2004. **68**(3): p. 295-302.
29. Woodcock, T.E. and T.M. Woodcock, *Revised Starling equation and the glycocalyx model of transvascular fluid exchange: an improved paradigm for prescribing intravenous fluid therapy.* Br J Anaesth, 2012. **108**(3): p. 384-94.
30. Palade, G.E., *Transport in quanta across the endothelium of blood capillaries.* Anatomical Record, 1960. **136**(254).
31. Palade, G.E., *Structural modulations of plasmalemmal vesicles.* Journal of Cell Biology, 1968. **37**(3): p. 633-649.
32. Hofman, P., et al., *Lack of blood-brain barrier properties in microvessels of the prelaminar optic nerve head.* Invest Ophthalmol Vis Sci, 2001. **42**(5): p. 895-901.
33. Chow, B.W. and C. Gu, *Gradual Suppression of Transcytosis Governs Functional Blood-Retinal Barrier Formation.* Neuron, 2017. **93**(6): p. 1325-1333 e3.
34. Simionescu, N., *Enzymatic tracers in the study of vascular permeability.* J Histochem Cytochem, 1979. **27**(8): p. 1120-30.
35. Klaassen, I., C.J. Van Noorden, and R.O. Schlingemann, *Molecular basis of the inner blood-retinal barrier and its breakdown in diabetic macular edema and other pathological conditions.* Prog Retin Eye Res, 2013. **34**: p. 19-48.
36. Toda, R., et al., *Comparison of drug permeabilities across the blood-retinal barrier, blood-aqueous humor barrier, and blood-brain barrier.* J Pharm Sci, 2011. **100**(9): p. 3904-11.
37. Sagaties, M.J., et al., *The structural basis of the inner blood-retina barrier in the eye of Macaca mulatta.* Invest Ophthalmol Vis Sci, 1987. **28**(12): p. 2000-14.
38. Liebner, S., et al., *Correlation of tight junction morphology with the expression of tight junction proteins in blood-brain barrier endothelial cells.* Eur J Cell Biol, 2000. **79**(10): p. 707-17.
39. Farquhar, M.G. and G.E. Palade, *Junctional complexes in various epithelia.* J Cell Biol, 1963. **17**: p. 375-412.
40. Reese, T.S. and M.J. Karnovsky, *Fine structural localization of a blood-brain barrier to exogenous peroxidase.* J Cell Biol, 1967. **34**(1): p. 207-17.
41. D'Atri, F. and S. Citi, *Molecular complexity of vertebrate tight junctions (Review).* Mol Membr Biol, 2002. **19**(2): p. 103-12.
42. van Meer, G. and K. Simons, *The function of tight junctions in maintaining differences in lipid composition between the apical and the basolateral cell surface domains of MDCK cells.* EMBO J, 1986. **5**(7): p. 1455-64.

43. Zahraoui, A., D. Louvard, and T. Galli, *Tight junction, a platform for trafficking and signaling protein complexes.* J Cell Biol, 2000. **151**(5): p. F31-6.
44. Yeaman, C., K.K. Grindstaff, and W.J. Nelson, *Mechanism of recruiting Sec6/8 (exocyst) complex to the apical junctional complex during polarization of epithelial cells.* J Cell Sci, 2004. **117**(Pt 4): p. 559-70.
45. Gonzalez-Mariscal, L., S. Lechuga, and E. Garay, *Role of tight junctions in cell proliferation and cancer.* Prog Histochem Cytochem, 2007. **42**(1): p. 1-57.
46. Bauer, H.C., et al., *New aspects of the molecular constituents of tissue barriers.* J Neural Transm (Vienna), 2011. **118**(1): p. 7-21.
47. Dejana, E., *Endothelial cell-cell junctions: happy together.* Nat Rev Mol Cell Biol, 2004. **5**(4): p. 261-70.
48. Schneeberger, E.E. and R.D. Lynch, *The tight junction: a multifunctional complex.* Am J Physiol Cell Physiol, 2004. **286**(6): p. C1213-28.
49. Morita, K., et al., *Claudin multigene family encoding four-transmembrane domain protein components of tight junction strands.* Proc Natl Acad Sci U S A, 1999. **96**(2): p. 511-6.
50. Turksen, K. and T.C. Troy, *Barriers built on claudins.* J Cell Sci, 2004. **117**(Pt 12): p. 2435-47.
51. Furuse, M., et al., *Claudin-1 and -2: novel integral membrane proteins localizing at tight junctions with no sequence similarity to occludin.* J Cell Biol, 1998. **141**(7): p. 1539-50.
52. Amasheh, S., et al., *Claudin-2 expression induces cation-selective channels in tight junctions of epithelial cells.* J Cell Sci, 2002. **115**(Pt 24): p. 4969-76.
53. Angelow, S. and A.S. Yu, *Structure-function studies of claudin extracellular domains by cysteine-scanning mutagenesis.* J Biol Chem, 2009. **284**(42): p. 29205-17.
54. Rossa, J., et al., *Claudin-3 and claudin-5 protein folding and assembly into the tight junction are controlled by non-conserved residues in the transmembrane 3 (TM3) and extracellular loop 2 (ECL2) segments.* J Biol Chem, 2014. **289**(11): p. 7641-53.
55. Krause, G., et al., *Structure and function of extracellular claudin domains.* Ann N Y Acad Sci, 2009. **1165**: p. 34-43.
56. Itoh, M., et al., *Direct binding of three tight junction-associated MAGUKs, ZO-1, ZO-2, and ZO-3, with the COOH termini of claudins.* J Cell Biol, 1999. **147**(6): p. 1351-63.
57. Furuse, M., H. Sasaki, and S. Tsukita, *Manner of interaction of heterogeneous claudin species within and between tight junction strands.* J Cell Biol, 1999. **147**(4): p. 891-903.
58. Gunzel, D. and A.S. Yu, *Claudins and the modulation of tight junction permeability.* Physiol Rev, 2013. **93**(2): p. 525-69.
59. Furuse, M., et al., *A single gene product, claudin-1 or -2, reconstitutes tight junction strands and recruits occludin in fibroblasts.* J Cell Biol, 1998. **143**(2): p. 391-401.
60. Mineta, K., et al., *Predicted expansion of the claudin multigene family.* FEBS Lett, 2011. **585**(4): p. 606-12.
61. Goncalves, A., A.F. Ambrosio, and R. Fernandes, *Regulation of claudins in blood-tissue barriers under physiological and pathological states.* Tissue Barriers, 2013. **1**(3): p. e24782.
62. Luo, Y., et al., *Differential expression of claudins in retinas during normal development and the angiogenesis of oxygen-induced retinopathy.* Invest Ophthalmol Vis Sci, 2011. **52**(10): p. 7556-64.
63. Nitta, T., et al., *Size-selective loosening of the blood-brain barrier in claudin-5-deficient mice.* J Cell Biol, 2003. **161**(3): p. 653-60.
64. Argaw, A.T., et al., *VEGF-mediated disruption of endothelial CLN-5 promotes blood-brain barrier breakdown.* Proc Natl Acad Sci U S A, 2009. **106**(6): p. 1977-82.

65. Muthusamy, A., et al., *Ischemia-reperfusion injury induces occludin phosphorylation/ubiquitination and retinal vascular permeability in a VEGFR-2-dependent manner.* J Cereb Blood Flow Metab, 2014. **34**(3): p. 522-31.
66. Furuse, M., et al., *Claudin-based tight junctions are crucial for the mammalian epidermal barrier: a lesson from claudin-1-deficient mice.* J Cell Biol, 2002. **156**(6): p. 1099-111.
67. Yu, Z., et al., *Dendrobium chrysotoxum Lindl. alleviates diabetic retinopathy by preventing retinal inflammation and tight junction protein decrease.* J Diabetes Res, 2015. **2015**: p. 518317.
68. Xu, H., et al., *Leukocyte diapedesis in vivo induces transient loss of tight junction protein at the blood-retina barrier.* Invest Ophthalmol Vis Sci, 2005. **46**(7): p. 2487-94.
69. Sanchez-Pulido, L., et al., *MARVEL: a conserved domain involved in membrane apposition events.* Trends Biochem Sci, 2002. **27**(12): p. 599-601.
70. Raleigh, D.R., et al., *Tight junction-associated MARVEL proteins marveld3, tricellulin, and occludin have distinct but overlapping functions.* Mol Biol Cell, 2010. **21**(7): p. 1200-13.
71. Furuse, M., et al., *Occludin: a novel integral membrane protein localizing at tight junctions.* J Cell Biol, 1993. **123**(6 Pt 2): p. 1777-88.
72. Feldman, G.J., J.M. Mullin, and M.P. Ryan, *Occludin: structure, function and regulation.* Adv Drug Deliv Rev, 2005. **57**(6): p. 883-917.
73. Traweger, A., et al., *The tight junction-specific protein occludin is a functional target of the E3 ubiquitin-protein ligase itch.* J Biol Chem, 2002. **277**(12): p. 10201-8.
74. Murakami, T., E.A. Felinski, and D.A. Antonetti, *Occludin phosphorylation and ubiquitination regulate tight junction trafficking and vascular endothelial growth factor-induced permeability.* J Biol Chem, 2009. **284**(31): p. 21036-46.
75. Furuse, M., et al., *Direct association of occludin with ZO-1 and its possible involvement in the localization of occludin at tight junctions.* J Cell Biol, 1994. **127**(6 Pt 1): p. 1617-26.
76. Tash, B.R., et al., *The occludin and ZO-1 complex, defined by small angle X-ray scattering and NMR, has implications for modulating tight junction permeability.* Proc Natl Acad Sci U S A, 2012. **109**(27): p. 10855-60.
77. Jesaitis, L.A. and D.A. Goodenough, *Molecular characterization and tissue distribution of ZO-2, a tight junction protein homologous to ZO-1 and the Drosophila discs-large tumor suppressor protein.* J Cell Biol, 1994. **124**(6): p. 949-61.
78. Haskins, J., et al., *ZO-3, a novel member of the MAGUK protein family found at the tight junction, interacts with ZO-1 and occludin.* J Cell Biol, 1998. **141**(1): p. 199-208.
79. Balda, M.S., et al., *Functional dissociation of paracellular permeability and transepithelial electrical resistance and disruption of the apical-basolateral intramembrane diffusion barrier by expression of a mutant tight junction membrane protein.* J Cell Biol, 1996. **134**(4): p. 1031-49.
80. Kevil, C.G., et al., *Expression of zonula occludens and adherens junctional proteins in human venous and arterial endothelial cells: role of occludin in endothelial solute barriers.* Microcirculation, 1998. **5**(2-3): p. 197-210.
81. Yu, A.S., et al., *Knockdown of occludin expression leads to diverse phenotypic alterations in epithelial cells.* Am J Physiol Cell Physiol, 2005. **288**(6): p. C1231-41.
82. Hirase, T., et al., *Occludin as a possible determinant of tight junction permeability in endothelial cells.* J Cell Sci, 1997. **110 (Pt 14)**: p. 1603-13.
83. Elsaid, M.F., et al., *Whole genome sequencing identifies a novel occludin mutation in microcephaly with band-like calcification and polymicrogyria that extends the phenotypic spectrum.* Am J Med Genet A, 2014. **164A**(6): p. 1614-7.
84. LeBlanc, M.A., et al., *A novel rearrangement of occludin causes brain calcification and renal dysfunction.* Hum Genet, 2013. **132**(11): p. 1223-34.

85. O'Driscoll, M.C., et al., *Recessive mutations in the gene encoding the tight junction protein occludin cause band-like calcification with simplified gyration and polymicrogyria.* Am J Hum Genet, 2010. **87**(3): p. 354-64.
86. Saitou, M., et al., *Occludin-deficient embryonic stem cells can differentiate into polarized epithelial cells bearing tight junctions.* J Cell Biol, 1998. **141**(2): p. 397-408.
87. Saitou, M., et al., *Complex phenotype of mice lacking occludin, a component of tight junction strands.* Mol Biol Cell, 2000. **11**(12): p. 4131-42.
88. Schulzke, J.D., et al., *Epithelial transport and barrier function in occludin-deficient mice.* Biochim Biophys Acta, 2005. **1669**(1): p. 34-42.
89. Sundstrom, J.M., et al., *Identification and analysis of occludin phosphosites: a combined mass spectrometry and bioinformatics approach.* J Proteome Res, 2009. **8**(2): p. 808-17.
90. Cummins, P.M., *Occludin: one protein, many forms.* Mol Cell Biol, 2012. **32**(2): p. 242-50.
91. Suzuki, T., et al., *PKC eta regulates occludin phosphorylation and epithelial tight junction integrity.* Proc Natl Acad Sci U S A, 2009. **106**(1): p. 61-6.
92. Elias, B.C., et al., *Phosphorylation of Tyr-398 and Tyr-402 in occludin prevents its interaction with ZO-1 and destabilizes its assembly at the tight junctions.* J Biol Chem, 2009. **284**(3): p. 1559-69.
93. Raleigh, D.R., et al., *Occludin S408 phosphorylation regulates tight junction protein interactions and barrier function.* J Cell Biol, 2011. **193**(3): p. 565-82.
94. Murakami, T., et al., *Protein kinase cbeta phosphorylates occludin regulating tight junction trafficking in vascular endothelial growth factor-induced permeability in vivo.* Diabetes, 2012. **61**(6): p. 1573-83.
95. Runkle, E.A., et al., *Occludin localizes to centrosomes and modifies mitotic entry.* J Biol Chem, 2011. **286**(35): p. 30847-58.
96. Liu, X., et al., *Occludin S490 Phosphorylation Regulates Vascular Endothelial Growth Factor-Induced Retinal Neovascularization.* Am J Pathol, 2016. **186**(9): p. 2486-99.
97. Bolinger, M.T., et al., *Occludin S471 Phosphorylation Contributes to Epithelial Monolayer Maturation.* Mol Cell Biol, 2016. **36**(15): p. 2051-66.
98. Ikenouchi, J., et al., *Tricellulin constitutes a novel barrier at tricellular contacts of epithelial cells.* J Cell Biol, 2005. **171**(6): p. 939-45.
99. Iwamoto, N., T. Higashi, and M. Furuse, *Localization of angulin-1/LSR and tricellulin at tricellular contacts of brain and retinal endothelial cells in vivo.* Cell Struct Funct, 2014. **39**(1): p. 1-8.
100. Riazuddin, S., et al., *Tricellulin is a tight-junction protein necessary for hearing.* Am J Hum Genet, 2006. **79**(6): p. 1040-51.
101. Kitajiri, S., et al., *Deafness in occludin-deficient mice with dislocation of tricellulin and progressive apoptosis of the hair cells.* Biol Open, 2014. **3**(8): p. 759-66.
102. Kamitani, T., et al., *Deletion of Tricellulin Causes Progressive Hearing Loss Associated with Degeneration of Cochlear Hair Cells.* Sci Rep, 2015. **5**: p. 18402.
103. Ikenouchi, J., et al., *Loss of occludin affects tricellular localization of tricellulin.* Mol Biol Cell, 2008. **19**(11): p. 4687-93.
104. Higashi, T., et al., *Analysis of the 'angulin' proteins LSR, ILDR1 and ILDR2--tricellulin recruitment, epithelial barrier function and implication in deafness pathogenesis.* J Cell Sci, 2013. **126**(Pt 4): p. 966-77.
105. Steed, E., et al., *Identification of MarvelD3 as a tight junction-associated transmembrane protein of the occludin family.* BMC Cell Biol, 2009. **10**: p. 95.
106. Martin-Padura, I., et al., *Junctional adhesion molecule, a novel member of the immunoglobulin superfamily that distributes at intercellular junctions and modulates monocyte transmigration.* J Cell Biol, 1998. **142**(1): p. 117-27.

107. Williams, L.A., et al., *Identification and characterisation of human Junctional Adhesion Molecule (JAM).* Mol Immunol, 1999. **36**(17): p. 1175-88.
108. Arrate, M.P., et al., *Cloning of human junctional adhesion molecule 3 (JAM3) and its identification as the JAM2 counter-receptor.* J Biol Chem, 2001. **276**(49): p. 45826-32.
109. Bazzoni, G., et al., *Interaction of junctional adhesion molecule with the tight junction components ZO-1, cingulin, and occludin.* J Biol Chem, 2000. **275**(27): p. 20520-6.
110. Luo, Y., et al., *Expression of JAM-A, AF-6, PAR-3 and PAR-6 during the assembly and remodeling of RPE tight junctions.* Brain Res, 2006. **1110**(1): p. 55-63.
111. Aurrand-Lions, M., et al., *Heterogeneity of endothelial junctions is reflected by differential expression and specific subcellular localization of the three JAM family members.* Blood, 2001. **98**(13): p. 3699-707.
112. Tomi, M. and K. Hosoya, *Application of magnetically isolated rat retinal vascular endothelial cells for the determination of transporter gene expression levels at the inner blood-retinal barrier.* J Neurochem, 2004. **91**(5): p. 1244-8.
113. Williams, D.W., et al., *JAM-A and ALCAM are therapeutic targets to inhibit diapedesis across the BBB of CD14+CD16+ monocytes in HIV-infected individuals.* J Leukoc Biol, 2015. **97**(2): p. 401-12.
114. Woodfin, A., et al., *JAM-A mediates neutrophil transmigration in a stimulus-specific manner in vivo: evidence for sequential roles for JAM-A and PECAM-1 in neutrophil transmigration.* Blood, 2007. **110**(6): p. 1848-56.
115. Daniele, L.L., et al., *Novel distribution of junctional adhesion molecule-C in the neural retina and retinal pigment epithelium.* J Comp Neurol, 2007. **505**(2): p. 166-76.
116. Economopoulou, M., et al., *Endothelial-specific deficiency of Junctional Adhesion Molecule-C promotes vessel normalisation in proliferative retinopathy.* Thromb Haemost, 2015. **114**(6): p. 1241-9.
117. Stevenson, B.R., et al., *Identification of ZO-1: a high molecular weight polypeptide associated with the tight junction (zonula occludens) in a variety of epithelia.* J Cell Biol, 1986. **103**(3): p. 755-66.
118. Gumbiner, B., T. Lowenkopf, and D. Apatira, *Identification of a 160-kDa polypeptide that binds to the tight junction protein ZO-1.* Proc Natl Acad Sci U S A, 1991. **88**(8): p. 3460-4.
119. Ebnet, K., et al., *Junctional adhesion molecule interacts with the PDZ domain-containing proteins AF-6 and ZO-1.* J Biol Chem, 2000. **275**(36): p. 27979-88.
120. Itoh, M., et al., *Involvement of ZO-1 in cadherin-based cell adhesion through its direct binding to alpha catenin and actin filaments.* J Cell Biol, 1997. **138**(1): p. 181-92.
121. Wittchen, E.S., J. Haskins, and B.R. Stevenson, *Protein interactions at the tight junction. Actin has multiple binding partners, and ZO-1 forms independent complexes with ZO-2 and ZO-3.* J Biol Chem, 1999. **274**(49): p. 35179-85.
122. Yamamoto, T., et al., *The Ras target AF-6 interacts with ZO-1 and serves as a peripheral component of tight junctions in epithelial cells.* J Cell Biol, 1997. **139**(3): p. 785-95.
123. Ooshio, T., et al., *Involvement of the interaction of afadin with ZO-1 in the formation of tight junctions in Madin-Darby canine kidney cells.* J Biol Chem, 2010. **285**(7): p. 5003-12.
124. Umeda, K., et al., *ZO-1 and ZO-2 independently determine where claudins are polymerized in tight-junction strand formation.* Cell, 2006. **126**(4): p. 741-54.
125. Katsuno, T., et al., *Deficiency of zonula occludens-1 causes embryonic lethal phenotype associated with defected yolk sac angiogenesis and apoptosis of embryonic cells.* Mol Biol Cell, 2008. **19**(6): p. 2465-75.
126. Yeh, W.L., et al., *Inhibition of hypoxia-induced increase of blood-brain barrier permeability by YC-1 through the antagonism of HIF-1alpha accumulation and VEGF expression.* Mol Pharmacol, 2007. **72**(2): p. 440-9.

127. Carmeliet, P., et al., *Targeted deficiency or cytosolic truncation of the VE-cadherin gene in mice impairs VEGF-mediated endothelial survival and angiogenesis.* Cell, 1999. **98**(2): p. 147-57.
128. Giannotta, M., M. Trani, and E. Dejana, *VE-cadherin and endothelial adherens junctions: active guardians of vascular integrity.* Dev Cell, 2013. **26**(5): p. 441-54.
129. Stamatovic, S.M., et al., *Junctional proteins of the blood-brain barrier: New insights into function and dysfunction.* Tissue Barriers, 2016. **4**(1): p. e1154641.
130. Wojciak-Stothard, B. and A.J. Ridley, *Rho GTPases and the regulation of endothelial permeability.* Vascul Pharmacol, 2002. **39**(4-5): p. 187-99.
131. Wilson, C.W. and W. Ye, *Regulation of vascular endothelial junction stability and remodeling through Rap1-Rasip1 signaling.* Cell Adh Migr, 2014. **8**(2): p. 76-83.
132. Amado-Azevedo, J., E.T. Valent, and G.P. Van Nieuw Amerongen, *Regulation of the endothelial barrier function: a filum granum of cellular forces, Rho-GTPase signaling and microenvironment.* Cell Tissue Res, 2014. **355**(3): p. 557-76.
133. Heasman, S.J. and A.J. Ridley, *Mammalian Rho GTPases: new insights into their functions from in vivo studies.* Nat Rev Mol Cell Biol, 2008. **9**(9): p. 690-701.
134. Boulter, E., et al., *Regulation of Rho GTPase crosstalk, degradation and activity by RhoGDI1.* Nat Cell Biol, 2010. **12**(5): p. 477-83.
135. Wennerberg, K., K.L. Rossman, and C.J. Der, *The Ras superfamily at a glance.* J Cell Sci, 2005. **118**(Pt 5): p. 843-6.
136. Bos, J.L., H. Rehmann, and A. Wittinghofer, *GEFs and GAPs: critical elements in the control of small G proteins.* Cell, 2007. **129**(5): p. 865-77.
137. Bourne, H.R., *GTPases: a family of molecular switches and clocks.* Philos Trans R Soc Lond B Biol Sci, 1995. **349**(1329): p. 283-9.
138. Citalan-Madrid, A.F., et al., *Small GTPases of the Ras superfamily regulate intestinal epithelial homeostasis and barrier function via common and unique mechanisms.* Tissue Barriers, 2013. **1**(5): p. e26938.
139. Mott, H.R. and D. Owen, *Structures of Ras superfamily effector complexes: What have we learnt in two decades?* Crit Rev Biochem Mol Biol, 2015. **50**(2): p. 85-133.
140. Lampugnani, M.G., et al., *VE-cadherin regulates endothelial actin activating Rac and increasing membrane association of Tiam.* Mol Biol Cell, 2002. **13**(4): p. 1175-89.
141. Ando, K., et al., *Rap1 potentiates endothelial cell junctions by spatially controlling myosin II activity and actin organization.* J Cell Biol, 2013. **202**(6): p. 901-16.
142. Amano, M., et al., *Phosphorylation and activation of myosin by Rho-associated kinase (Rho-kinase).* J Biol Chem, 1996. **271**(34): p. 20246-9.
143. Dudek, S.M. and J.G. Garcia, *Cytoskeletal regulation of pulmonary vascular permeability.* J Appl Physiol (1985), 2001. **91**(4): p. 1487-500.
144. Xie, H., et al., *Role of RhoA/ROCK signaling in endothelial-monocyte-activating polypeptide II opening of the blood-tumor barrier: role of RhoA/ROCK signaling in EMAP II opening of the BTB.* J Mol Neurosci, 2012. **46**(3): p. 666-76.
145. Bos, J.L., *Epac: a new cAMP target and new avenues in cAMP research.* Nat Rev Mol Cell Biol, 2003. **4**(9): p. 733-8.
146. Post, A., et al., *Rasip1 mediates Rap1 regulation of Rho in endothelial barrier function through ArhGAP29.* Proc Natl Acad Sci U S A, 2013. **110**(28): p. 11427-32.
147. Hall, A., *Rho GTPases and the control of cell behaviour.* Biochem Soc Trans, 2005. **33**(Pt 5): p. 891-5.
148. Hall, A., *Rho family GTPases.* Biochem Soc Trans, 2012. **40**(6): p. 1378-82.
149. Essler, M., et al., *Thrombin inactivates myosin light chain phosphatase via Rho and its target Rho kinase in human endothelial cells.* J Biol Chem, 1998. **273**(34): p. 21867-74.

150. Faurobert, E., et al., *CCM1-ICAP-1 complex controls beta1 integrin-dependent endothelial contractility and fibronectin remodeling.* J Cell Biol, 2013. **202**(3): p. 545-61.
151. Beckers, C.M., V.W. van Hinsbergh, and G.P. van Nieuw Amerongen, *Driving Rho GTPase activity in endothelial cells regulates barrier integrity.* Thromb Haemost, 2010. **103**(1): p. 40-55.
152. Loirand, G., V. Sauzeau, and P. Pacaud, *Small G proteins in the cardiovascular system: physiological and pathological aspects.* Physiol Rev, 2013. **93**(4): p. 1659-720.
153. Bryan, B.A., et al., *RhoA/ROCK signaling is essential for multiple aspects of VEGF-mediated angiogenesis.* FASEB J, 2010. **24**(9): p. 3186-95.
154. Arita, R., et al., *Rho kinase inhibition by fasudil ameliorates diabetes-induced microvascular damage.* Diabetes, 2009. **58**(1): p. 215-26.
155. van Nieuw Amerongen, G.P., et al., *Involvement of Rho kinase in endothelial barrier maintenance.* Arterioscler Thromb Vasc Biol, 2007. **27**(11): p. 2332-9.
156. Terry, S.J., et al., *Spatially restricted activation of RhoA signalling at epithelial junctions by p114RhoGEF drives junction formation and morphogenesis.* Nat Cell Biol, 2011. **13**(2): p. 159-66.
157. Braga, V.M., et al., *The small GTPases Rho and Rac are required for the establishment of cadherin-dependent cell-cell contacts.* J Cell Biol, 1997. **137**(6): p. 1421-31.
158. Kouklis, P., et al., *Cdc42 regulates the restoration of endothelial barrier function.* Circ Res, 2004. **94**(2): p. 159-66.
159. Broman, M.T., D. Mehta, and A.B. Malik, *Cdc42 regulates the restoration of endothelial adherens junctions and permeability.* Trends Cardiovasc Med, 2007. **17**(5): p. 151-6.
160. Mataraza, J.M., et al., *Identification and characterization of the Cdc42-binding site of IQGAP1.* Biochem Biophys Res Commun, 2003. **305**(2): p. 315-21.
161. Briggs, M.W. and D.B. Sacks, *IQGAP1 as signal integrator: Ca2+, calmodulin, Cdc42 and the cytoskeleton.* FEBS Lett, 2003. **542**(1-3): p. 7-11.
162. Wojciak-Stothard, B., et al., *Rho and Rac but not Cdc42 regulate endothelial cell permeability.* J Cell Sci, 2001. **114**(Pt 7): p. 1343-55.
163. Gavard, J. and J.S. Gutkind, *VEGF controls endothelial-cell permeability by promoting the beta-arrestin-dependent endocytosis of VE-cadherin.* Nat Cell Biol, 2006. **8**(11): p. 1223-34.
164. de Rooij, J., et al., *Epac is a Rap1 guanine-nucleotide-exchange factor directly activated by cyclic AMP.* Nature, 1998. **396**(6710): p. 474-7.
165. Roberts, O.L. and C. Dart, *cAMP signalling in the vasculature: the role of Epac (exchange protein directly activated by cAMP).* Biochem Soc Trans, 2014. **42**(1): p. 89-97.
166. Bos, J.L., *Epac proteins: multi-purpose cAMP targets.* Trends Biochem Sci, 2006. **31**(12): p. 680-6.
167. Rehmann, H., et al., *Structure of Epac2 in complex with a cyclic AMP analogue and RAP1B.* Nature, 2008. **455**(7209): p. 124-7.
168. Rehmann, H., et al., *Structure and regulation of the cAMP-binding domains of Epac2.* Nat Struct Biol, 2003. **10**(1): p. 26-32.
169. Wang, P., et al., *Exchange proteins directly activated by cAMP (EPACs): Emerging therapeutic targets.* Bioorg Med Chem Lett, 2017. **27**(8): p. 1633-1639.
170. Kai, A.K., et al., *Exchange protein activated by cAMP 1 (Epac1)-deficient mice develop beta-cell dysfunction and metabolic syndrome.* FASEB J, 2013. **27**(10): p. 4122-35.
171. Yan, J., et al., *Enhanced leptin sensitivity, reduced adiposity, and improved glucose homeostasis in mice lacking exchange protein directly activated by cyclic AMP isoform 1.* Mol Cell Biol, 2013. **33**(5): p. 918-26.
172. Yang, Y., et al., *EPAC null mutation impairs learning and social interactions via aberrant regulation of miR-124 and Zif268 translation.* Neuron, 2012. **73**(4): p. 774-88.
173. Bos, J.L., J. de Rooij, and K.A. Reedquist, *Rap1 signalling: adhering to new models.* Nat Rev Mol Cell Biol, 2001. **2**(5): p. 369-77.

174. Rousseau-Merck, M.F., et al., *Chromosome mapping of the human RAS-related RAP1A, RAP1B, and RAP2 genes to chromosomes 1p12----p13, 12q14, and 13q34, respectively.* Cytogenet Cell Genet, 1990. **53**(1): p. 2-4.
175. van Dam, T.J., J.L. Bos, and B. Snel, *Evolution of the Ras-like small GTPases and their regulators.* Small GTPases, 2011. **2**(1): p. 4-16.
176. Bos, J.L., *Ras-like GTPases.* Biochim Biophys Acta, 1997. **1333**(2): p. M19-31.
177. Pannekoek, W.J., et al., *Cell-cell junction formation: the role of Rap1 and Rap1 guanine nucleotide exchange factors.* Biochim Biophys Acta, 2009. **1788**(4): p. 790-6.
178. Lakshmikanthan, S., et al., *Rap1 promotes VEGFR2 activation and angiogenesis by a mechanism involving integrin alphavbeta(3).* Blood, 2011. **118**(7): p. 2015-26.
179. Li, Y., et al., *Rap1a null mice have altered myeloid cell functions suggesting distinct roles for the closely related Rap1a and 1b proteins.* J Immunol, 2007. **179**(12): p. 8322-31.
180. Chrzanowska-Wodnicka, M., et al., *Defective angiogenesis, endothelial migration, proliferation, and MAPK signaling in Rap1b-deficient mice.* Blood, 2008. **111**(5): p. 2647-56.
181. Chrzanowska-Wodnicka, M., et al., *Small GTPase Rap1 Is Essential for Mouse Development and Formation of Functional Vasculature.* PLoS One, 2015. **10**(12): p. e0145689.
182. Duchniewicz, M., et al., *Rap1A-deficient T and B cells show impaired integrin-mediated cell adhesion.* Mol Cell Biol, 2006. **26**(2): p. 643-53.
183. Walls, J.R., et al., *Three-dimensional analysis of vascular development in the mouse embryo.* PLoS One, 2008. **3**(8): p. e2853.
184. Chrzanowska-Wodnicka, M., et al., *Rap1b is required for normal platelet function and hemostasis in mice.* J Clin Invest, 2005. **115**(3): p. 680-7.
185. Enserink, J.M., et al., *A novel Epac-specific cAMP analogue demonstrates independent regulation of Rap1 and ERK.* Nat Cell Biol, 2002. **4**(11): p. 901-6.
186. Vliem, M.J., et al., *8-pCPT-2'-O-Me-cAMP-AM: an improved Epac-selective cAMP analogue.* Chembiochem, 2008. **9**(13): p. 2052-4.
187. Cullere, X., et al., *Regulation of vascular endothelial barrier function by Epac, a cAMP-activated exchange factor for Rap GTPase.* Blood, 2005. **105**(5): p. 1950-5.
188. Kooistra, M.R., et al., *Epac1 regulates integrity of endothelial cell junctions through VE-cadherin.* FEBS Lett, 2005. **579**(22): p. 4966-72.
189. Fukuhara, S., et al., *Cyclic AMP potentiates vascular endothelial cadherin-mediated cell-cell contact to enhance endothelial barrier function through an Epac-Rap1 signaling pathway.* Mol Cell Biol, 2005. **25**(1): p. 136-46.
190. Adamson, R.H., et al., *Epac/Rap1 pathway regulates microvascular hyperpermeability induced by PAF in rat mesentery.* Am J Physiol Heart Circ Physiol, 2008. **294**(3): p. H1188-96.
191. Pannekoek, W.J., et al., *Rap1 and Rap2 antagonistically control endothelial barrier resistance.* PLoS One, 2013. **8**(2): p. e57903.
192. Birukova, A.A., et al., *Rap-afadin axis in control of Rho signaling and endothelial barrier recovery.* Mol Biol Cell, 2013. **24**(17): p. 2678-88.
193. Hoshino, T., et al., *Regulation of E-cadherin endocytosis by nectin through afadin, Rap1, and p120ctn.* J Biol Chem, 2005. **280**(25): p. 24095-103.
194. Sehrawat, S., et al., *Role of Epac1, an exchange factor for Rap GTPases, in endothelial microtubule dynamics and barrier function.* Mol Biol Cell, 2008. **19**(3): p. 1261-70.
195. Mitin, N.Y., et al., *Identification and characterization of rain, a novel Ras-interacting protein with a unique subcellular localization.* J Biol Chem, 2004. **279**(21): p. 22353-61.
196. Rogers, S.L., et al., *Regulation of melanosome movement in the cell cycle by reversible association with myosin V.* J Cell Biol, 1999. **146**(6): p. 1265-76.

197. Xu, K., et al., *Blood vessel tubulogenesis requires Rasip1 regulation of GTPase signaling.* Dev Cell, 2011. **20**(4): p. 526-39.
198. Wallgard, E., et al., *Identification of a core set of 58 gene transcripts with broad and specific expression in the microvasculature.* Arterioscler Thromb Vasc Biol, 2008. **28**(8): p. 1469-76.
199. Xu, K., et al., *Rasip1 is required for endothelial cell motility, angiogenesis and vessel formation.* Dev Biol, 2009. **329**(2): p. 269-79.
200. Koo, Y., et al., *Rasip1 is essential to blood vessel stability and angiogenic blood vessel growth.* Angiogenesis, 2016. **19**(2): p. 173-90.
201. Wilson, C.W., et al., *Rasip1 regulates vertebrate vascular endothelial junction stability through Epac1-Rap1 signaling.* Blood, 2013. **122**(22): p. 3678-90.
202. de Kreuk, B.J., et al., *Heart of glass anchors Rasip1 at endothelial cell-cell junctions to support vascular integrity.* Elife, 2016. **5**: p. e11394.
203. Gingras, A.R., et al., *Structural Basis of Dimeric Rasip1 RA Domain Recognition of the Ras Subfamily of GTP-Binding Proteins.* Structure, 2016. **24**(12): p. 2152-2162.
204. Rehmann, H. and J.L. Bos, *Ras Association-Domain Dimers Bring Proteins Together.* Structure, 2016. **24**(12): p. 2039-2040.
205. Post, A., et al., *Rap1 Spatially Controls ArhGAP29 To Inhibit Rho Signaling during Endothelial Barrier Regulation.* Mol Cell Biol, 2015. **35**(14): p. 2495-502.
206. Aveleira, C.A., et al., *TNF-alpha signals through PKCzeta/NF-kappaB to alter the tight junction complex and increase retinal endothelial cell permeability.* Diabetes, 2010. **59**(11): p. 2872-82.
207. Simo, R., J.M. Sundstrom, and D.A. Antonetti, *Ocular Anti-VEGF therapy for diabetic retinopathy: the role of VEGF in the pathogenesis of diabetic retinopathy.* Diabetes Care, 2014. **37**(4): p. 893-9.
208. He, P., M. Zeng, and F.E. Curry, *Dominant role of cAMP in regulation of microvessel permeability.* Am J Physiol Heart Circ Physiol, 2000. **278**(4): p. H1124-33.
209. Adamson, R.H., et al., *Microvascular permeability and number of tight junctions are modulated by cAMP.* Am J Physiol, 1998. **274**(6 Pt 2): p. H1885-94.
210. de Rooij, J., et al., *Mechanism of regulation of the Epac family of cAMP-dependent RapGEFs.* J Biol Chem, 2000. **275**(27): p. 20829-36.
211. Kawasaki, H., et al., *A family of cAMP-binding proteins that directly activate Rap1.* Science, 1998. **282**(5397): p. 2275-9.
212. Kooistra, M.R., N. Dube, and J.L. Bos, *Rap1: a key regulator in cell-cell junction formation.* J Cell Sci, 2007. **120**(Pt 1): p. 17-22.
213. Baumer, Y., D. Drenckhahn, and J. Waschke, *cAMP induced Rac 1-mediated cytoskeletal reorganization in microvascular endothelium.* Histochem Cell Biol, 2008. **129**(6): p. 765-78.
214. Titchenell, P.M., et al., *Novel atypical PKC inhibitors prevent vascular endothelial growth factor-induced blood-retinal barrier dysfunction.* Biochem J, 2012. **446**(3): p. 455-67.
215. Antonetti, D.A. and E.B. Wolpert, *Isolation and characterization of retinal endothelial cells.* Methods Mol Med, 2003. **89**: p. 365-74.
216. Harhaj, N.S., et al., *VEGF activation of protein kinase C stimulates occludin phosphorylation and contributes to endothelial permeability.* Invest Ophthalmol Vis Sci, 2006. **47**(11): p. 5106-15.
217. Wittchen, E.S., et al., *Rap1 GTPase activation and barrier enhancement in rpe inhibits choroidal neovascularization in vivo.* PLoS One, 2013. **8**(9): p. e73070.
218. Whitaker, C.M. and N.G. Cooper, *Differential distribution of exchange proteins directly activated by cyclic AMP within the adult rat retina.* Neuroscience, 2010. **165**(3): p. 955-67.
219. Penzes, P., K.M. Woolfrey, and D.P. Srivastava, *Epac2-mediated dendritic spine remodeling: implications for disease.* Mol Cell Neurosci, 2011. **46**(2): p. 368-80.

220. Liu, J., et al., *Epac2-deficiency leads to more severe retinal swelling, glial reactivity and oxidative stress in transient middle cerebral artery occlusion induced ischemic retinopathy.* Sci China Life Sci, 2015. **58**(6): p. 521-30.
221. Boettner, B. and L. Van Aelst, *Control of cell adhesion dynamics by Rap1 signaling.* Curr Opin Cell Biol, 2009. **21**(5): p. 684-93.
222. Glading, A., et al., *KRIT-1/CCM1 is a Rap1 effector that regulates endothelial cell cell junctions.* J Cell Biol, 2007. **179**(2): p. 247-54.
223. van Buul, J.D., D. Geerts, and S. Huveneers, *Rho GAPs and GEFs: controling switches in endothelial cell adhesion.* Cell Adh Migr, 2014. **8**(2): p. 108-24.
224. Ramos, C.J. and D.A. Antonetti, *The role of small GTPases and EPAC-Rap signaling in the regulation of the blood-brain and blood-retinal barriers.* Tissue Barriers, 2017. **5**(3): p. e1339768.
225. Wittchen, E.S. and M.E. Hartnett, *The small GTPase Rap1 is a novel regulator of RPE cell barrier function.* Invest Ophthalmol Vis Sci, 2011. **52**(10): p. 7455-63.
226. Yuan, Z., W. Zhang, and W. Tan, *A labile pool of IQGAP1 disassembles endothelial adherens junctions.* Int J Mol Sci, 2013. **14**(7): p. 13377-90.
227. Tian, Y., et al., *Hepatocyte growth factor-induced Asef-IQGAP1 complex controls cytoskeletal remodeling and endothelial barrier.* J Biol Chem, 2015. **290**(7): p. 4097-109.
228. Wang, H., et al., *Retinal pigment epithelial cell expression of active Rap 1a by scAAV2 inhibits choroidal neovascularization.* Mol Ther Methods Clin Dev, 2016. **3**: p. 16056.
229. Cook, S.J., et al., *RapV12 antagonizes Ras-dependent activation of ERK1 and ERK2 by LPA and EGF in Rat-1 fibroblasts.* EMBO J, 1993. **12**(9): p. 3475-85.
230. Roskoski, R., Jr., *ERK1/2 MAP kinases: structure, function, and regulation.* Pharmacol Res, 2012. **66**(2): p. 105-43.
231. Antonetti, D.A., et al., *Diabetic retinopathy: seeing beyond glucose-induced microvascular disease.* Diabetes, 2006. **55**(9): p. 2401-11.
232. Hartnett, M.E., W. Baehr, and Y.Z. Le, *Diabetic retinopathy, an overview.* Vision Res, 2017.
233. Lee, R., T.Y. Wong, and C. Sabanayagam, *Epidemiology of diabetic retinopathy, diabetic macular edema and related vision loss.* Eye Vis (Lond), 2015. **2**: p. 17.
234. Rowley, W.R., et al., *Diabetes 2030: Insights from Yesterday, Today, and Future Trends.* Popul Health Manag, 2017. **20**(1): p. 6-12.
235. Diabetic Retinopathy Clinical Research, N., et al., *Randomized trial evaluating ranibizumab plus prompt or deferred laser or triamcinolone plus prompt laser for diabetic macular edema.* Ophthalmology, 2010. **117**(6): p. 1064-1077 e35.
236. Robinson, C.J. and S.E. Stringer, *The splice variants of vascular endothelial growth factor (VEGF) and their receptors.* J Cell Sci, 2001. **114**(Pt 5): p. 853-65.
237. Evans, I., *An Overview of VEGF-Mediated Signal Transduction.* Methods Mol Biol, 2015. **1332**: p. 91-120.
238. Takahashi, H. and M. Shibuya, *The vascular endothelial growth factor (VEGF)/VEGF receptor system and its role under physiological and pathological conditions.* Clin Sci (Lond), 2005. **109**(3): p. 227-41.
239. Aiello, L.P., et al., *Vascular endothelial growth factor in ocular fluid of patients with diabetic retinopathy and other retinal disorders.* N Engl J Med, 1994. **331**(22): p. 1480-7.
240. Adamis, A.P., et al., *Increased vascular endothelial growth factor levels in the vitreous of eyes with proliferative diabetic retinopathy.* Am J Ophthalmol, 1994. **118**(4): p. 445-50.
241. Semeraro, F., et al., *Diabetic Retinopathy: Vascular and Inflammatory Disease.* J Diabetes Res, 2015. **2015**: p. 582060.
242. Rosenbaum, J.T., et al., *Ocular inflammatory effects of intravitreally-injected tumor necrosis factor.* Am J Pathol, 1988. **133**(1): p. 47-53.

243. Yoshida, S., A. Yoshida, and T. Ishibashi, *Induction of IL-8, MCP-1, and bFGF by TNF-alpha in retinal glial cells: implications for retinal neovascularization during post-ischemic inflammation.* Graefes Arch Clin Exp Ophthalmol, 2004. **242**(5): p. 409-13.
244. Carmeliet, P., et al., *Role of HIF-1alpha in hypoxia-mediated apoptosis, cell proliferation and tumour angiogenesis.* Nature, 1998. **394**(6692): p. 485-90.
245. Semenza, G.L., *HIF-1: mediator of physiological and pathophysiological responses to hypoxia.* J Appl Physiol (1985), 2000. **88**(4): p. 1474-80.
246. Koch, S., et al., *Signal transduction by vascular endothelial growth factor receptors.* Biochem J, 2011. **437**(2): p. 169-83.
247. Ho, Q.T. and C.J. Kuo, *Vascular endothelial growth factor: biology and therapeutic applications.* Int J Biochem Cell Biol, 2007. **39**(7-8): p. 1349-57.
248. Takahashi, T., et al., *A single autophosphorylation site on KDR/Flk-1 is essential for VEGF-A-dependent activation of PLC-gamma and DNA synthesis in vascular endothelial cells.* EMBO J, 2001. **20**(11): p. 2768-78.
249. Matsumoto, T., et al., *VEGF receptor-2 Y951 signaling and a role for the adapter molecule TSAd in tumor angiogenesis.* EMBO J, 2005. **24**(13): p. 2342-53.
250. Dougher, M. and B.I. Terman, *Autophosphorylation of KDR in the kinase domain is required for maximal VEGF-stimulated kinase activity and receptor internalization.* Oncogene, 1999. **18**(8): p. 1619-27.
251. Antonetti, D.A., et al., *Vascular endothelial growth factor induces rapid phosphorylation of tight junction proteins occludin and zonula occluden 1. A potential mechanism for vascular permeability in diabetic retinopathy and tumors.* J Biol Chem, 1999. **274**(33): p. 23463-7.
252. Pearce, L.R., D. Komander, and D.R. Alessi, *The nuts and bolts of AGC protein kinases.* Nat Rev Mol Cell Biol, 2010. **11**(1): p. 9-22.
253. Steinberg, S.F., *Structural basis of protein kinase C isoform function.* Physiol Rev, 2008. **88**(4): p. 1341-78.
254. Chou, M.M., et al., *Regulation of protein kinase C zeta by PI 3-kinase and PDK-1.* Curr Biol, 1998. **8**(19): p. 1069-77.
255. Jayapandian, M., et al., *Michigan Molecular Interactions (MiMI): putting the jigsaw puzzle together.* Nucleic Acids Res, 2007. **35**(Database issue): p. D566-71.
256. Titchenell, P.M., et al., *Synthesis and structure-activity relationships of 2-amino-3-carboxy-4-phenylthiophenes as novel atypical protein kinase C inhibitors.* Bioorg Med Chem Lett, 2013. **23**(10): p. 3034-8.
257. Cunha-Vaz, J., J.R. Faria de Abreu, and A.J. Campos, *Early breakdown of the blood-retinal barrier in diabetes.* Br J Ophthalmol, 1975. **59**(11): p. 649-56.
258. Eshaq, R.S., et al., *Diabetic retinopathy: Breaking the barrier.* Pathophysiology, 2017.
259. Nguyen, Q.D., et al., *Two-year outcomes of the ranibizumab for edema of the mAcula in diabetes (READ-2) study.* Ophthalmology, 2010. **117**(11): p. 2146-51.
260. Massin, P., et al., *Intravitreal triamcinolone acetonide for diabetic diffuse macular edema: preliminary results of a prospective controlled trial.* Ophthalmology, 2004. **111**(2): p. 218-24; discussion 224-5.
261. Sutter, F.K., J.M. Simpson, and M.C. Gillies, *Intravitreal triamcinolone for diabetic macular edema that persists after laser treatment: three-month efficacy and safety results of a prospective, randomized, double-masked, placebo-controlled clinical trial.* Ophthalmology, 2004. **111**(11): p. 2044-9.
262. Ciardella, A.P., et al., *Intravitreal triamcinolone for the treatment of refractory diabetic macular oedema with hard exudates: an optical coherence tomography study.* Br J Ophthalmol, 2004. **88**(9): p. 1131-6.

263. Gillies, M.C., et al., *Intravitreal triamcinolone for refractory diabetic macular edema: two-year results of a double-masked, placebo-controlled, randomized clinical trial.* Ophthalmology, 2006. **113**(9): p. 1533-8.
264. Moshfeghi, D.M., et al., *Acute endophthalmitis following intravitreal triamcinolone acetonide injection.* Am J Ophthalmol, 2003. **136**(5): p. 791-6.
265. van Hinsbergh, V.W. and G.P. van Nieuw Amerongen, *Intracellular signalling involved in modulating human endothelial barrier function.* J Anat, 2002. **200**(6): p. 549-60.
266. van Nieuw Amerongen, G.P., et al., *Activation of RhoA by thrombin in endothelial hyperpermeability: role of Rho kinase and protein tyrosine kinases.* Circ Res, 2000. **87**(4): p. 335-40.
267. Antonetti, D.A., et al., *Vascular permeability in experimental diabetes is associated with reduced endothelial occludin content: vascular endothelial growth factor decreases occludin in retinal endothelial cells. Penn State Retina Research Group.* Diabetes, 1998. **47**(12): p. 1953-9.
268. Harhaj, N.S. and D.A. Antonetti, *Regulation of tight junctions and loss of barrier function in pathophysiology.* Int J Biochem Cell Biol, 2004. **36**(7): p. 1206-37.
269. Birukova, A.A., et al., *Afadin controls p120-catenin-ZO-1 interactions leading to endothelial barrier enhancement by oxidized phospholipids.* J Cell Physiol, 2012. **227**(5): p. 1883-90.
270. Duran, A., M.T. Diaz-Meco, and J. Moscat, *Essential role of RelA Ser311 phosphorylation by zetaPKC in NF-kappaB transcriptional activation.* EMBO J, 2003. **22**(15): p. 3910-8.
271. Leitges, M., et al., *Targeted disruption of the zetaPKC gene results in the impairment of the NF-kappaB pathway.* Mol Cell, 2001. **8**(4): p. 771-80.